VOLUME 25, NUMBER 1
IN TWO PARTS

JANUARY, 1937
PART 1

PROCEEDINGS
of
The Institute of Radio Engineers

Application Blank for Associate Membership on Page XII

Institute of Radio Engineers Forthcoming Meetings

CINCINNATI SECTION
January 19, 1937

CLEVELAND SECTION
January 28, 1937

DETROIT SECTION
January 15, 1937

EMPORIUM SECTION
January 14, 1937

LOS ANGELES SECTION
January 19, 1937

NEW YORK MEETING
January 6, 1937
February 3, 1937

PHILADELPHIA SECTION
January 7, 1937
February 4, 1937

SAN FRANCISCO SECTION
January 20, 1937

SEATTLE SECTION
January 8, 1937

TORONTO SECTION
January 11, 1937

WASHINGTON SECTION
January 11, 1937

Underwood & Underwood

HAROLD H. BEVERAGE

President of the Institute, 1937

Harold Henry Beverage was born in North Haven, Maine, on October 14, 1893. In 1915 he received a Bachelor of Science degree in electrical engineering from the University of Maine and entered the General Electric Company test course. During the next four years he was laboratory assistant to Dr. Alexanderson and participated in the development of the high-frequency alternator later used in the high-powered transatlantic transmitting stations.

From 1920 to 1929 his time was devoted to research on communication receivers for the Radio Corporation of America. During this period his work on directional antennas brought him the Morris Liebmann Memorial Prize of the Institute.

He was transferred to RCA Communications as chief research engineer in 1929.

He joined the Institute as an Associate in 1915, transferred to Member grade in 1926, and was transferred to Fellow grade in 1928.

December Meeting of Board of Directors

The regular meeting of the Board of Directors was held in the Institute office on December 2, 1936. Those present were Alan Hazeltine, president; Melville Eastham, treasurer; E. H. Armstrong, Arthur Batcheller, H. H. Beverage, Ralph Bown (guest), Virgil M. Graham, L. C. F. Horle, C. M. Jansky, Jr., E. L. Nelson, Haraden Pratt, H. M. Turner, and H. P. Westman, Secretary.

Seventy-five applications for Associate membership, two for Junior, and ten for Student membership were approved.

A report on the recent Rochester Fall Meeting gave a total registration of 455 of whom 87 were from the local area. There were 148 American and Canadian organizations represented.

An application for the formation of an Institute section with headquarters in Indianapolis, Indiana, was approved.

The establishment of a Montreal Section of the Institute was authorized also.

An invitation for a representative of the Institute to address via high-frequency radiotelephony a dinner in honor of the early pioneers of radio being held in Sydney by the Institution of Radio Engineers (Australia) was accepted.

A resolution favoring the adoption of the proposed twelve month, equal quarters calendar sponsored by the World Calendar Association was adopted.

The editor was authorized to include in the PROCEEDINGS a section in which letters from the membership and others on both Institute and technical matters might be published.

Committee Work

TECHNICAL COMMITTEES

ELECTRONICS COMMITTEE

A meeting of the Electronics Committee was held in the Institute office on Friday, December 11. Those present were B. J. Thompson, chairman; R. S. Burnap, E. L. Chaffee, F. Holborn, F. R. Lack, George Lewis, Knox McIlwain, G. F. Metcalf, and H. P. Westman, secretary.

The committee gave final consideration to the review of its field during 1936 which it is preparing for presentation at the annual meeting of the Institute. It considered also comments from the Standards

Committee in regard to the report prepared by it which is under review of the Standards Committee.

Electronics Committee—Subcommittee on High-Frequency Tubes

The Subcommittee on High-Frequency Tubes operating under the Electronics Committee met in the Institute office on November 30 and devoted its time to the preparation of a review of that field during 1936. Those present were B. J. Thompson, chairman; K. C. DeWalt, G. R. Kilgore, F. B. Llewellyn, A. L. Samuel, and H. P. Westman, secretary.

Standards Committee

L. C. F. Horle, chairman; J. Blanchard (representing William Wilson), Melville Eastham, H. F. Olson, J. C. Schelleng, B. J. Thompson, H. J. Vennes, H. A. Wheeler, and H. P. Westman, secretary, were present at a meeting of the Standards Committee held in the Institute office on December 3. The committee completed its review of the reports submitted by the Electronics Committee which except for some minor considerations, is now to be acted on by the Board of Directors. It reviewed also a report on loud-speaker testing submitted to it by the Electroacoustics Committee.

Institute Meetings

Chicago Section

A meeting of the Chicago Section was held on November 27 in the Hotel LaSalle. H. C. Vance, vice chairman, presided and 140 attended the meeting. Twenty-five attended the dinner which preceded the meeting.

A paper on "Résumé of the Theory and Application of Acoustic Networks in Radio Receiver Cabinets" was presented by Hugh Knowles, chief engineer of the Jensen Radio Manufacturing Company and was discussed by Messrs. Krause and Maki.

Cleveland Section

The Cleveland Section met on October 22 at Case School of Applied Science. The attendance was twenty-six and R. M. Pierce, chairman, presided.

A paper on "Cross Modulation in Radio Receivers" was presented by W. W. Rockwell, technical supervisor of WLW. In it he presented

evidence to disprove the theory of the "Luxemburg effect" which attributed cross modulation to disturbances in the ionosphere caused by high power radiation. One cause of this effect is rectification occurring in the vicinity of the receiver by loose and corroded joints in power lines and drain spouts. "Tunable hum" was discussed and seems to be caused by rectification in the receiver power wiring. Elimination has been effected by disturbing the power wiring by mechanical shock. Intermittent effects are sometimes caused by wet and dry weather conditions. During wet weather the trouble disappears which indicates the trouble to be outside the house. Both superheterodyne and tuned radio-frequency receivers are bothered by this trouble which affects equally noise, weak signals, and strong signals. These conditions can be reproduced in the laboratory by tuning a large antenna with a variometer shunted by a diode detector and using a small antenna on the receiver. Cross moduation can thus be produced.

A paper prepared by A. F. Van Dyck of the RCA License Laboratory on "Suggested Empirical Standards and Mileage Separation Tables for Broadcast Stations" was read by the chairman. It was based on an average selectivity curve for all 1935 receivers listing at less than a hundred dollars. He advocated a seven-to-one signal strength ratio on ten-kilocycle removed channels instead of the present one-half-to-one ratio standard.

The November meeting of the section was held on the 19th at Case School of Applied Science with Chairman Pierce presiding. There were 106 present.

A paper by J. J. Lamb, technical editor of *QST*, was on "Improvements Reducing Signal and Noise Interference in Communications Receivers." Amplitude, frequency, and phase selectivity were discussed. Characteristic selectivity curves of crystal filter circuits were shown. Frequency selectivity is best secured by the use of a crystal filter, while amplitude selectivity can be obtained by the use of the noise silencer. This noise silencer is a circuit which momentarily cuts the signal when there is a burst of noise. A demonstration followed to indicate the effectiveness of these methods of reducing interference.

Connecticut Valley Section

The Connecticut Valley Section met jointly with the Connecticut Technical Council, an association of technical societies of Connecticut, at the Connecticut State College on October 17 to inspect the college equipment for engineering instruction and endorse plans for bettering its engineering facilities.

The program included a football game between Connecticut State College and Worcester Polytechnic Institute, an informal dinner which was followed by general speeches, and a meeting of those interested in radio which was held at Beech Hall. M. E. Bond, chairman of the section, presided at this meeting which was attended by fifty-one. D. E. Noble, professor of electrical engineering, described the high-frequency transmitter and antenna system used for relaying programs to the broadcast stations in Hartford. The receiving installation was described by E. R. Sanders of WTIC. The meeting was closed with a trip to the Engineering Building where the transmitter and other equipment were inspected.

The November meeting of the section was held on the 12th at Yale University with Chairman Bond presiding and the attendance was seventy. There were thirty-seven at the dinner which preceded the meeting.

A paper on "Coils and Coil Engineering" was presented by K. W. Jarvis, vice president of the Norwalk Engineering Corporation. In it he discussed radio-frequency coils and some of the difficulties encountered in their design and manufacture. He described and showed samples of a new type of winding which he has developed and which gives improved operation over a bank-wound coil of approximately ten to fifteen per cent in Q and a reduction in distributed capacitance of approximately twenty-five per cent. Winding machines which produce solenoid, universal, or bank-wound coils were described and run at higher speed than most of the existing machines. The control of the number of turns is by photoelectric cells and accurate to within one tenth of a turn. Disks with holes in them are used for this purpose. Two impulses are required to stop the machine; the first applied ten turns from the finish removes the power and the second at the finish stops the machine.

Testing is done at one thousand cycles and at one or two radio frequencies. For the two-frequency test, the frequency is changed automatically. Cathode-ray tubes are used as indicators in matching coils.

Detroit Section

The Detroit Section met on November 20 at Broadcast Station WWJ to hear a paper on "Modern Broadcast Speech Input Equipment" presented by W. L. Black of the technical staff of the Bell Telephone Laboratories. E. C. Denstaedt, chairman, presided and there were 175 present. Thirty attended the dinner which preceded the meeting.

Mr. Black described the construction and operation of modern studio equipment basing his remarks on the installation at WWJ. Reversed feedback in audio-frequency amplifiers to reduce distortion was discussed. It was pointed out that there is a definite limit to the amount of feedback which should be used and that it is not a "cure-all." Its application causes a loss in the gain of the amplifier which may necessitate additional amplifiers which in turn introduce further distortion. Improvements in microphone quality have decreased microphone efficiency in output. The output is approaching the point where noise levels are comparable and an increase of amplifier gain cannot be used. Increased efficiency in high quality microphones would be a valuable improvement.

Emporium Section

The November 6 meeting of the Emporium Section was held in the American Legion Club Rooms and presided over by R. R. Hoffman, chairman. There were fifty-nine present.

J. J. Rogan, patent attorney of New York City, spoke on "Patents and Engineering." He first defined an invention and then illustrated first by showing in a negative manner what did not constitute an invention and then pointing out a number of essentials which an invention must include. Assuming an invention, he then gave the proofs needed and outlined the necessary steps to be taken to secure a patent. The necessity for the keeping of accurate records and the importance of a clear disclosure of the idea to another party was strongly stressed and illustrated by the recital of actual cases. The constitutional basis for patents and their value when granted was discussed and the route followed by a patent application outlined. Chief differences between the United States system and various foreign systems were pointed out. The paper was discussed by Messrs. Abbot, Bachman, Bowie, Kahl, Stringfellow, and Miss Sommers.

A second paper on "Laminated Bakelite" was presented by R. L. Foote, sales manager in the Ohio territory for the Synthane Corporation. He first described artificial resins and outlined their processes of manufacture. Their uses in laminated bakelite were discussed and the difference between this type of bakelite and that found in moulded products pointed out. Physical and electrical properties of laminated bakelite were given and its use in radio discussed. A comparative picture was then drawn of its properties and usefulness in its various forms as compared to those others commonly used in insulating materials. Various forms of laminated bakelite were exhibited and two reels of motion pictures showed the fabrication of the product. The paper was discussed by Messrs. Bachman, Bowie, Kievit, and Rogan.

A second meeting of the Emporium Section was held in November on the 20th at the American Legion Club Rooms. Chairman Hoffman presided and there were fifty-six present.

A paper on "Radio Manufacturing in Europe" was presented by George Lewis, liaison engineer of the International Telephone and Telegraph Company. Mr. Lewis pointed out the prevailing practice of taxing radio receivers in Europe on the basis of the number of tubes. This results in the use of comparatively high Q networks in conjunction with very high impedance, high mutual conductance, and pentode tubes to realize high per stage gain. This makes tube manufacture difficult with correspondingly high shrinkage and unit cost and poor uniformity of product. It was pointed out that receiver design especially as effecting eye appeal is so highly nationalized as to be indicative of the political nationalization which characterizes Europe. There are almost as many types of audio-frequency response systems as there are kinds of accents. A map indicating relative broadcast power saturation for the world was shown and discussed together with tables showing relative saturation for radios, telephones, and pleasure automobiles. Government controlled education by radio programs was discussed and the keen competition for program audiences especially in the field of political propagandizing was pointed out. The paper was concluded with a brief discussion of the relative qualities of the broadcast programs abroad and in the United States and there was a short statement on the use of microwaves for telephone circuits between certain points in Europe. The paper was discussed by Messrs. Abbot, Bachman, Bowie, Carter, Grankvist, Hoffman, Kievit, Miller, Ratchford, Soderback, Wise, and West.

New York Meeting

Three papers were presented at the New York meeting of the Institute held on November 12 in the Engineering Societies Building and presided over by President Hazeltine. The first was on "The Broadcast Organization in Europe" by Raymond Braillard who is chairman of the technical committee and director of the Center of Control of the International Broadcasting Union at Brussels, Belgium. The second paper was on "Theory of the Propagation Electromagnetic Waves Around a Finitely Conducting Sphere" by Balth. van Der Pol, chief of scientific research for N. V. Philips' Radio at Eindhoven, Holland. The third paper, on "The Status of Television in Great Britain" by Noel Ashbridge, chief engineer of the British Broadcasting Corporation, was presented in his absence by L. W. Hayes of the same organization.

The Institute was fortunate in having as its guests a number of outstanding engineers from Europe who were attending the celebrations of the Tenth Anniversary of the founding of the National Broadcasting Company.

The December meeting was held on the second in the Engineering Societies Building and presided over by President Hazeltine.

A paper on "RCA Television Field Test System" was presented by R. R. Beal, chairman of the television co-ordination committee of the Radio Corporation of America. In it he described the experimental high definition television system being tested under field conditions in New York City. The installation comprises a complete complement of facilities with talent and film studios in the RCA Building, Radio City, and with the video and audio transmitter in the Empire State Building. The transmitting system employs the iconoscope as the pickup element, and the receiver, the kinescope as the reproducing element. Pictures were given of the component parts of the installation, the scope of the field work was described, and a summary given of the progress in the several phases of the field work.

Philadelphia Section

On November 5 a meeting of the Philadelphia Section was held in the Engineers Club. There were 200 in attendance and Irving Wolff, chairman, presided.

A paper on "Cosmic-Ray Observations in the Stratosphere" was presented by W. F. G. Swann, director of the Bartol Research Foundation of the Franklin Institute. Particular reference was made by Dr. Swann to the three stratosphere flights in which he and the members of his laboratory participated. The first and third were made under the suspices of the National Geographic Society and the U. S. Army Air Corps. The second was made by Dr. and Mrs. Picard. For all three flights the Bartol Foundation supplied a system of what might be called cosmic-ray telescopes which are pointed in different directions to measure the ray intensity at the various altitudes obtained in the flights.

Most recent observations confirm the conclusions that cosmic-ray intensity in the horizontal direction is abnormally large and while the intensity increases with altitude, above a critical height it diminishes progressively. This is considered to have a very significant bearing upon the nature of the cosmic rays as measured and upon the relation of the primary rays which enter the atmosphere to the secondaries produced therein. Motion pictures of incidents pertaining to some of

the flights were shown. The speaker surveyed the fundamental principles and facts concerned with cosmic rays and their origin. While their origin is not completely known, it is concluded that the rays come from origins far beyond our solar system. The paper was discussed by Messrs. Packard, McIlwain, Murray, and Wolff.

Pittsburgh Section

A meeting of the Pittsburgh Section was held on October 20 at the Carnegie Institute of Technology and attended by twenty-four. B. Lazich, chairman, presided.

A paper on "Developments and Trends of Short-Wave Radio" was presented by Anthony Mag of the radio interference department of the Duquesne Light Company. He summarized the work being done on five-meter receivers. Also, a number of transmitters were displayed. Various types of equipment used in tests between Pittsburgh and Uniontown were described. Several types of antennas were discussed. The paper was discussed by Messrs. Gabler, Mufty, Stark and others.

After adjournment, a demonstration of two-way short-wave radio communication between an automobile and one of the local transmitting stations was given.

The November meeting of the section was held on the 17th at the University of Pittsburgh with Chairman Lazich presiding. The attendance was thirty-three.

A paper on "Visible Transmitter and Receiver Analysis" was presented jointly by J. B. Dearing of the RCA Manufacturing Company and G. A. Scott, professor of physics at the University of Pittsburgh. In it were shown the usefulness of the cathode-ray oscillograph in analyzing receiver and transmitter performance. The oscillograph was first described and its uses outlined. Among the procedures described were the alignment of receivers by use of the variable frequency signal generator, a determination of frequency-response characteristics using a single generator modulated by a beat frequency oscillator, effects of mismatching and mistuning of transmitter tank circuits, and ways of checking percentage of modulation and amplitude distortion. An elaborate setup of equipment was used to illustrate many parts of the paper.

San Francisco Section

Two meetings of the San Francisco Section were held in November. The first on the 4th was in the Auditorium Annex Room of the Telephone Building and attended by twenty. V. J. Freiermuth, vice chairman, presided.

It was devoted to discussions of the two papers which have been

published in the PROCEEDINGS. The first was on the "Design of Doublet Antenna Systems" by H. A. Wheeler and V. E. Whitman and was reviewed by H. G. Blanchard of Stanford University. The second paper was "The Secondary Emission Multiplier—A New Electronic Device" by V. K. Zworykin, G. A. Morton, and L. Malter which was reviewed by R. Bennett, Lieutenant, U. S. Navy.

The second meeting was on the 18th at the University of California and attended by fifty-three. There were ten at the dinner which preceded it. R. D. Kirkland, chairman, presided.

"The Electrical Response of the Hearing Mechanism" was the title of a paper presented by L. J. Black, instructor in electrical engineering at the University of California and W. P. Covell, assistant professor in charge of otological research of the University of California. Illustrations were shown of the anatomy of the ear and curves of the results of experiments in the electrical response of the hearing mechanism in animals. A record was played which was made by using the amplified electrical response in a cat's ear.

The December 1 meeting of the San Francisco Section was held jointly with the American Signal Corps Association. R. D. Kirkland, chairman, presided and there were ninety present. Thirty-nine attended the dinner which preceded the meeting.

A paper on "Lightweight High-Frequency Power Equipment for Driving Miscellaneous Aircraft Units" was the subject of a paper by R. M. Heintz of Heintz and Kaufman. He described aircraft auxiliary power problems and trends. He then described a three-phase four-cylinder gasoline engine-generator unit giving an output of 7.5 kilovolt-amperes at 360 cycles and weighing 145 pounds. Radio transmitters, receivers, and ship telephone communication equipment was then described. A number of pieces of equipment were available for inspection.

As this was the annual meeting, the Institute group held a short business meeting at which V. J. Freiermuth of the Pacific Telephone and Telegraph Company was named chairman; W. N. Eldred of Heintz and Kaufman, vice chairman; and Carl J. Penther of the Shell Development Company, secretary-treasurer.

TORONTO SECTION

There were 105 present at the October meeting of the Toronto Section held at the University of Toronto and presided over by B. deF. Bayly, chairman.

R. A. Hackbusch, chief engineer of Stromberg Carlson Telephone

Manufacturing Company of Canada, presented a paper on "Radio Design Considerations." He introduced the subject by pointing out how all branches of the radio industry were bound together in the common cause of transferring a program from the studio to the listener. Changes in the broadcast spectrum were outlined and the problems created discussed. Statistics were presented showing that the high-frequency bands are not extensively used by the radio listener. The tendency toward the use of ultra-high-frequency bands was based on improvement in quality of transmission and reduced costs of transmitting and radiating systems. Quality of reproduction was next discussed and an attempt made to place a percentage figure on the performance of various systems in relating the frequency band reproduced to a band sufficiently wide to result in imperceptible distortion. The use of methods of avoiding cabinet resonance in loud-speaker systems was covered and the acoustical labyrinth method outlined in detail. A demonstration of high fidelity records was given and the effect of cutting off certain frequency bands demonstrated.

The November meeting of the Toronto Section was held on the 13th and attended by fifty-seven. Chairman Bayly presided and the meeting was at the University of Toronto.

H. S. Knowles, chief engineer of the Jensen Radio Manufacturing Company presented a paper on "New Developments in Loud-speakers." He pointed out that infinite baffles were not the ultimate in obtaining best reproduction in ordinary rooms. Reflected sounds plays a great part in the effect on the listener, which makes important the characteristics of the room. A general impression that a single loud-speaker does not adequately cover the complete audio-frequency range has led to the use of multiple speakers. Some methods improve the effectiveness of the single speaker and increase its frequency range of reproduction The acoustical labyrinth is a tuned sound transmission line attached to the back of the speaker. It is of such dimensions that the desired frequencies leave the port in phase with the waves from the front of the speaker diaphragm.

Two speakers may be used by exciting one 180 degrees out of phase with the other by inserting a low-pass filter section. Also a combination of a large diaphragm speaker and a "tweeter" may be used to increase the frequency range. Equations for designing wide range sound systems were developed from equivalent electrical transmission line equations. When using any of the new systems of coupling it is necessary to construct the cabinet to prevent radiation at spurious frequencies. This is accomplished by damping with absorbing materials.

Personal Mention

E. C. Anderson, formerly with RCA Institutes, has joined the staff of Philco Radio and Television Corporation, Philadelphia, Pa.

J. W. Conklin, previously with RCA Communications, is now on the engineering staff of the RCA Manufacturing Company, Camden, N. J.

J. H. Foley, Lieutenant, U.S.N., has been transferred from the U.S.S. *Humphreys* to the U.S.S. *San Francisco*, basing at San Francisco, Calif.

K. H. Martin, previously with RCA Manufacturing Company, is now a research engineer for First National Television, Inc., Kansas City, Mo.

H. G. Miller, formerly at Kansas State College, has joined the research department of the Philco Radio and Television Corporation, Philadelphia, Pa.

N. S. Neilson, previously at the Billings Polytechnic Institute, has joined the instruction staff of General Motors Institute at Flint, Mich.

L. C. Paslay, formerly on the staff of the Kansas State College, is now president of the National Geophysical Company of Dallas, Tex.

W. B. Wells has been transferred from the Naval Research Laboratory to the Bureau of Engineering, Navy Department, Washington, D. C.

M. P. Wilder, previously with Ken-Rad Corporation, has joined the engineering staff of the RCA Manufacturing Company at Harrison, N. J.

V. J. Andrew has resigned from Doolittle and Faulknor to establish a firm engaged in consulting engineering and the manufacture of broadcast equipment.

T. S. Baker formerly with Press Wireless, Inc., has accepted a temporary appointment at the U. S. Signal Corps at Washington, D. C., as superintendent of radio inspection.

J. R. Bruce has left the Beam Wireless Station at Salisbury, Southern Rhodesia, to join the Eastern Telegraph Company at Ascension Island.

A. P. Dillow of the U. S. Coast Guard has been transferred to the communication base at Curtis Bay, Md.

W. H. Grosselfinger of the Western Electric Company has been transferred from Kearny, N. J., to New York City as sales engineer.

W. S. Harmon previously with Emerson Radio and Phonograph Corporation has been made chief engineer of Mission Bell Radio Manufacturing Company of Los Angeles.

O. C. Maier, Captain, USA, Signal Corps has been transferred from the California Institute of Technology to March Field, Calif.

R. G. Piety has left United Research Corporation to become affiliated with the Independent Research Service Company of New York City.

W. W. Reynolds of the U. S. Coast Guard has been transferred from Washington D. C. to Staten Island, N. Y.

M. Van Voorst, Captain, USA, has been transferred from Fort Monmouth, to the Charlestown Armory, Boston, Mass.

Proceedings of the Institute of Radio Engineers
Volume 25, Number 1, Part 1 *January, 1937*

TECHNICAL PAPERS

PARTIAL SUPPRESSION OF ONE SIDE BAND IN TELEVISION RECEPTION*

By

W. J. Poch and D. W. Epstein

(RCA Manufacturing Company, Inc., Camden, New Jersey.)

Summary—*An experimental and theoretical study was made for the purpose of determining the advisability of operating a television system with the carrier located near one edge of the over-all selectivity curve. Satisfactory results were obtained when operating a television system with the carrier at one edge of the over-all selectivity characteristic.*

Fidelity and phase characteristics were experimentally determined with the carrier located at the center and near one edge of the selectivity curve. Fidelity and delay characteristics were also calculated for various carrier locations on the selectivity curve. Although calculations show that for large percentages of modulation and with the carrier detuned, any detector will reproduce not only the original modulation frequencies but also various combination frequencies, observations on picture quality indicated that the distortion due to linear detection produces no noticeable detrimental effects on the picture quality.

The fact that fewer stages of amplification are necessary in the intermediate-frequency amplifier of the receiver when the carrier is tuned to one edge of the intermediate-frequency selectivity curve makes it very desirable to adopt this system.

Introduction

EARLY television development followed the precedents established in sound broadcasting. A radio carrier was amplitude modulated by the video signals resulting from scanning and the transmission included both side bands. In the receivers the selectivity or band width was made such as to pass both upper and lower side bands when the carrier was modulated with the highest desired modulating frequency. Progress in television development has been marked by a continual increase in the number of scanning lines and requiring, in turn, increases in the communication band. This race, as it became, between the terminal apparatus—ability to increase resolution, i.e., number of lines—and the communication portions of the system—ability to increase band width in the amplifiers and circuits exhibiting selectivity characteristics—first found one element in the lead and then the other. At times when the receiver band-pass characteristics were more limiting than other elements, it was early determined ex-

* Decimal classification: R361 × R583. Original manuscript received by the Institute, November 27, 1936. Presented before Rochester Fall Meeting, Rochester, New York, November 18, 1936.

perimentally that a better picture was obtained when the receiver was slightly detuned. Thus, by detuning, the picture carrier was placed near one edge of the selectivity characteristic.

Later when this condition was more thoroughly appreciated, an analysis was made of its importance and usefulness. Suppose we deliberately design a receiver so the resulting intermediate frequency is placed near one edge of the intermediate-frequency circuit selectivity characteristic and so that carrier and all of one side band but only a small portion of the other side band is accepted, with the over-all selectivity being insufficient to remove entirely the second side band. We shall term this a selective side-band receiver. An immediate advantage is that we nearly double the modulation frequency range that the receiver will pass. This is of great importance where the band width for one side band approaches the limits of circuit and tubes and where it is inadvisable to reduce gain or selectivity.

It is a well-known fact that for circuits passing broad bands, the gain per stage is inversely proportional to the band width. This means that two intermediate-frequency amplifiers having the same number of stages, one for selective side-band and the other for double side-band operation, will have a difference in gain of 2^n, where n is the number of stages. For six stages this means a difference in gain of 64 to 1. If the gain per stage of the selective side-band receivers were eight, the double side-band receiver must have three additional stages to have the same over-all gain.

Before taking the important step of making this change in the receivers, it was thought necessary to make a further investigation of this problem. An experimental transmitter and receiver system, whose condition of operation could be controlled and upon which measurements could be easily made, was set up. This apparatus was arranged so that it would be used either as a double or a selective side-band system with a simple and quick change-over arrangement. It was also arranged so that part of the suppression of one side band was done in the transmitter, to determine whether this would introduce any special difficulties. The data taken on this system were also verified by a mathematical investigation.

Because of the profound influence selective side-band suppression is likely to have on practical systems of television, it is considered of interest and importance to describe these early tests and to outline the mathematical verification.

Apparatus Used in Experimental Work

Fig. 1 is a block diagram of the transmitter and receiver equipment. The only adjustment necessary for changing from double side-band to

selective side-band operation was to shift the master oscillator frequency from 4.25 to 4 megacycles. Suppose that the master oscillator was generating 4.25 megacycles, the condition necessary for normal double side-band operation. The modulator then delivered an 8.5-megacycle modulated carrier at the input of the transmitter intermediate-frequency amplifier. Care had been taken to make the modulation amplifier and the modulator itself with a fidelity characteristic flat to 1000 kilocycles. The output of the intermediate-frequency amplifier, still an 8.5-megacycle carrier but with side bands trimmed to 500 kilocycles on each side, was used to modulate another oscillator operating at 63.5 megacycles. Only the resulting lower side band was

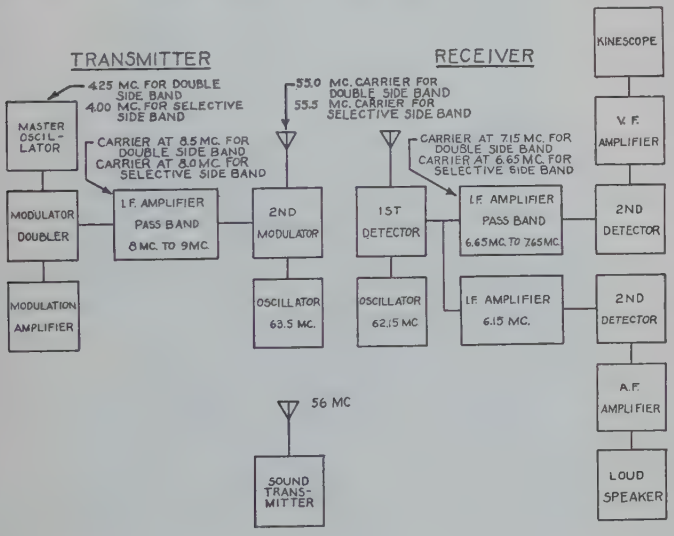
TRANSMITTER
RECEIVER
4.25 MC. FOR DOUBLE SIDE BAND
4.00 MC. FOR SELECTIVE SIDE BAND
53.0 MC. CARRIER FOR DOUBLE SIDE BAND
55.5 MC. CARRIER FOR SELECTIVE SIDE BAND
MASTER OSCIL-LATOR
CARRIER AT 8.5 MC. FOR DOUBLE SIDE BAND
CARRIER AT 8.0 MC. FOR SELECTIVE SIDE BAND
CARRIER AT 7.15 MC. FOR DOUBLE SIDE BAND
CARRIER AT 6.65 MC. FOR SELECTIVE SIDE BAND
KINESCOPE
V. F. AMPLIFIER
MODULATOR DOUBLER
I.F. AMPLIFIER PASS BAND 8 MC. TO 9 MC.
2ND MODULATOR
1ST DETECTOR
I.F. AMPLIFIER PASS BAND 6.65 MC. TO 7.65 MC.
2ND DETECTOR
MODULATION AMPLIFIER
OSCILLATOR 63.5 MC.
OSCILLATOR 62.15 MC
I.F. AMPLIFIER 6.15 MC.
2ND DETECTOR
A.F. AMPLIFIER
56 MC
SOUND TRANS-MITTER
LOUD SPEAKER

Fig. 1

used. This was a carrier at 55 megacycles with side bands extending to 500 kilocycles on both sides. The receiver was also tuned in such a way that the incoming carrier was located in the center of the receiver selectivity characteristic, so that again both side bands were treated alike. The second detector and video frequency amplifier which were adjusted to have a fidelity characteristic good to 1000 kilocycles, brought the modulated signal to the grid of the "kinescope."

Now suppose that the frequency of the master oscillator was shifted from 4.25 to 4 megacycles, the condition for selective side-band operation. The carrier output of the modulator doubler was now at 8 megacycles which brought the carrier to one edge of the transmitter intermediate-frequency pass-band characteristic. The output of this amplifier was still a carrier at 8 megacycles but with the upper side band

extending to 1000 kilocycles and the lower side band greatly attenuated, except at low modulation frequencies. Similarly, in the receiver whose tuning adjustment had not been altered, the carrier was also moved to one edge of the selectivity characteristic, causing one side band to be reduced still more. At low video frequencies normal demodulation of a carrier and both side bands occurred at the second detector. At the higher video frequencies only the carrier and one side

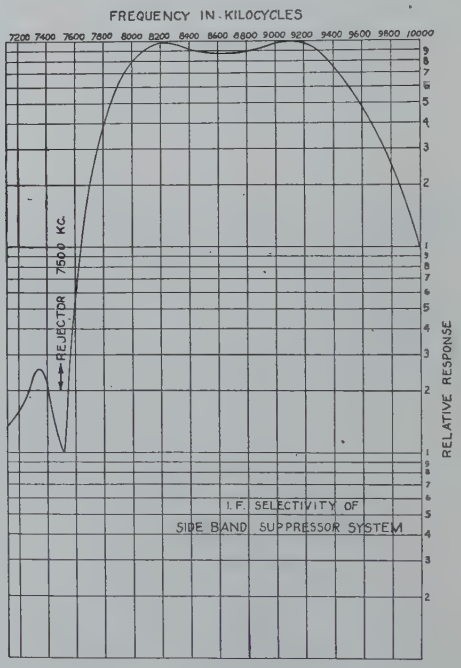
FREQUENCY IN KILOCYCLES
7200 7400 7600 7800 8000 8200 8400 8600 8800 9000 9200 9400 9600 9800 10000
7600 KC.
REJECTOR
RELATIVE RESPONSE
I. F. SELECTIVITY OF
SIDE BAND SUPPRESSOR SYSTEM

Fig. 2

band were present. In between was a range of frequencies in which one side band was being rapidly attenuated. This problem of detection will be discussed in more detail later.

The sound transmitter and the sound channel of the receiver which had a sharp selectivity characteristic compared with that of the picture channel, were used to check the tuning of the receiver. The frequency spacing between picture and sound transmitters was checked by tuning a broadcast receiver to the difference frequency.

Selectivity Measurements

Figs. 2 and 3 show the selectivity characteristics of the transmitter and receiver intermediate-frequency amplifiers. These were taken in

the usual manner with a calibrated oscillator and vacuum tube voltmeter. Rejector circuits were used in both of these amplifiers which increased the attenuation of the unwanted side band. In the receiver, the rejector circuits were tuned to the sound intermediate frequency to prevent interference from the sound transmitter in the picture channel. Note that these curves show a generous 1000-kilocycle band width. An over-all selectivity measurement was not made but should

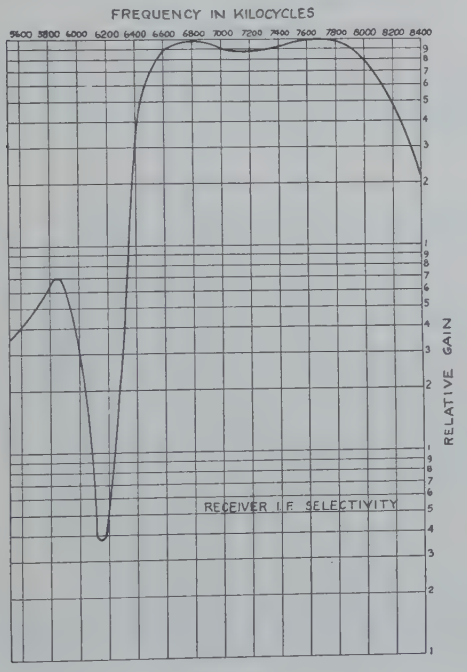

Fig. 3

correspond to the product of the two curves shown since the radio-frequency output circuit at the transmitter and the input system of the receiver did not have sufficient selectivity to affect the other curves.

Measurement of Fidelity and Phase Characteristics

Measurements of fidelity and phase characteristics were made in the video frequency range between 10 and 1000 kilocycles since no effects due to suppressing one side band were found below 10 kilocycles. The fidelity characteristics were taken with a beat frequency oscillator and vacuum tube voltmeter having an upper frequency limit of 1000 kilocycles. A cathode-ray oscillograph also having a 1000-kilocycle frequency range was used in conjunction with the beat

frequency oscillator to obtain the phase characteristics. This was done by the familiar method of connecting the output of the beat oscillator to the horizontal deflecting circuit of the oscillograph and the output voltage of the circuit being tested to the vertical deflecting circuit. From measurements of the resulting ellipse the phase angle between the input and output voltages can be calculated. To avoid wave shape errors, modulation on the transmitter was kept below about 25 per cent. The most desirable characteristics are, naturally, a flat frequency response and the phase shift proportional to frequency.

Fig. 4 shows the resulting fidelity curves. The over-all curve for double side-band operation shows the expected loss in response above 500 kilocycles due to trimming of the side bands. The over-all curve

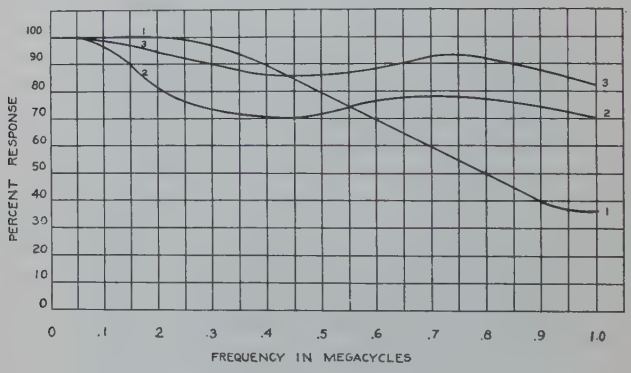

Fig. 4—Measured fidelity.

1. Over-all fidelity double side-band operation.
2. Over-all fidelity selective side-band operation.
3. Picture amplifier fidelity of receiver.

for selective side-band operation is perhaps better than might be anticipated. Since at low modulation frequencies both side bands are present at the second detector and at the higher frequencies only one, we would expect the fidelity curve to drop down approximately 50 per cent at a fairly low frequency and then continue to about double the frequency limit for double side-band operation before dropping down again. This effect, however, is also dependent upon the exact position of the carrier on the edge of the selectivity curve. The farther down we put the carrier on the side of the curve, the less will be the first dip downward in the response curve. It is possible, of course, to carry this procedure so far that the high-frequency response will actually be greater than the low-frequency response. In this particular case, the over-all selectivity curve of the system and the posi-

tion of the carrier relative to it were such that the response curve shown in Fig. 4 was produced.

Fig. 5 shows the phase delay characteristics corresponding to the previous frequency characteristics. The phase shift, as measured by the ellipse method, was converted to phase delay by the following equation:

$$\text{Phase delay} = \frac{\text{phase angle}}{360^\circ \times \text{frequency}}.$$

This expression gives the actual time required for a cycle of a given frequency to go between input and output of the amplifier system being measured. Obviously, if this time is the same for all video frequencies,

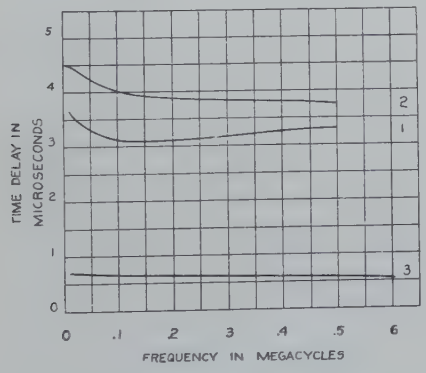

Fig. 5—Measured phase delay.

1. Over-all phase delay using double side-band transmitter.
2. Over-all phase delay using selective side-band transmitter.
3. Receiver picture amplifier alone.

there will be no phase distortion. This condition for a constant phase delay is equivalent to the previously mentioned condition for having the phase shift proportional to frequency. The variation in phase delay over the video-frequency band may be taken as a measure of the phase distortion.

Fidelity and delay characteristics for conditions similar to those in this experimental work were also calculated and are given in the next section.

Calculation of Fidelity and Delay Characteristics

In order to calculate these characteristics it is necessary to know the over-all selectivity and phase characteristics of the system. Accordingly, the selectivity and phase curves for one of the coupling

transformers used in the intermediate-frequency system were calculated. These curves are shown in Fig. 6. Assuming no radio-frequency selectivity and that all the coupling circuits are identical, the selectivity and phase characteristics of the receiver or receiver and transmitter may be deduced from Fig. 6 by merely raising the ordinates of the selectivity curve to the nth power and multiplying the ordinates of the phase curve by n, where n is the number of identical coupling circuits used in the system. Fig. 7 shows the selectivity and phase characteristics for four intermediate-frequency coupling circuits in cascade as

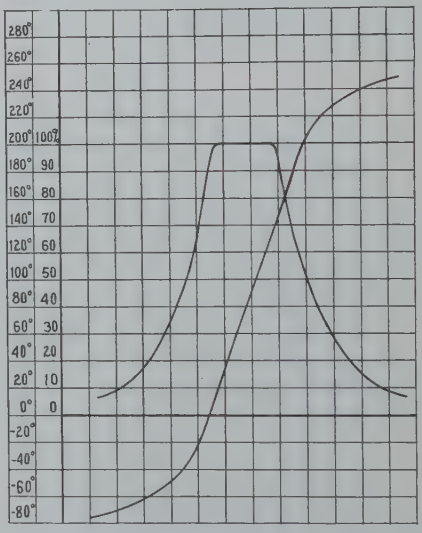

Fig. 6—Selectivity and phase of intermediate-frequency transformer.

obtained from Fig. 6. These curves may be taken as the selectivity and phase characteristics of the receiver or transmitter alone.

Before proceeding with the calculation of the fidelity and delay characteristics as obtained from the selectivity and phase curves of the intermediate frequency, it is worth reviewing, for the sake of clarity, the action of the intermediate-frequency and second detector on a carrier modulated by a single frequency. For this purpose, consider the simple case of a receiver in which the input to the intermediate-frequency amplifier consists of a carrier of frequency f_0 modulated with the video frequency f_1. The input to the intermediate-frequency amplifier may then be written as

$$e = E \cos \omega_0 t + \frac{mE}{2} \cos (\omega_0 + \omega_1)t + \frac{mE}{2} \cos (\omega_0 - \omega_1)t \qquad (1)$$

where $\omega = 2\pi f$, E is the amplitude of the unmodulated carrier, and m is the percentage of modulation. After passing through the selective circuits of the intermediate-frequency amplifier, the voltage output becomes

$$v = E\left[A_c \cos(\omega_0 t + \phi_0) + \frac{mA_u}{2}\cos\{(\omega_0 + \omega_1)t + \phi_u\} + \frac{mA_L}{2}\cos\{(\omega_0 - \omega_1)t + \phi_L\}\right] \quad (2)$$

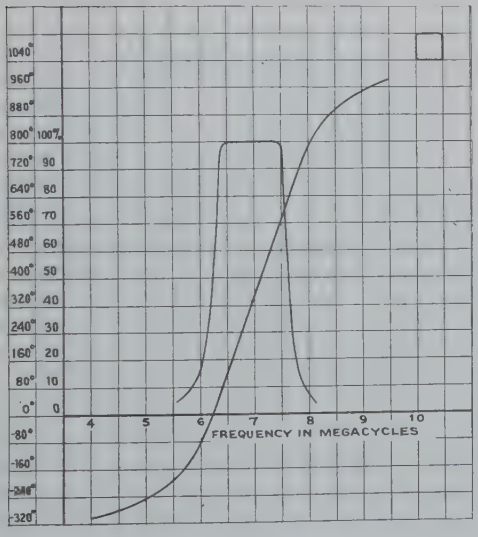

Fig. 7—Selectivity and phase characteristics of the intermediate-frequency amplifier.

where A_c, A_u, and A_L are the amplitude ratios of output to input of the intermediate-frequency amplifier for the frequencies f_0, f_0+f_1, and f_0-f_1, respectively, and ϕ_0, ϕ_u, and ϕ_L are the phase shifts introduced by the selective circuits of the intermediate frequency for the respective frequencies.

Equation (2) gives the input to the second detector The output of the second detector may be obtained by first determining the envelope of the modulated carrier given by (2). To determine the envelope at the input to the second detector it is but necessary to transform (2) into the form

$$v = V_e \cos(\omega_0 t + \phi)$$

and then V_e gives the form of the envelope. Performing this transformation there results that

$$V_e = E\Big[A_c^2 + \frac{m^2}{4}\left\{A_u^2 + A_L^2 + 2A_uA_L\cos(2\omega_1 t + \phi_u - \phi_L)\right\}$$

$$+ mA_c\left\{A_u\cos(\omega_1 t + \phi_u - \phi_0) + A_L\cos(\omega_1 t + \phi_0 - \phi_L)\right\}\Big]^{1/2}. \quad (3)$$

Equation (3) thus gives the shape of the carrier envelope at the input to the second detector.

It is worth noting, in passing, that the phase of the modulated carrier, ϕ, is given by

$$\tan\phi = \frac{A_c\sin\phi_0 + \frac{mA_v}{2}\sin(\omega_1 t + \phi_u) - \frac{mA_L}{2}\sin(\omega_1 t - \phi_L)}{A_c\cos\phi_0 + \frac{mA_u}{2}\cos(\omega_1 t + \phi_u) + \frac{mA_L}{2}\cos(\omega_1 t - \phi_L)} \quad (4)$$

and that in general when one of the side bands is partially suppressed $\tan\phi$ is a function of time so that some phase modulation exists.

Referring to (3) it may be seen that for low percentages of modulation the output of an n-law detector[1] is given by

$$V_e^n = E^n\Big[A_c^n + \frac{nm}{2}A_c^{n-1}\left\{A_u\cos(\omega_1 t + \phi_u - \phi_0) + A_L\cos(\omega_1 t + \phi_0 - \phi_L)\right\}\Big]. \quad (5)$$

Equation (5) shows that for small percentages of modulation the detector will reproduce only the original modulation frequencies. Assuming, therefore, a small percentage of modulation one may, with the aid of (5), calculate fidelity and delay characteristics from the selectivity and phase curves of the intermediate frequency. Thus the output of the second detector at the frequency f_1 is, by (5), proportional to

$$A_u\cos(2\pi f_1 t + \phi_u - \phi_0) + A_L\cos(2\pi f_1 t + \phi_0 - \phi_L)$$

where A_u and A_L are the ratios of output to input amplitudes for the frequencies f_0+f_1 and f_0-f_1, respectively, as obtained from a selectivity curve such as that shown in Fig. 7 and where ϕ_0 is the phase of the carrier and ϕ_u and ϕ_L are the phases for the frequencies f_0+f_1 and f_0-f_1, respectively, as obtained from the phase curve of Fig. 7. Adding the above two terms there results that

$$A_u\cos(2\pi f_1 t + \phi_u - \phi_0) + A_L\cos(2\pi f_1 t + \phi_0 - \phi_L) = V_{f_1}\cos(2\pi f_1 t - \theta)$$

[1] $n=1$ for a linear detector, $n=2$ for a square detector, etc.

where,

$$V_{f_1} = \sqrt{A_u^2 + A_L^2 + 2A_uA_L \cos(\phi_u + \phi_L)} \tag{6}$$

and,

$$\tan\theta = \frac{A_u \sin(\phi_u - \phi_0) + A_L \sin(\phi_0 - \phi_L)}{A_u \cos(\phi_u - \phi_0) + A_L \cos(\phi_0 - \phi_L)}. \tag{7}$$

The fidelity and phase characteristics may then be calculated by using (6) and (7) and the curves of Fig. 7. As was mentioned previously, the phase delay in seconds at any frequency f is $\theta/2\pi f$ where θ is in radians and f in cycles per second.

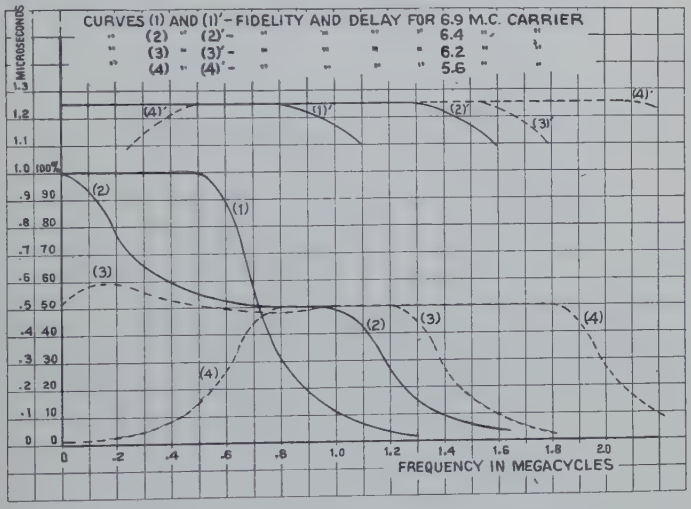

Fig. 8—Fidelity and delay characteristics.

Fidelity and delay characteristics corresponding to various intermediate-frequency carrier frequencies were calculated with the aid of (6) and (7) and are shown in Fig. 8. These fidelity curves correspond to those of a receiver with no radio-frequency detector or video distortion and with the selectivity shown in Fig. 7. Curves (1), (2), (3), and (4) of Fig. 8 correspond to the fidelity of the receiver for intermediate-frequency carrier frequencies 6.9, 6.4, 6.2, and 5.6 megacycles, respectively.

In obtaining Fig. 8 it is assumed that the transmitter passes both side bands. If the transmitter partially suppresses one side band, it may still be assumed that the transmitter passes both side bands but that the receiver selectivity has been increased. Fig. 9 gives the selectivity and phase characteristics corresponding to those of receiver and

transmitter. The fidelity characteristics for such a receiver calculated from Fig. 9 are shown in Fig. 10. Thus Fig. 10 gives the fidelity of a

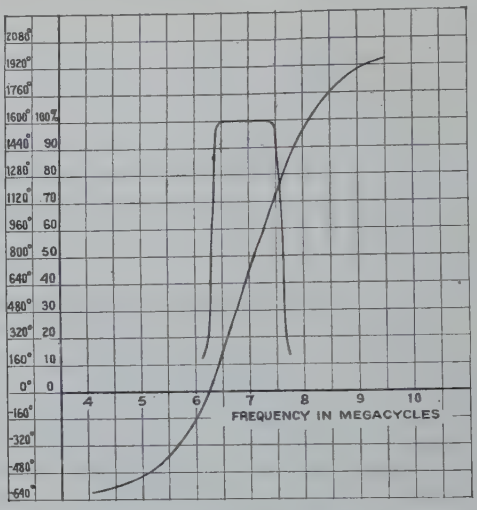

Fig. 9—Selectivity and phase equivalent to that of receiver and transmitter.

receiver having the selectivity shown in Fig. 7 when the transmitter has the same selectivity. Curves (1) and (2) of Fig. 10 correspond to a carrier at 6.4 and 6.25 megacycles, respectively.

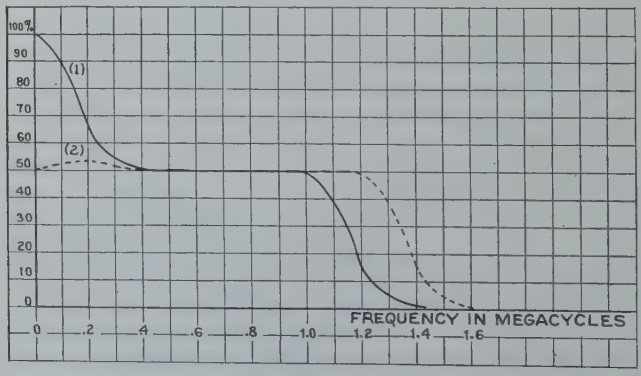

Fig. 10—Curve (1) fidelity for 6.4-megacycle carrier, obtained from Fig. 9. Curve (2) fidelity for 6.25-megacycle carrier, obtained from Fig. 9.

Referring to Fig. 8 it is to be seen that: Curve (1), corresponding to double side-band reception, is practically flat in the frequency range 0 to 0.6 megacycles. No phase distortion is present in the frequency

range 0 to 0.8 megacycles. Curve (2), obtained with the carrier on one edge of the selectivity curve, emphasizes the lower frequencies more than the higher. No phase distortion is present in the frequency range 0 to 1.3 megacycles. Curve (3) is the best fidelity characteristic and is obtained when the carrier (with two side bands) is located halfway down the selectivity curve of Fig. 1. The delay characteristic given by curve (3) of Fig. 8 is flat in the frequency range 0 to 1.5 megacycles, and hence there is no phase distortion, as all frequencies are delayed by the same time. The time of delay is seen to be about 1.25 microseconds. The characteristic is practically flat in the frequency range 0 to 1.3 megacycles. Curve (4) shows the low frequencies badly attenuated. Phase distortion exists for low and high frequencies.

The curves of Fig. 8, therefore, show that with the assumptions made and with the transmitter passing both side bands, it is best to tune in about halfway down on the selectivity curve in order to obtain the optimum fidelity curve with a given selectivity curve of the receiver.

The curves of Fig. 10 similarly show that with the transmitter partially suppressing one side band it is best to attenuate the carrier at the transmitter and receiver so that the total attenuation is down to 50 per cent. Thus if the transmitter attenuates the carrier to 71 per cent and the receiver to 71 per cent of this the result is about 50 per cent. However, as is shown by curve (4) of Fig. 8, the carrier should not be attenuated by transmitter or receiver any further than to 30 per cent, for at 30 per cent and below phase distortion appears. With phase distortion objectionable transients occur.

Results with Picture Modulation

Coming back to the experimental transmitter and receiver setup again, tests were made on the system using picture modulation for both double and selective side-band operation. The previous measurements and calculations should lead us to expect that with selective side-band operation, there should be much better detail due to the additional high-frequency response. At the time these measurements were made, the picture scanning equipment had an upper frequency limit of 500 kilocycles so that when pictures under both conditions of operation were compared, most observers agreed that there was very little difference between the two. Since that time the upper frequency limit of the picture pickup equipment has been increased and the expected increase in detail clearly demonstrated. Changing from double side-band to selective side-band operation, therefore, means an approximately two-to-one improvement in detail which results in a distinctly clearer and sharper picture.

Second Detector Distortion

The conclusions drawn from the calculated fidelity characteristics shown in Figs. 8 and 10 were based on the assumption that the detector distortion is negligible. This was shown to be true for any detector so long as the percentage of modulation is sufficiently small. The conclusions have to be modified when detector distortion with large percentages of modulation is considered.

Referring to (3) it may be seen that for double side-band reception where $A_u = A_L$ and $\phi_u - \phi_0 = \phi_0 - \phi_L$ the form of the carrier envelope becomes

$$V_e = E\left[A_c + mA_u \cos\left(\omega_1 t + \frac{\phi_u - \phi_L}{2}\right)\right] \tag{8}$$

so that a linear detector will introduce no distortion for any percentage of modulation. If one of the side bands, say the lower, is completely suppressed then $A_L = 0$ and (3) reduces to

$$V_e = E\left[A_c^2 + \frac{m^2}{4} A_u^2 + mA_cA_u \cos(\omega_1 t + \phi_u - \phi_0)\right]^{1/2}. \tag{9}$$

Hence, the output of a square detector will be

$$V_e^2 = E^2\left[A_c^2 + \frac{m^2}{4} A_u^2 + mA_cA_u \cos(\omega_1 t + \phi_u - \phi_0)\right] \tag{10}$$

so that no distortion is introduced if a square detector is used. If one of the side bands is but partially suppressed then it follows from (3) that, for high percentages of modulation, there is, in general, no detector which will reproduce only the modulating frequency.

Some estimate of the second detector distortion may be made by assuming that one of the side bands is totally suppressed and that a linear detector[2] is used on the envelope given by (9). Fig. 10 gives the per cent of harmonics introduced by a linear detector as the percentage of modulation[3] is increased. It is seen that the introduction of these harmonics occurring at high percentages of modulation would be objectionable in the case of sound reception. However, in television it is not the frequency *per se* but rather the wave form of the signal that is important. The solid line of Fig. 11 shows a single side-band carrier envelope (the upper half of which is the output of a linear detector) and the dotted line shows the fundamental sine wave. In television reception the two wave forms would appear as practically identical.

[2] 100 per cent modulation means a carrier modulated to 100 per cent with both side bands present.

[3] Since a linear detector is usually used in practice,

In discussing detector distortion for large percentages of modulation it is not sufficient to consider the envelope given by (3), but rather it is necessary to consider the envelope of a carrier modulated with any

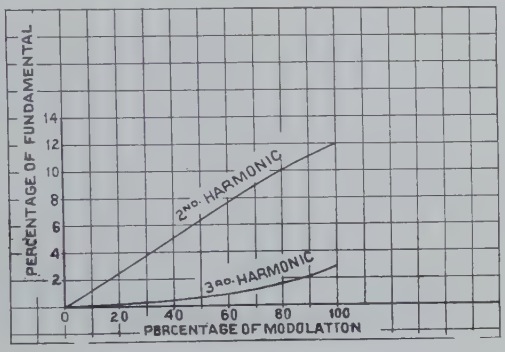

Fig. 11—Variation of harmonic distortion with percentage of modulation.

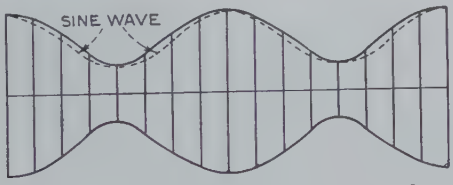

Fig. 12—Single side-band carrier envelope.

number of frequencies. By a method identical with that used in deducing (3) it may be deduced that the envelope of a carrier modulated with n frequencies is at the input to the second detector.

$$
\begin{aligned}
V_e = E\Bigg[& A_c^2 + \frac{m^2}{4}\sum_{i=1}^{n}(A_{L_i}^2 + A_{u_i}^2) \\
& + \frac{m^2}{2}\sum_{i=1}^{n} A_{L_i}A_{u_i}\cos(2\omega_i t + \phi_0 - \phi_{L_i}) \\
& + \frac{m^2}{4}\sum_{\substack{i=1\\ i\neq j}}^{n}\sum_{j=1}^{n}\{A_{L_i}A_{Lj}\cos[(\omega_i - \omega_j)t + \phi_{Lj} - \phi_{L_i}] \\
& + A_{u_i}A_{u_j}\cos[(\omega_i - \omega_j) + \phi_{u_i} - \phi_{u_j}] \\
& + 2A_{L_i}A_{u_j}\cos[(\omega_i + \omega_j) + \phi_{u_j} - \phi_{L_i}]\} \\
& + mA_c\sum_{i=1}^{n}\{A_{L_i}\cos(\omega_i t + \phi_0 - \phi_{L_i}) \\
& + A_{u_i}\cos(\omega_i t + \phi_{u_i} - \phi_0)\}\Bigg]^{1/2}.
\end{aligned}
\tag{11}
$$

It is to be noted that for large percentages of modulation any detector will reproduce not only the original modulation frequencies but also a great many others resulting from various combinations of the modulating frequencies.

With the effect of the second detector in mind, picture signal was again put on the experimental transmitter operating to suppress one side band and effects due to this type of distortion looked for. The picture modulation was increased to a value where saturation in the modulator began to be noticeable. All observers agreed that up to this value of modulation no difference in the picture compared to one at a lower value of modulation could be noticed. This supports the theory that distortion of this type causes no appreciable harmful effect in the picture. It also indicates that the amount and type of distortion which can be tolerated in a picture signal is quite different than that in a sound signal.

Location of the Carrier on the Selectivity Curve

The calculated fidelity curves showed how the over-all frequency characteristic was greatly influenced by the exact position of the carrier at the edge of the selectivity curve. When the carrier was tuned at the 50 per cent response point of the over-all selectivity curve a very good over-all fidelity curve was obtained. At this point, however, the selectivity curve is quite steep and slight variations in tuning cause considerable changes in the over-all frequency characteristic. It also means that to obtain uniform results from a number of receivers their selectivity and tuning characteristics must be held to very close tolerances. We have found that a reasonable compromise is to have the carrier approximately 25 per cent down from maximum response. At this point the selectivity curve has not yet become very steep and the slight drop in high-frequency response can be compensated for in the video-frequency amplifier following the second detector.

Transmitter Considerations

Since the time these measurements and calculations were made a moderate power test transmitter was installed in Camden to provide a signal at a receiver location a mile away. No attempt was made to suppress one side band in the transmitter but all the receivers used with it were of the selective side-band type. Excellent results were obtained with this system and the difference in detail between double side-band and selective side-band operation could be easily demonstrated by tuning from the center to the edge of the receiver selectivity curve. The suppression of one side band at the transmitter becomes a

very difficult problem at the frequencies which are used for television. If this can be successfully done then the band width of one channel for television transmission can be considerably reduced. The power requirements of the transmitter are expected to be approximately the same, whether double side-band or selective side-band operation is used. While the input signal may be thought of as being reduced due to the absence of one side band, the gain in the input circuits can be increased due to the smaller band width necessary. This increases the signal-to-noise ratio on the grid of the first tube which compensates for the loss of one side band.

Conclusion

This investigation has shown that no serious difficulties are encountered when a television system is operated with the carrier at one edge of the over-all selectivity curve. The necessity for fewer stages of amplification in the intermediate-frequency amplifier of the receiver makes it very desirable to adopt this system. In addition to this, if one side band can be suppressed at the transmitter there will be a considerable saving in channel requirements.

Proceedings of the Institute of Radio Engineers
Volume 25, Number 1, Part 1 *January, 1937*

ULTRA-HIGH-FREQUENCY WAVE PROPAGATION OVER PLANE EARTH AND FRESH WATER*

By

R. C. Colwell and A. W. Friend
(West Virginia University, Morgantown, West Virginia)

Summary—*The propagation of 59- to 98-megacycle waves over plane earth and fresh water was measured and a simple equation for the field strength was developed. Propagation over very deep fresh water was found to be no better than that over plane dry earth.*

MANY measurements of ultra-high-frequency wave propagation have been made and checked with optical theory with varying degrees of accuracy.†

While in the process of developing the equipment for other measurements, it was decided to test the devices by making measurements of wave propagation, *near the surface*, over plane earth and fresh water.

The frequency range chosen was 59 to 98 megacycles. The maximum power used was 40 watts input to a $\lambda/2$ vertical rod antenna. The signal strength measuring equipment consisted of $\lambda/2$ rod antenna with either a thermogalvanometer or a crystal detector and a microammeter connected to indicate the current at the center of the antenna. Fig 1(A) shows the circuit diagram for the crystal receiver. The thermogalvanometer may be used in place of the crystal detector.

Using the thermogalvanometer and a calibration chart the field strength was calibrated directly from the receiving antenna current. This method was applicable only for the high field intensity area near the transmitter.

The crystal field strength meter required calibration of the indicated microamperes against the received field strength. This was accomplished for high values of field strength by taking readings on both the thermogalvanometer and the crystal current microammeter at every station. The crystal and its meter were thus calibrated from the thermogalvanometer. In order to calibrate the crystal signal strength a series of readings was taken by starting with a calibrated reading and then reducing the transmitted power to a lower value and calculating the new field strength. When the receiver meter had been calibrated for this field strength, the transmitter power was returned to normal and the receiver was moved away until the field strength was equal to that calculated with the previously reduced power output. The trans-

* Decimal classification: R113.7. Original manuscript received by the Institute July 1, 1936; revised manuscript received by the Institute, August 28, 1936.
† See Bibliography.

mitter power was then lowered again to the value used previously and the new low field strength was used as a lower calibration point for the receiver. This process was continued until the lowest readable field strength for the crystal detector receiver was determined. This was found to be a field strength of about 15 millivolts per meter. A selected commercial type of fixed crystal detector was used; and the calibration has remained constant at normal temperatures for a period of more than one year. Care must be exercised in using the crystal, so as not to overload it in a strong field and burn out the contact point. The best crystal material has been found to be fused silicon.

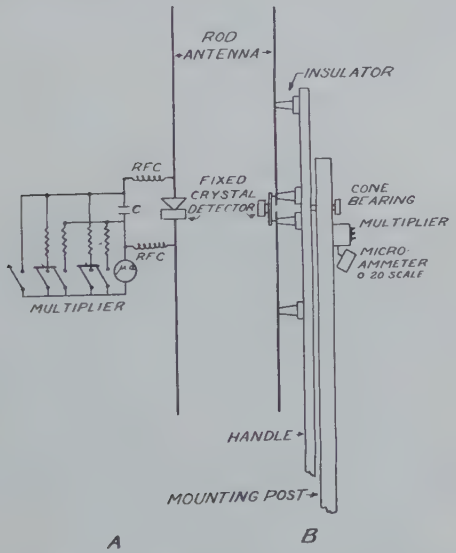

Fig. 1—Signal receiving equipment.

For making the field strength measurements, the $\lambda/2$ transmitting antenna was mounted at a convenient height above the earth (as indicated on the figures showing the attenuation curves) and the $\lambda/2$ receiving antenna was set upon a suitable wooden mounting (Fig. 1 (B)). The transmitter was turned on and allowed to warm up to a stable operating condition, after which it was not changed during the course of a single series of measurements.

The receiving equipment was erected at a series of points along a radial line from the transmitting antenna. The influence of the observer and all other field distorting objects were eliminated by choosing a plane earth surface free from any projecting objects and by having all persons in the vicinity lie flat on the earth at points sufficiently far away from the equipment to eliminate any detectable influence upon the readings. Most of the readings were made by the use of binoculars.

Experimental Results

A composite curve (Fig. 2) of all propagation measurements made on 59 megacycles over plane earth and fresh water was produced by correcting all tests to a condition of transmitting antenna current of fixed value. Similar curves for the higher frequencies (87 megacycles over plane earth and 98 megacycles over fresh water) were plotted together in Fig. 3. It will be noticed that although the waves passing over fresh water were of about ten per cent higher frequency they were

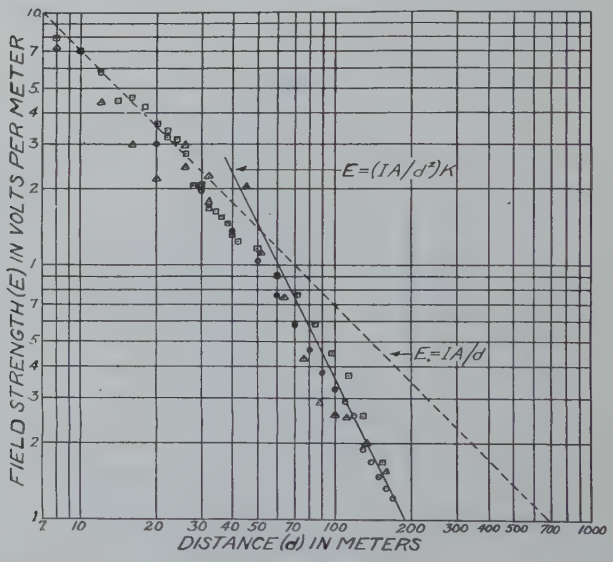

Fig. 2—Propagation of 59-megacycle waves over plane earth and fresh water.
⊙—Airport—damp earth.
⊡—Farm—dry sod.
△—Lake Lynn—deep fresh water.
Antenna heights—$h_1 = 1.6$ meters—$h_2 = 2.1$ meters.

attenuated approximately the same as the lower frequency waves over plane earth. This fact is probably due to *slightly* better propagation characteristics over water. The over-water measurements were made on Lake Lynn (a part of Cheat River). This lake contains fresh mountain stream water.

These propagation curves for various earth conditions and propagation over a short distance are found to agree closely with a curve plotted from an inverse square equation, beyond a distance which makes the ratio of the distance of propagation to the product of the antenna heights sufficiently great (d/h_1h_2 = about 10 or 12). At shorter

distances the inverse distance law for free space propagation is followed. The equation for the field strength in free space condition is the well-known $E_0 = 60\ \pi\ HI/\lambda d$. When a half-wave doublet is used this becomes $E_0 = 60\ I/d$, since $H = \lambda/\pi$; or for any type of antenna we may use $E = IA/d$, letting $A = 60\pi H/\lambda$.

H = the "effective height" of the antenna
I = the transmitting antenna current in amperes
λ = the wave length in meters
d = the distance in meters.

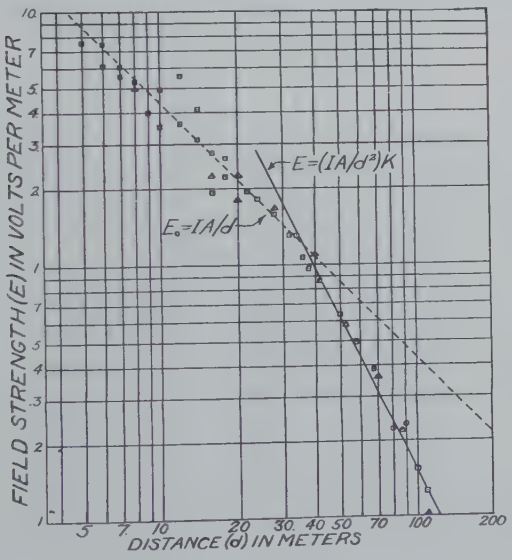

Fig. 3—Propagation of waves.

87 megacycles over plane earth.
98 megacycles over fresh water.
⊡—Farm—dry sod.
△—Lake Lynn—deep fresh water.
Antenna heights—$h_1 = 1.4$ meters—$h_1 = 2.2$ meters.

The equation

$$E_0 = IA/d \qquad (1)$$

has been plotted along with the experimental points of the curves (Figs. 2 and 3) as a dashed line to show the excellent agreement.

At a definite point on each curve it will be noted that an abrupt bend occurs and that a new straight line is followed by the experimental points when plotted on logarithmic paper. An inverse distance squared formula fits this part of the curve very closely.

By merely inserting a constant (K) in the free space equation to

correct for the apparent value of I if we assumed the inverse square law at all distances, and by using $1/d^2$ instead of $1/d$ the new equation may be evolved. This gives

$$E = I\,KA/d^2 \tag{2}$$

for the field strength at any distance (over a plane) from the transmitting antenna, when $d/h_1h_2 > 10$.

The constant (K) may be thought of as being a multiplier for the antenna current (I) to give the value of current (I') which would be required to produce the measured field strength (E) at any distance (d) if the inverse square law extended entirely back to the transmitter. Then,

$$I' = IK. \tag{3}$$

The constant (K) may be determined experimentally by setting up a transmitter with the antenna in the desired location and using an uncalibrated linear field strength meter. The readings will show the free space portion of the curve, and then the inverse distance squared portion. By extending the two straight parts of the curve until they intersect (so that $E_0 = E$), (1) and (2) may be equated to each other at the indicated distance (d). Then $K = d$, the distance in meters to the intersection of the two straight lines. If K is known from the experimental data, the field strength (E) at any distance (d), when $d/h_1h_2 > 10$, may be calculated by substituting the proper value of A, for the antenna, in (3). If a calibrated field strength meter is used to check a few of the experimental field test points the value of A may be determined experimentally for *any* antenna system.

Burrows, Decino, and Hunt have deduced and experimentally verified an equation for the field strength at much greater distances for the conditions which can still be assumed to approximate a plane earth. That equation is

$$E = 240\pi^2 HIh_1h_2/\lambda^2 d^2 \cdot (9) \tag{4}$$

The direct relation of this equation to (2) is at once apparent. Since $A = 60\pi H/\lambda$, K must be equal to $4\pi h_1h_2/\lambda$ *if* (2) and (4) are identical. Either of these equations may be used to plot the curves of Figs. 2 and 3 if the proper earth constants are chosen to obtain H.

Briefly, there has been deduced a simple workable formula for determining field strength at any location, for a given antenna system, and it is quite evident that there is no great difference in the propagation characteristics observed over plane earth and fresh water for the frequencies between 59 and 98 megacycles.

Bibliography

(1). R. L. Smith-Rose, and J. S. McPetrie, *Proc. Phys. Soc.* (London), vol. 43, part 5, no. 240, p. 592, (1931).
(2). G. H. Munro, *J.I.E.E.* (London), vol. 71, no. 426, p. 135, (1932).
(3). L. F. Jones, Proc. I.R.E., vol. 23, pp. 349-368; March, (1933).
(4). B. Trevor and P. S. Carter, Proc. I.R.E., vol. 21, pp. 387–426; March, (1933).
(5). J. C. Schelleng, C. R. Burrows, and E. B. Ferrell, Proc. I.R.E., vol. 21, pp. 427–463; March, (1933).
(6). C. R. Englund, A. B. Crawford, and W. W. Mumford, Proc. I.R.E., vol. 21, pp. 464–492; March, (1933).
(7). C. B. Feldman, Proc. I.R.E., vol. 21, pp. 764–802; June, (1933).
(8). C. R. Burrows, A. Decino, and L. E. Hunt, *Elec. Eng.*, vol. 54, p. 115; January, (1935).
(9). C. R. Burrows, A. Decino, and L. E. Hunt, Proc. I.R.E., vol. 23, pp. 1507–1535; December, (1935).

Proceedings of the Institute of Radio Engineers
Volume 25, Number 1, Part 1 *January, 1937*

COMPARISON OF DATA ON THE IONOSPHERE, SUNSPOTS, AND TERRESTRIAL MAGNETISM*

By

Elbert B. Judson

(National Bureau of Standards, Washington, D. C.

Summary.—*Ionosphere data of the National Bureau of Standards from 1930 to 1935 are compared with data on the earth's magnetic field intensity and sunspot numbers. Seasonal variation of F_2 critical frequency and virtual height are compared with sunspot numbers and magnetic activity. Correlation of annual averages of the ionosphere critical frequencies with sunspot numbers is shown. Variations of midnight F_2 critical frequencies are compared with variations of sunspot numbers and magnetic activity.*

IT has shown[1] that there are relations between variations in radio field intensities and similar variations in sunspot activity and disturbances in the earth's magnetic field. The dependence of long-distance radio transmission upon the ionosphere is well known, and it is therefore of interest to examine the possible relations between ionosphere data and data on sunspot activity and terrestrial magnetism. It is the purpose of this paper to compare ionosphere data obtained at the National Bureau of Standards from 1930 to 1935 with sunspot activity and variations of the earth's magnetic field during the same period.

The theory and method of measurement of ionosphere phenomena have been treated elsewhere.[2,3] There are three principal regions of the ionosphere capable of returning radio waves back to the earth; the E region, about 100 to 120 kilometers in virtual height, the F_1 region, about 200 to 230 kilometers in virtual height, and the F_2 region, about 240 to 500 kilometers in virtual height, depending upon the season and time of day. The presence of the F_1 region is most marked during the

* Decimal classification: R113.5. Original manuscript received by the Institute, September 14, 1936. Publication approved by the Director of the National Bureau of Standards of the U. S. Department of Commerce. Presented before Tenth Annual Convention, Detroit, Michigan, July 3, 1935. Published in *Nat. Bur. Stand. Jour. Res.*, vol. 17, pp. 323–330; September, 1936.

[1] G. W. Pickard, "Correlation of radio reception with solar activity and terrestrial magnetism," Proc. I.R.E., vol. 15, pp. 83–97; February, (1927); pp. 749–766; September, (1927).

C. N. Anderson, "Notes on the effect of solar disturbances on transatlantic radio transmission," Proc. I.R.E., vol. 17, pp. 1528–1535; September, (1929).

L. W. Austin, "Comparison between sunspot numbers, intensity of the earth's magnetic field and strength of radiotelegraphic signals, *Jour. Wash. Acad. Sci.*, vol. 20, pp. 73–74 (1930); and others.

[2] Pedersen, "Propagation of Radio Waves," Chapters V and VI.

[3] S. S. Kirby, L. V. Berkner, and D. M. Stuart, "Studies of the ionosphere and their application to radio transmission," Proc. I.R.E., vol. 22, pp. 481–521; April, (1934). (Also references contained therein.) *Nat. Bur. Stand. Jour. Res.*, vol. 12, pp. 15–51, 1934 (RP632).

summer day. At night the F_1 and F_2 regions combine to form the night F region as shown in Fig. 1.

Two important kinds of data are available for each region from ionosphere measurements; namely, the critical frequency or penetration frequency[4] in the virtual height of the region. From the critical frequency the ionization density is calculated.

The critical frequency of each region has a definite diurnal characteristic. The *E* critical frequency increases rapidly near sunrise and later more slowly to a maximum at noon, decreasing slowly during the afternoon and rapidly near sunset. The F_1 region does not form until

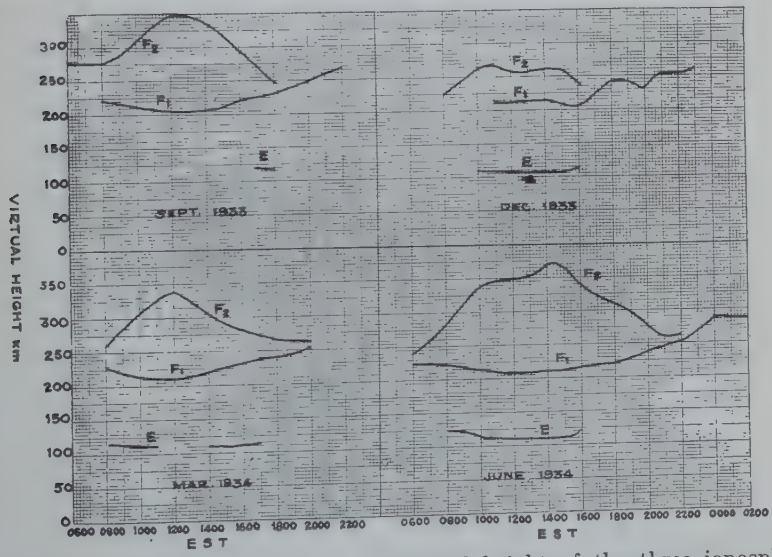

Fig. 1—Average diurnal variation of virtual height of the three ionosphere regions for four seasons.

several hours after sunrise and then f_{F_1} increases slowly to a maximum near noon, decreasing slowly during the afternoon until the F_1 region disappears several hours before sunset. The diurnal curves for f_E and $f^0_{F_1}$ are given in detail by Gilliland.[5] The F_2 critical frequency varies more irregularly than those of the E or F_1 regions. During the winter

[4] The critical or penetration frequency is defined as the lowest radio frequency of a wave which penetrates the region at normal incidence. The critical frequency of the ordinary ray of the F_1 region is referred to as $f^0_{F_1}$. The critical frequency of the ordinary ray of the F_2 is known as $f^0_{F_2}$, and for the extraordinary ray, $f^x_{F_2}$. There is a separation of approximately 800 kilocycles between the critical frequency of the ordinary and extraordinary rays in the F regions. The critical frequency of the E region is given as f_E.

[5] T. R. Gilliland, "Multifrequency ionosphere recording and its significance," *Nat. Bur. Stand. Jour Res.*, vol. 14, pp. 283-303; March, (1935) (RP769); Proc. I.R.E., vol. 23, pp. 1076–1101, September, (1935).

f_{F_2} is highest just after noon and lowest just before sunrise, while during the summer it is highest just about sunset.

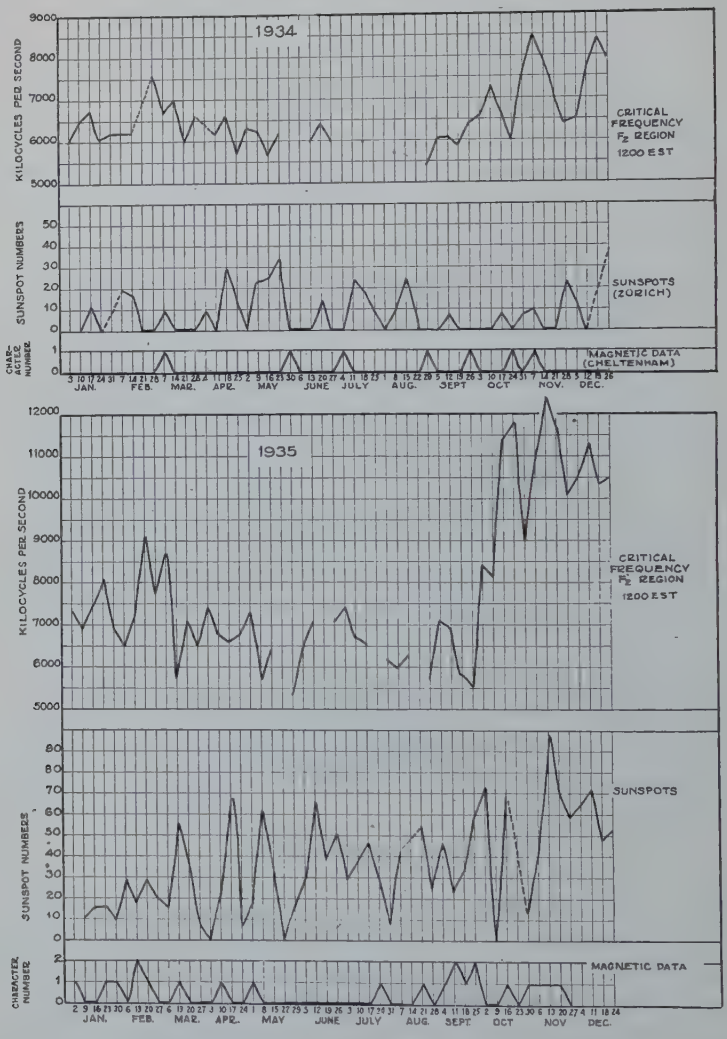

Fig. 2—Comparison of 1934 and 1935 weekly noon F_2 critical frequencies with sunspot numbers and magnetic activity.

Since there is greater variation in the critical frequency and virtual height of the F_2 region than of the other regions, and since there are data available for this region over a longer period of time, this paper deals mainly with the F_2 region.

Noon critical frequency and virtual height measurements have

been made manually once each week in the vicinity of Washington, D. C., since early in 1930. Since May, 1933, automatic multifrequency records have been made hourly in the frequency band 2500–4400 kilocycles. Although more complete and accurate data are available for 1933 and 1935, the earlier data give indications of some value.

Fig. 2 shows weekly noon values of the F_2 critical frequency extraordinary ray during 1934 and 1935, compared with the sunspot numbers and the magnetic character of the days. The sunspot numbers are the Zurich provisional numbers, while the magnetic character number for each day is that reported by the Cheltenham Magnetic Observatory of the U. S. Coast and Geodetic Survey. The noon (1200 E.S.T.) are not necessarily the maximum points of the diurnal curves. They were selected because the majority of observations during 1930, 1931, and 1932 were taken at or near noon. Here the curve for the year 1934 is placed directly above that of 1935 for comparison. The dotted portion of each curve indicates periods when no data were available. The blank spaces in the critical frequency curves represent times when no reflections from the F_2 region were returned, or when the F_2 region was masked by a sporadic E layer.[6]

It will be noticed that the critical frequency values for 1935 were generally higher than for the corresponding time in 1934. Sunspot numbers and magnetic activity were greater in 1935 than in 1934. An examination of the individual days in both years showed no consistent agreement between the curves for the critical frequency and those for the cosmic data. A decrease in critical frequency seemed as likely to happen on quiet days as on magnetically active days. The low values of critical frequency during the summers of 1934 and 1935 and the high values during the winters are indicative of the regular seasonal variation.

Weekly values of noon F_2 critical frequency (extraordinary ray $f^x_{F_2}$) and the virtual height of the F_2 region (for Washington, D. C.) were averaged by months, for September, 1930, to December, 1935, inclusive, and are plotted in Fig. 3. The F_2 virtual heights plotted were those observed between 4000 and 5000 kilocycles. The monthly averages of sunspot numbers and the variations of the horizontal component of the earth's magnetic field are also shown in Fig. 3.

An examination of the critical frequency and virtual height curves shows the marked seasonal variation repeating each year and usually having high daytime critical frequencies around February and another

[6] S. S. Kirby and E. B. Judson, "Recent studies of the ionosphere," *Nat. Bur. Stand. Jour. Res.*, vol. 14, pp. 469–486; April, (1935). (RP780); Proc. I.R.E., vol. 23, pp. 733–751; July, (1935).

in November of each year. Much lower values of critical frequency are obtained during the summer months. It is of interest to note that when the $f^x_{F_2}$ is high the virtual height is low, and vice versa. This condition has also been found to hold for individual days.

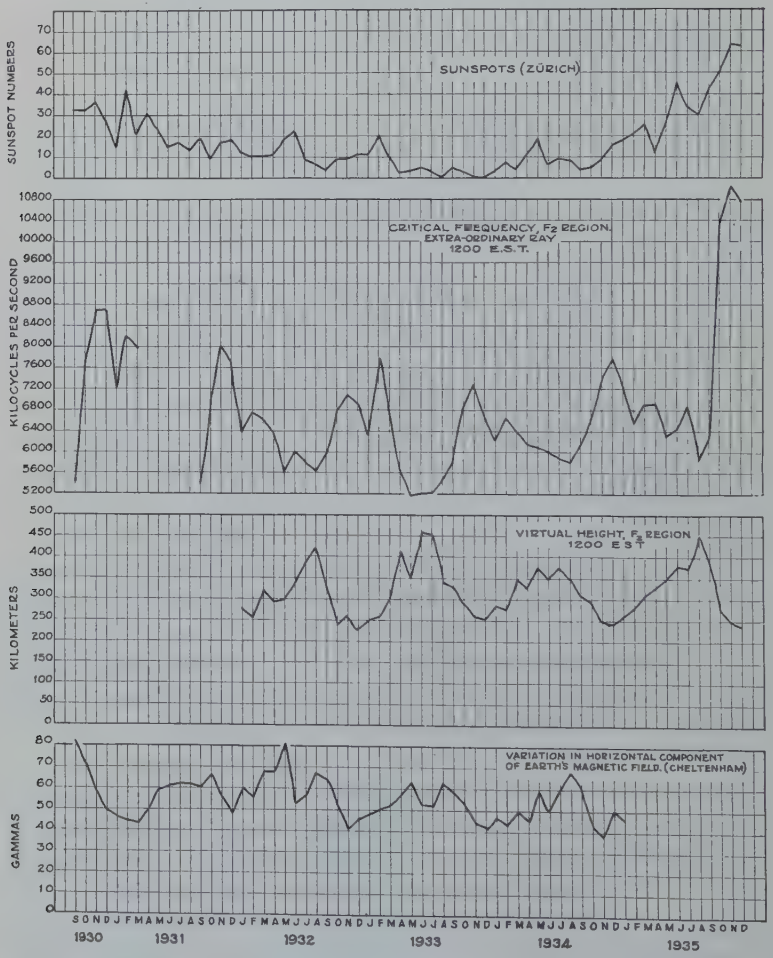

Fig. 3—Seasonal and annual variation of monthly averages of F_2 critical frequency, F_2 virtual height, sunspot numbers, and magnetic activity.

The graph of the variation in the horizontal component of the earth's magnetic field is placed directly below that of virtual height and critical frequency to show the similarity in the seasonal variations. The seasonal curve of virtual heights follows fairly well the seasonal curve of magnetic disturbances. The critical frequency curve and the curve

for the magnetic variations appear to have an inverse relationship. From these comparisons it could not however be concluded that low critical frequencies regularly occur during short periods of pronounced

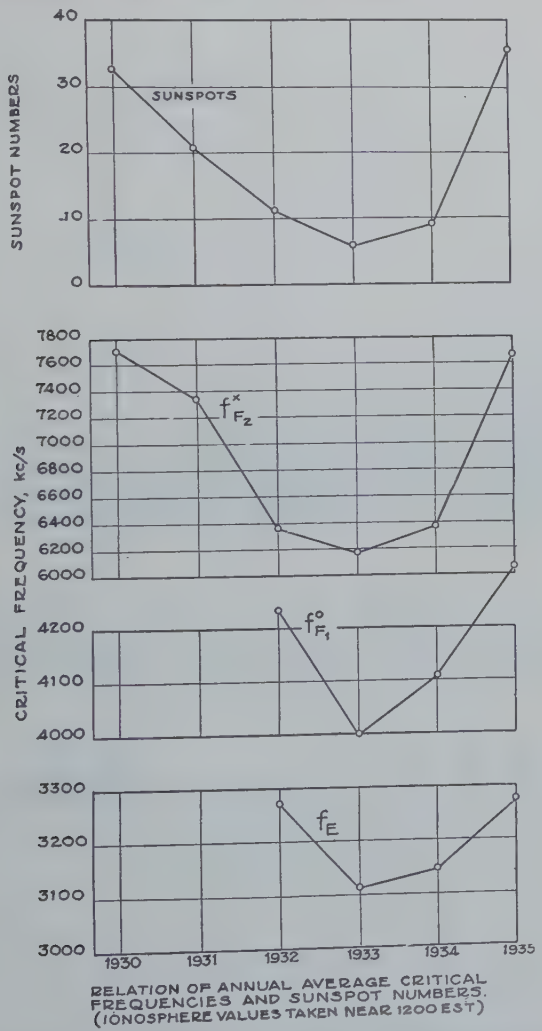

Fig. 4—Annual averages of critical frequencies for the three ionosphere regions compared with the annual average of sunspot numbers.

magnetic activity. A comparison of the critical frequency curve with the average sunspot curve shows no certain correlation between the two phenomena for corresponding months. There is, however, a similar general trend when considering the envelopes of the two curves.

Annual averages of critical frequencies and sunspots were next considered. In Fig. 4 the annual averages of sunspot numbers, the critical frequency (extraordinary ray) of the F_2 region, the ordinary ray of the F_1 region, and the critical frequency of the E region, are plotted for comparison. The sunspot numbers and F_2 critical frequency curves are closely related, reaching a minimum in 1933, and rising rapidly together from 1934 to 1935. The F_1 and E region critical frequencies seem to vary similarly, but the trend is much less pronounced (the ordinates in the figure for F_1 and E are different in scale from those of the F_2).

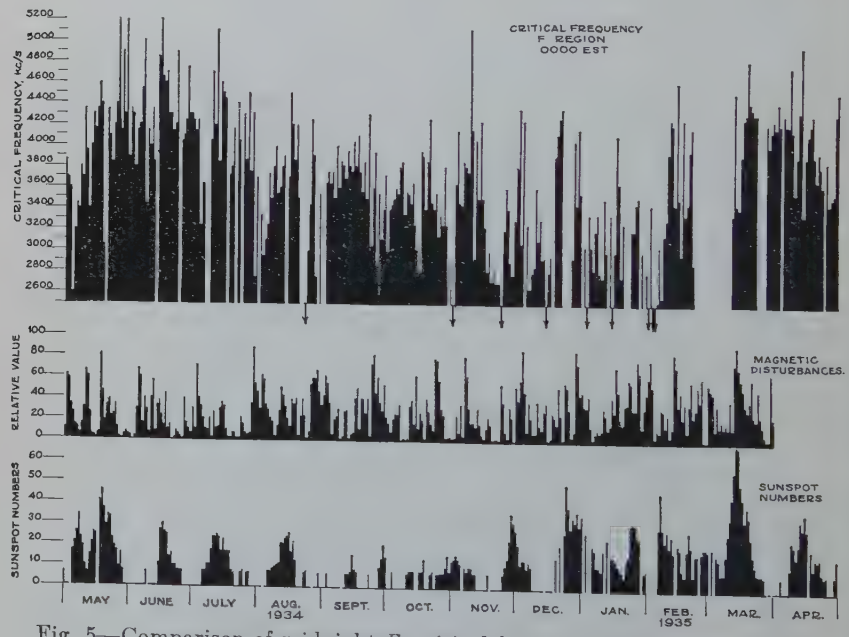

Fig. 5—Comparison of midnight F_2 critical frequency with magnetic disturbances and sunspot numbers.

The correlation of these annual averages is suggestive of the possibility of forecasting the most suitable radio frequencies which might be utilized for communication purposes during certain periods of the sunspot cycle. The maximum frequency which would return to earth would be approximately the value of the critical frequency at normal incidence multiplied by the secant of the angle of incidence.[3] For the F_2 region the maximum value of the secant would be between 3 and 4 depending upon the height of the region above ground.

Records of midnight F region critical frequencies are obtained nightly from a multifrequency automatic recorder developed by Gilli-

land.[7] In Fig 5 these night values are plotted in block form, for one year, May, 1934, to April, 1935, inclusive. For purposes of comparison the magnetic activity and sunspot numbers are plotted in a similar form and placed in a corresponding position under the ionosphere diagram. The magnetic disturbances are taken from the DeBilt magnetic character figures for forty-four different locations through the world. The value for an individual day on the curve in Fig. 5 represents the sum of the DeBilt character figures. The sunspot numbers are the provisional numbers (Zurich) for each day. The F critical frequency shown is for the extraordinary ray. Blank spaces extending to the bottom of the block show that the record was either spoiled or missing. The arrows pointing downward from the bottom of the block show that the critical frequency was below 2500 kilocycles. (2500 kilocycles is the lower limit of frequency of the automatic recorder.)

Comparison of the critical frequency diagram with that for magnetic disturbances shows that in quite a number of instances a drop in the critical frequency happens on a night when there is increased magnetic activity. Best agreement appears in the summer months.

The highest groups of critical frequencies appear to be associated with minimum groups of magnetic activity.

Sunspot numbers show very little correlation with the critical frequency curve.

The seasonal variation for midnight critical frequencies for this particular year shows the values high in the summer and lower in the winter months (November and December, 1934, and January 1935). The low point in sunspot numbers occurred during September, October, and November, 1934.

Values of E and F_1 critical frequencies in general seem to be little if any disturbed with increased magnetic activity. Monthly averages of the F_2 critical frequency show a definite seasonal variation which has repeated since 1930. Two maxima occur in the seasonal curve for each year, approximately in February and November. Low values of f_{F_2} predominate in the summer.

The virtual height of the F_2 region has a seasonal variation inversely related to that of the critical frequency. The height is a maximum in the summer months and a minimum in the winter. Over long periods the values of daytime f_{F_2} are high when the magnetic activity is low and vice versa. The values of daytime F_2 virtual heights are high when the magnetic activity is high and vice versa.

[7] T. R. Gilliland, "Note on a multifrequency automatic recorder of ionosphere heights," *Bur. Stand. Jour. Res.*, vol. 11, pp. 561–566; October, (1933) (RP608); Proc. I.R.E., vol. 22, pp. 236–246; February, (1934).

Comparisons of critical frequency and sunspot numbers on individual days as well as of the monthly averages show no direct relation. Annual averages, however, show a good correlation between the critical frequencies of the ionosphere regions and sunspot numbers. For all regions the annual average critical frequencies were high when the sunspot numbers were high.

Midnight F_2 critical frequencies are often low during periods of high magnetic activity, especially in the summer months; this condition was not found during the winter.

Proceedings of the Institute of Radio Engineers
Volume 25, Number 1, Part 1 *January, 1937*

SIMPLIFIED METHODS FOR COMPUTING PERFORMANCE OF TRANSMITTING TUBES*

By

W. G. Wagener

(RCA Radiotron Division, RCA Manufacturing Company, Inc., Harrison, New Jersey)

Summary—*Simplified methods are given for quickly computing with reasonable accuracy the performance of transmitting tubes in the usual radio-frequency and audio-frequency applications. These applications cover the cases where the current wave shapes within the tube are pulses of current which flow for less than the full cycle.*

The factors controlling the shape of these pulses are discussed and a simplified analysis of the pulses is presented.

The problems of choosing the optimum conditions for a transmitting tube are discussed and the conditions for fully utilizing a tube's capabilities in the different classes of service are presented. These methods are illustrated thoroughly by calculations for a standard transmitting tube.

I. Introduction

IN designing equipment, or in studying the actual performance of existing installations, it is invaluable to have knowledge of the capabilities of the individual component parts. The performance of standard types of transmitting tubes as component parts in the usual power amplifier services can be computed with a very useful accuracy. When the user has the ability to calculate a tube's capabilities and requirements, the design of the associated circuit and equipment becomes definite and straightforward. At the same time, an appreciation of what a transmitting tube should do and why, will aid greatly in analyzing trouble or in clarifying observed behavior in practical installations. Similarly, the attainment of modulation characteristics of greater linearity will be greatly aided by a knowledge of the tube requirements. Fortunately when performance of transmitting tubes in the usual modes of operation is to be calculated, a number of simplifying assumptions are reasonable and justifiable. The accuracy of the results will probably be well within the accuracy with which tube circuit conditions are known and within the reasonable variations of individual tubes from the average of a group.

If a complete and exact computation of any individual tube is desired, an understanding of the simpler methods will indicate just what more thorough mathematical or graphical solutions are needed. These exact solutions may be made readily as an extension of the

* Decimal classification: R253. Original manuscript received by the Institute, September 29, 1936. Presented before Eleventh Annual Convention, Cleveland, Ohio, May 13, 1936.

simplified methods to be presented. However, for more practical purposes the accuracy desired does not justify such exact analysis.

Because all radio-frequency power amplifiers operate in such a manner that plate and grid currents flow for only a fraction of the cycle, the wave forms are not those of simple direct or sine wave currents. It is this complicating factor that has discouraged the application of the standard electrical circuit methods of analysis to transmitting tubes. However, such pulses can be broken down easily into their equivalent direct-current and alternating-current components. All calculations will then follow the familiar simple methods.

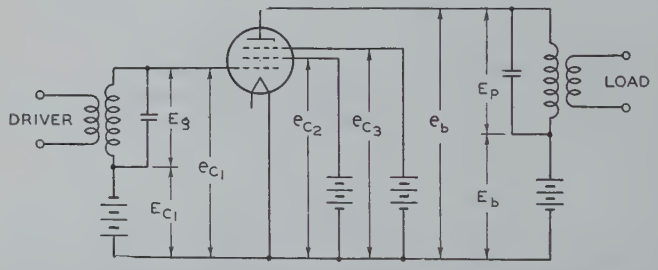

Fig. 1—Schematic radio-frequency power amplifier circuit.

In order to understand the behavior of tubes operated in this manner, it will be necessary to investigate the composition of these pulses of current. In general the principal features that must be known are:

1. The shape of the current pulse.
2. The peak value, or greatest instantaneous current.
3. The direct-current component.
4. The fundamental alternating-current component.
5. The higher harmonic component in cases of frequency multiplication.

II. Factors Controlling the Current Pulse

In order to ascertain the shape of the current pulses, it will be necessary to investigate the action of a typical power amplifier circuit and to see how a vacuum tube will respond to the various voltages acting within such a circuit. Fig. 1 represents a typical radio-frequency power amplifier circuit and indicates the voltages acting on the tube. For completeness a five-electrode tube is shown; for a tetrode or triode analysis, the surplus electrodes are omitted. It is seen that each electrode has a direct voltage applied to it. In addition, the input and output circuits each have a parallel resonant circuit in series with the supply voltages.

Because the resonant circuits store oscillating energy and because this energy is many times the energy extracted each cycle by the loading, the voltages developed across the circuits will be practically pure sine waves over the full cycle. Thus, the control grid and the plate of the tube can be considered as having applied to them by the outside circuit a combined direct voltage and fundamental sine wave voltage.

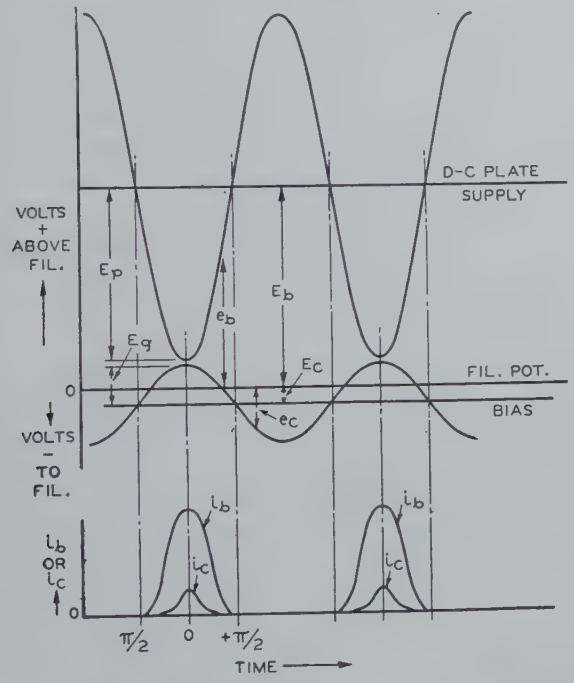

Fig. 2—Typical plate and grid voltages developed in a class C radio-frequency power amplifier, and the resultant tube currents.

In the case of two tubes operated as class B audio-frequency amplifiers, the sine wave analysis is also permissible because the two tubes are known to develop an almost pure fundamental sine wave in the output transformer and to have this voltage applied to the plate of each tube throughout a full audio cycle.

Fig. 2 shows the typical magnitude and phase of the instantaneous plate and grid voltages thoughout a radio-frequency cycle. These voltages acting on the tube cause the pulses of plate and grid current to flow with the shapes as indicated. It will be seen that the plate voltage has a sine wave of peak value (E_p) superimposed on the direct-current component (E_b). The resultant instantaneous voltage is e_b.

Similarly, the instantaneous grid voltage (e_c) is the resultant of a sine wave with a peak value of E_g superimposed on the negative direct-current bias (E_c). The plate current flows as a result of the combined action of these two instantaneous grid and plate voltages (e_c and e_b). As can be seen, the plate current generally flows for less than half a cycle. The grid current flows for a shorter period of time than the plate current.

Aside from the incidental electrostatic capacities of the electrodes which become part of the associated circuit, the vacuum tube is a pure resistive device at all ordinary frequencies and has no reactive impedances. This statement follows logically because the tube does not store appreciable electrostatic or electromagnetic energy. Further, the associated circuits are normally operated close to resonance so that the developed fundamental alternating voltages are in phase with the tube currents. Thus, the problem of the tube and the applied circuits can be treated solely on the basis of pure resistances. At the instant the grid voltage is at its most positive crest, the plate voltage has dropped to its lowest value.

It will now be advisable to see how such voltage combinations, acting on the plate and grid of a tube along with any direct voltages applied to the screen or suppressor, if either is present, will control the flow of plate current. The total space current (i_s) from the cathode emitter depends on the geometry of the tube and the combined effect of the electrode voltages acting in the plane of the control grid as follows:

$$i_s = G\left[e_{c_1} + \frac{e_{c_2}}{\mu_2} + \frac{e_{c_3}}{\mu_3} + \frac{e_b}{\mu_b} \right]^{3/2}$$

where,

e_{c_1} is the control grid voltage.

e_{c_2}/μ_2 is the effect of the No. 2 grid (screen) voltage (e_{c_2}) at the control grid as reduced by the amplification factor (μ_2) of grid No. 1 with respect to grid No. 2.

e_{c_3}/μ_3 is the effect of the No. 3 grid voltage (e_{c_3}) at the control grid as reduced by the amplification factor (μ_3) of grid No. 1 with respect to grid No. 3.

e_b/μ_b is the effect of the plate voltage (e_b) at the control grid as reduced by the over-all amplification factor (μ_b).

This equation assumes that the voltages are sufficiently positive to form no virtual cathode between the control grid and plate. The space current will flow only while the total effective voltage expressed by the brackets is positive.

In the case of a tetrode or a pentode, the factors μ_3 and μ_b are sufficiently large so that the effect of the suppressor voltage and the plate voltage can usually be neglected. Thus, for a tetrode or pentode, the space current is governed almost solely by $e_{c_1}+(e_{c_2}/\mu_2)$. This formula does not cover the case where the suppressor voltage is sufficiently low or negative to control the space current by forming a virtual cathode in the vicinity of the suppressor.

Because the plate current is less than the cathode space current by the current drawn to other grids and is also influenced in a small way by space charges in front of the plate at low plate voltages and by secondary electrons from other grids, the current that reaches the plate seldom follows a three-halves power law and can be represented by

$$i_b = G_1\left(e_{c_1} + \frac{e_{c_2}}{\mu_2}\right)^x \qquad \text{for a multigrid tube}$$

or,

$$i_b = G_1\left(e_{c_1} + \frac{e_b}{\mu}\right)^x \qquad \text{for a triode}$$

where x is an exponent fairly close to 1.0.

As was shown earlier, e_{c_1} and e_b are composite voltages and can be represented by

$$e_{c_1} = E_{c_1} + E_g \cos \omega t$$
$$e_b = E_b - E_p \cos \omega t.$$

The negative sign indicates that the alternating-current plate component is a voltage drop and hence is 180 degrees out of phase with the applied alternating grid voltage. Thus, for a triode,

$$i_b = G_1\left[E_{c_1} + E_g \cos \omega t + \frac{E_b - E_p \cos \omega t}{\mu}\right]^x.$$

The solution for a multigrid tube will not be carried further because it is always a simplification of the triode case. Thus, $(E_b - E_p \cos \omega t)/\mu$ can be replaced by e_{c_2}/μ_2 and will usually have no alternating-current component.

The above equation becomes

$$i_b = G_1\left[E_{c_1} + \frac{E_b}{\mu} + \left(E_g - \frac{E_p}{\mu}\right) \cos \omega t\right]^x$$

or,

$i_b = G_1$ (direct voltage component and alternating voltage component)^x.

If now the direct voltage component is negative, as it is in class

U OF I
LIBRARY

C amplifiers, no current will flow until the alternating voltage component becomes sufficiently positive to overcome the direct component. This action is shown in Fig. 3 where the portion of the cycle during which the resultant effective voltage is positive is indicated by the shaded portion. At the instant the effective voltage rises above the zero effective voltage level and becomes positive, the plate current begins to flow as shown by the typical plate current pulse. The grid current flows over a smaller portion of the cycle because the zero effective voltage level occurs at the plate current "cutoff" point where the

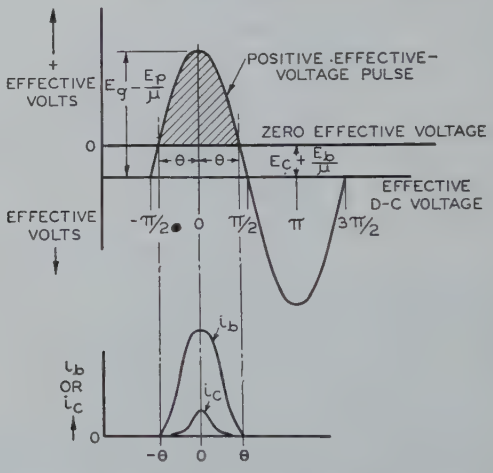

Fig. 3—Resultant effective voltage acting at cathode of tube to cause the flow of space current.

instantaneous grid voltage is always still negative. The grid voltage then rises into the positive region for a shorter duration of the cycle.

Because the alternating-current cycle is represented as a cosine wave, the effective voltage is maximum at $\omega t = 0$. As ωt increases toward $\pi/2$, the zero effective voltage level is crossed at some angle θ each side of maximum. At this point, the value of the cosine wave is just equal to the negative direct-current component and hence

$$\left(E_g - \frac{E_p}{\mu}\right) \cos\theta = -\left(E_{c_1} + \frac{E_b}{\mu}\right)$$

or,

$$\cos\theta = \frac{-\left(E_{c_1} + \frac{E_b}{\mu}\right)}{E_g - \frac{E_p}{\mu}}.$$

Thus, the angle of plate current cutoff (θ) is defined as the angle whose cosine equals the ratio of the direct-current component amplitude to the alternating-current component amplitude. For simplicity, θ will be called the cutoff angle. The plate current flow then occurs over a portion of the cycle equal to 2θ. Similarly, the flow of grid current occurs over twice the angle (θ_{grid}) where

$$\cos \theta_{\text{grid}} = \frac{-E_{c_1}}{E_g}$$

because the alternating-current component ($E_g \cos \omega t$) overcomes the bias (E_{c_1}) at $\omega t = \theta_{\text{grid}}$.

Thus, the angles (θ and θ_{grid}) specify when the resultant effective voltage governing plate current flow, and the actual grid voltage governing grid current flow, become positive. Hence, the plate current flows over 2θ of the cycle and grid current flows over $2\theta_{\text{grid}}$ of the cycle. It remains now to establish the approximate shape of the plate current pulse that must flow between $-\theta$ and $+\theta$ and the grid current pulse that flows between $-\theta_{\text{grid}}$ and $+\theta_{\text{grid}}$. In other words, what is the exponent x in the equation and is it a constant?

III. Shape and Analysis of the Current Pulse

Analysis of several actual plate current pulses, that are typical of the pulses obtained in tubes, shows that although x is not constant it may be treated as practically equal to unity in establishing the ratio of the peak to the direct-current value, and the ratio of fundamental alternating-current component to direct-current component as a function of the angle of flow (2θ). Fig. 4 shows a pure sine pulse with $x = 1.0$ for $\theta = 75$ degrees. The direct-current component and the fundamental alternating-current component (which with the higher order harmonics form the pulse) are also shown. The ratio of the peak to the direct-current value is 3.7 and the ratio of the alternating-current fundamental crest amplitude to the direct-current amplitude is 1.70. The pulses shown by dashes are actual plate current pulses which have been drawn with the same direct-current component and whose alternating-current fundamental is the same within the accuracy of the solid line curve (AC). Note that the maximum values are quite close to the pure sine wave maximum. For comparison the extreme case in which the pulse is a squared sine wave ($x = 2.0$) with the same angle and same direct-current component is also shown in dots. It is interesting to see that the alternating-current fundamental is not widely different. In fact this ratio of alternating-current to direct-current component varies relatively slowly with both θ and x.

Thus, for analysis of the plate current pulse and the plate circuit performance, it is quite reasonable to treat x as 1.0 for the peak, direct-current, and alternating-current values. For x to be unity is the same as ascribing to the tube the quality of linear performance. That this is reasonable is also borne out by the well-recognized experience that class B audio-frequency amplifiers and class B linear power amplifiers can be made to operate with a small degree of distortion. In class B work, the cutoff angle (θ) is constant and linearity is due to the effective first power exponent in the equation relating plate current and effective voltage.

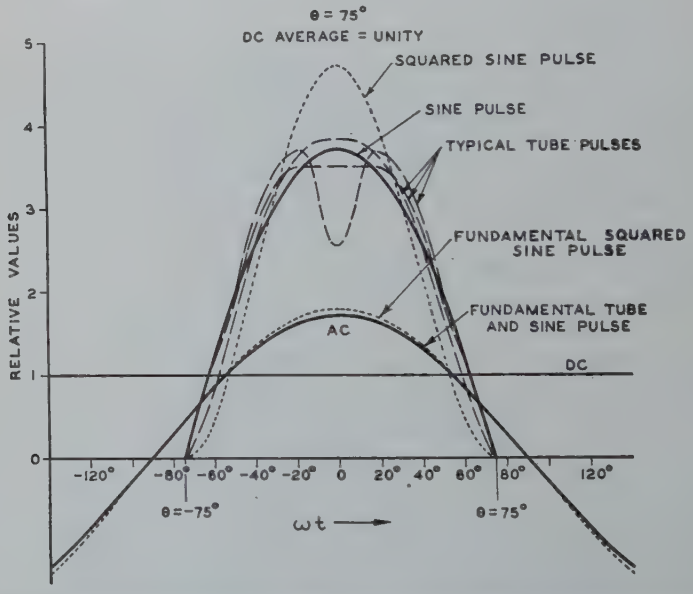

Fig. 4—Typical plate current pulses having the same direct-current values.

Analyses of various pulse shapes as a function of the cutoff angle and degree of linearity of the pulse have been made frequently. Perhaps the most recent and most complete for the immediate purpose of class B and C computations are those made by F. E. Terman and J. H. Fern,[1] and by F. E. Terman and W. C. Roake.[2] The former gives the harmonic components as a function of angle of flow and is valuable for computations of harmonic operation. A solution which is also

[1] F. E. Terman and J. H. Ferns, "The calculation of class C amplifier and harmonic generator performance of screen-grid and similar tubes," Proc. I.R.E., vol. 22, pp. 359-373; March, (1934).

[2] F. E. Terman and W. C. Roake, "Calculation and design of class C amplifiers," Proc. I.R.E., vol. 24, pp. 620-632; April, (1936).

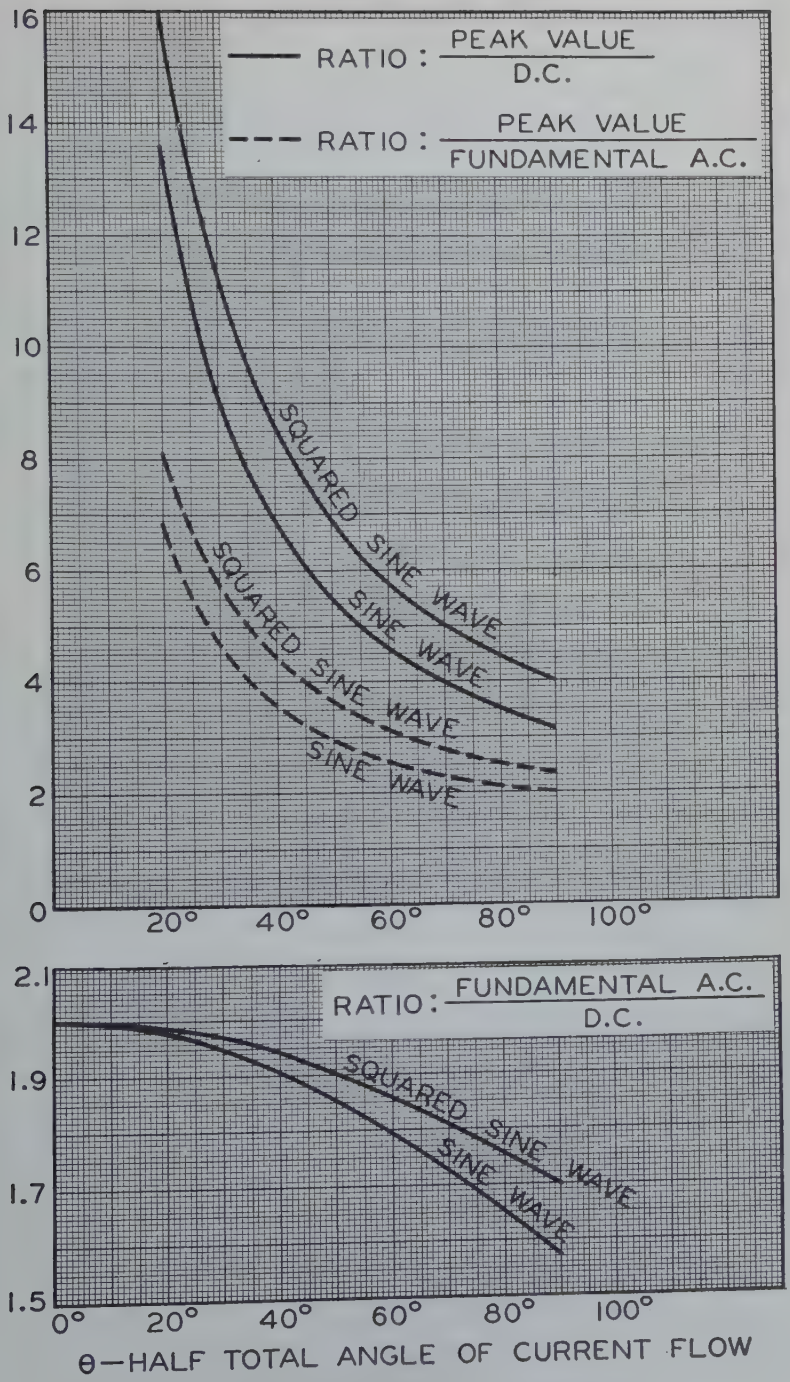

Fig. 5—Principal components of simple pulses.

applicable to class AB work, or to waves with flat tops such as might be obtained with limited emission, has been given by Yuziro Kusunose.[3] For convenience, the curves of the ratio of peak value to direct-current component, peak value to alternating-current component, and the ratio of alternating-current to direct-current component for a cut-off sine wave and a squared cutoff sine wave ($x=2.0$) are given in Fig. 5 as a function of θ. For completeness, the basic formulas for the analysis of these two pulses with all harmonic components are given in the Appendix.

In case the exact graphical or mathematical analysis of these pulses is desired in an individual case, the results may be applied in the same manner in these computations as the results of this simplified analysis. The final results will then be quite accurate because the assumption of the sinusoidal variation of input and output radio-frequency voltage is very reasonable. The analysis of the actual current pulses that would be picked off step by step as indicated in Fig. 8 could be made by a graphical Fourier analysis. A simple way of doing this has been outlined by I. E. Mouromtseff and H. N. Kozanowski.[4]

IV. Optimum Tube Operating Conditions

Now that a full knowledge of the important components of the current pulses expected in a transmitting tube is at hand, it is necessary to determine how such pulses are developed in a tube in order to utilize fully the capabilities of the tube. Because the power in the output resonant circuit is proportional to both the alternating voltage developed across the impedance of this circuit and the alternating-current component of current flow into this impedance, an individual tube's capabilities will be most fully developed when these alternating-current factors are at their maximum values. This brings up the question of the inherent limitations of a vacuum tube which will determine the maximum values of the alternating-current components.

The principal limitations are the maximum voltage that can be applied, the peak value of the current that can be drawn continuously from the emitter, and the maximum power losses that can be permitted within the tube consistent with the full life expectancy of the tube. These values are established by the manufacturers whose experience is incorporated in the ratings given the tube. Thus, a solution that is consistent with the tube requirements and the normal operation as

[3] Yuziro Kusunose, "Calculations on vacuum tubes and the design of triodes," Bulletin No. 237 of the Researches of the Electrotechnical Laboratory, Tokyo, Japan, September, (1928).

[4] I. E. Mouromtseff and H. N. Kozanowski, "Analysis of the operation of vacuum tubes as class C amplifiers," Proc. I.R.E., vol. 23, pp. 752–778; July, (1935).

expected in the hands of qualified persons is given in the maximum rated values of direct plate voltage, direct plate current, direct-current plate power input, plate dissipation, direct-current grid bias, and direct grid current, as listed under the various classes of operation.

It will now be interesting to see what happens in a triode operating as a class C amplifier with a fixed amount of input power (with both E_b and I_b constant), as the plate load impedance is varied. Variation of the load impedance means that the developed alternating plate voltage will vary and that the grid circuit conditions must be adjusted to keep the direct plate current constant. Fig. 6 shows how the power output increases to a maximum and the grid driving current rises very rapidly in the neighborhood of the maximum output region.

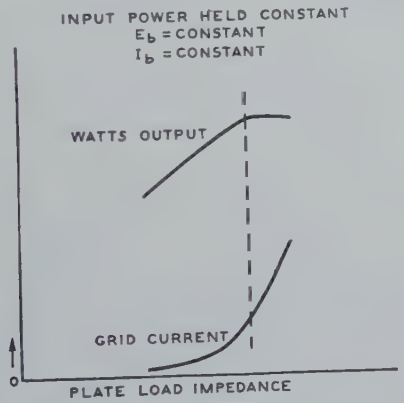

Fig. 6—Power amplifier performance with constant power input.

Thus, an optimum operating impedance is indicated. This optimum operating impedance is the value which develops the maximum output with the lowest grid current and, hence, the lowest driving power.

It is possible to calculate the optimum load impedance from the desired voltage value and current value required in the plate circuit. As explained previously, the maximum or peak value of the current pulse occurs at the instant the grid is at its maximum positive value ($+e_{c\max}$) and the plate voltage is at its minimum value ($e_{b\min}$). This point of maximum current on the static tube curves defines the upper limit of the operating curve which is traced across the static curves during a full radio-frequency cycle. It is point (A) in Fig. 8. From the location of this point in terms of $i_{b\max}$, $e_{c\max}$, and $e_{b\min}$, the full operation of the tube may be forecast.

In the triode, the optimum operating impedance indicated in Fig. 6 corresponds to the impedance necessary to place the maximum

current point at $e_{c\max} = e_{b\min}$. In this region if $e_{b\min}$ is allowed to fall below $e_{c\max}$, no further increase in peak plate current occurs although the grid current rises very rapidly. This is then the point at which the top of the plate current pulse begins to develop depressions or valleys due to the very low value of the instantaneous plate voltage compared to the other voltages in the tube. In a tetrode or pentode, this point may be found by an inspection of the static plate i_b vs. e_b curves in the region of low plate voltage and positive grid voltage, and where a further increase in positive grid voltage does not raise the plate current but only results in an increase of grid current.

Thus, a tube is fully utilized when the largest downswing of plate voltage is developed and when this downswing does not result in a serious dip in the crest value of the plate current pulse. The location of this maximum current point may frequently be varied in individual cases in view of the fact that a small change in plate circuit efficiency results in large changes of grid driving power since the peaks of grid current drawn vary so rapidly at this balance point.

V. Choice of Tube Maximum Current Point and Plate Circuit Analysis

It is the location of the maximum current point on the tube characteristics which is the key to the complete solution of any operating problem. This point can be found directly from the desired or actual operating conditions.

In the first place the power input to the tube is usually known for any application in terms of the plate voltage and plate current. Depending on the type of operation, the operating angle (θ) will be known approximately. From θ the ratio of the peak value of the current pulse to the direct-current component is established and may be found from Fig. 5. This factor times the plate current (I_b) fixes the desired peak plate current. This peak plate current ($i_{b\max}$) is then located on the static curves, and its position fixes the maximum value of the instantaneous grid voltage. The minimum value of the instantaneous plate voltage will also be determined with the choice of this point.

As has been stated for the triode, the location of this point is most favorably fixed in the region where the instantaneous values of grid and plate voltage are about equal. The exact location depends on the amount of grid current one wishes to draw. For the tetrode or pentode, this point is set at the lowest possible value of plate voltage before the individual curves on the i_b vs. e_b characteristics begin to knee over rapidly. Again, the exact point varies slightly with the amount of grid current desired. In a tetrode or pentode, the point lies roughly in

the region in which the minimum value of plate voltage approaches the screen voltage or the positive suppressor voltage, respectively.

From the location of this peak value of plate current on the tube curves, the swing of the plate voltage (E_p) from the direct plate voltage is known. The swing of the positive grid voltage above the filament potential is fixed. From the expression for the cosine of the cutoff angle, the plate voltage components, and the grid swing above filament, it is possible to calculate the required grid bias. Thus,

$$\cos\theta = \frac{-\left(E_c + \frac{E_b}{\mu}\right)}{E_g - \frac{E_p}{\mu}}$$

but,

$$E_g = e_{c\max} + (-E_c).$$

By rearrangement,

$$E_c = \frac{1}{1-\cos\theta}\left[\left(-e_{c\max} + \frac{E_p}{\mu}\right)\cos\theta - \frac{E_b}{\mu}\right).$$

It is now possible to calculate the alternating grid voltage (E_g) as the sum of the absolute values of $+e_{c\max}$ and the negative grid bias.

From the cutoff angle θ, the ratio of alternating fundamental current (I_p) to the direct current (I_b) is known. Hence, I_p is determined. The power output, the power input, and the efficiency may now be computed as follows:

$$\text{Power output,} \quad \text{P.O.} = \frac{I_p}{\sqrt{2}}\frac{E_p}{\sqrt{2}} = 1/2 I_p E_p$$

$$\text{Power input,} \quad \text{P.I.} = I_b E_b$$

$$\text{Plate circuit efficiency} = \frac{1/2 I_p E_p}{I_b E_b}.$$

Thus, the maximum current point is determined and the plate circuit analysis is complete.

VI. Analysis of Grid Circuit

As may be seen by reference to Fig. 2, the rapid rise of grid current produced as the plate voltage swings down in the region of the grid voltage gives the pulse of grid current quite a peaked form. The form of the pulse, as well as its total magnitude, varies rapidly. Such peaked pulses have been found to be fairly close to a squared sine wave form

(exponent equal to 2.0). See Fig. 7, where two sample grid current waves are drawn alongside a squared sine wave of the same peak value and angle of flow. Although this squared sine wave is only an approximation of the exact wave, it is reasonable in view of the rapid variation of the direct grid current with slight changes of adjustments. Hence, the approximation is of real value in estimating the values of direct grid current from the known peak values.

In the complete solution, the total alternating grid voltage swing is known and the direct grid current can be calculated from the peak value reached at the known maximum current point and the ratio of peak to direct current for the angle of grid current flow. The power represented by these values is quite close to the product, $E_g I_c$, where

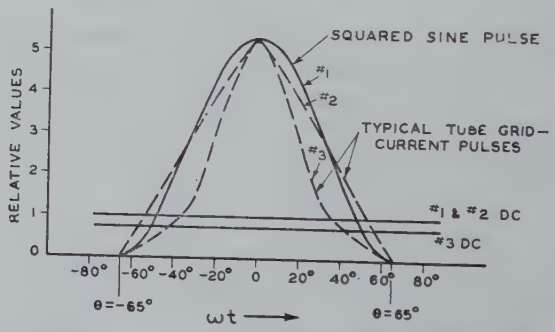

Fig. 7—Typical grid current pulses having the same peak values.

E_g is the crest amplitude of the alternating voltage in the grid circuit, and I_c is the direct grid current. This relation has been demonstrated recently by H. P. Thomas,[5] though he shows that probably $0.9\, E_g I_c$ is a closer approximation. As was pointed out by F. E. Terman,[6] this result follows logically from the fact that practically the whole grid current flows while the alternating grid voltage is near its peak amplitude (E_g).

VII. Typical Tube Performance Calculations

To show the complete calculations for a typical transmitting tube, let us take a type 203-A triode. For class C operation, the angle θ is usually in the neighborhood of 60 to 80 degrees as a practical balance between plate circuit efficiency, grid driving power, and reasonable peak emission requirements of the filament or cathode.

[5] H. P. Thomas, "Determination of grid driving power in radio-frequency power amplifiers," Proc. I.R.E., vol. 21, pp. 1134–1141; August, (1933).

[6] F. E. Terman, "Radio Engineering," p. 234, McGraw-Hill Book Company, Inc., (1932).

1. Calculation of Radio-frequency Power Amplifier

(a). Class C Telegraphy.

In this service, the type 203-A tube has the following maximum ratings:

Direct plate voltage, $E_b = 1250$ volts
Direct plate current, $I_b = 175$ milliamperes
Direct-current plate power input, $P.\ I. = 220$ watts
Direct grid current, $I_c = 60$ milliamperes
Plate dissipation = 100 watts

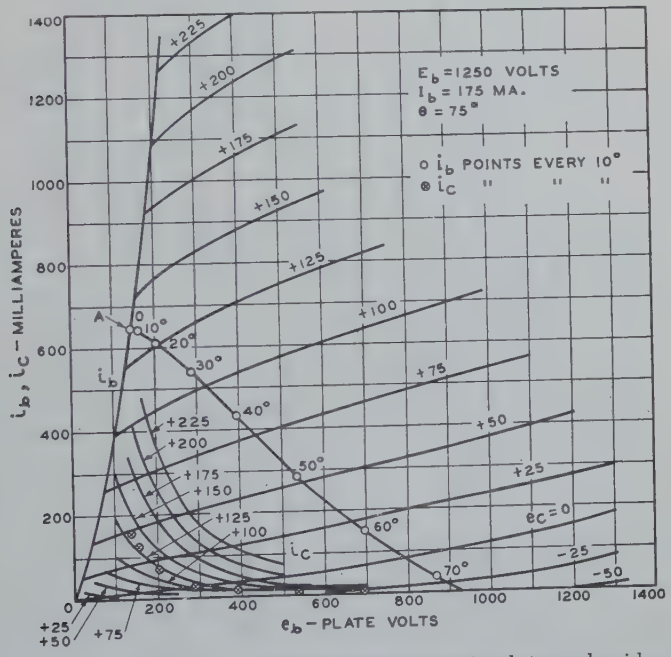

Fig. 8—Typical operating points plotted on static plate and grid curves of a type 203-A tube.

Let us take the following conditions for the computations: $E_b = 1250$ volts, $I_b = 175$ milliamperes, and $\theta = 75$ degrees

The tube maximum current point will be established on the line where $+e_{c\max} = e_{b\min}$. Referring to Fig. 5, at $\theta = 75$ degrees for the sine wave case, it is seen that the ratio of peak to direct-current value ($i_{b\max}/I_b$) is 3.7, and the ratio of alternating-current component to direct-current component (I_p/I_b) is 1.7. Hence,

$$i_{b\max} = 3.7 \times 175 = 647 \text{ milliamperes.}$$

At this point, the voltage requirements are found from the i_b vs. e_b curves of Fig. 8 to be

$$e_{c\max} = 140 \text{ volts, and } e_{b\min} = 140 \text{ volts}$$

Using these voltages, and from Fig. 8, we find $i_{c\max} = 160$ milliamperes. Then,

$$E_p = E_b - e_{b\min} = 1250 - 140 = 1110 \text{ volts}$$

and,

$$E_c = \frac{1}{1 - \cos\theta}\left[\left(-e_{c\max} + \frac{E_p}{\mu}\right)\cos\theta - \frac{E_b}{\mu}\right]$$

$$= \frac{1}{1 - 0.260}\left[\left(-140 + \frac{1110}{25}\right)0.260 - \frac{1250}{25}\right]$$

$$= -101 \text{ volts.}$$

Therefore, the total grid swing is

$$E_g = e_{c\max} + (-E_c) = 140 + 101 = 241 \text{ volts.}$$

As $I_p/I_b = 1.7$, we have

$$I_p = 1.7 \times 175 = 297 \text{ milliamperes}$$

$$\text{P.O.} = 1/2 I_p E_p = 1/2 \times 0.297 \times 1110 = 165 \text{ watts}$$

$$\text{P.I.} = I_b E_b = 0.175 \times 1250 = 219 \text{ watts}$$

$$\text{Efficiency} = \frac{\text{P.O.}}{\text{P.I.}} = \frac{165}{219} = 75 \text{ per cent.}$$

In the grid circuit, we have

$$\cos\theta_{\text{grid}} = \frac{-E_c}{E_g} = \frac{+101}{241} = 0.42$$

$$\theta_{\text{grid}} = 65 \text{ degrees.}$$

From the squared sine wave, wave, $i_{c\max}/I_c = 5.4$. Therefore,

$$I_c = 160/5.4 = 30 \text{ milliamperes.}$$

Grid driving power $= 0.9 \times 241 \times 0.030 = 6.5$ watts.

(*b*). *Class C Telephony, Plate Modulated.*

In this service, the tube is operated in a manner similar to that of the previous class C telegraphy application. However, the plate supply voltage (E_b) instead of being a pure direct voltage has superimposed on it an audio-frequency voltage. The amplitude of the audio voltage

varies with the intensity of the modulating signal. The largest signal that can be superimposed without introducing serious distortion is that whose alternating-current amplitude equals the direct plate voltage. This signal acts to drive the supply voltage up to twice its normal value and down to zero, during the audio cycle.

An idea of the tube capabilities may be obtained by carrying out calculations at the carrier, or zero-modulating signal condition, and at the crest of the cycle of the largest permissible audio signal where the plate voltage has been doubled and the tube conditions are at

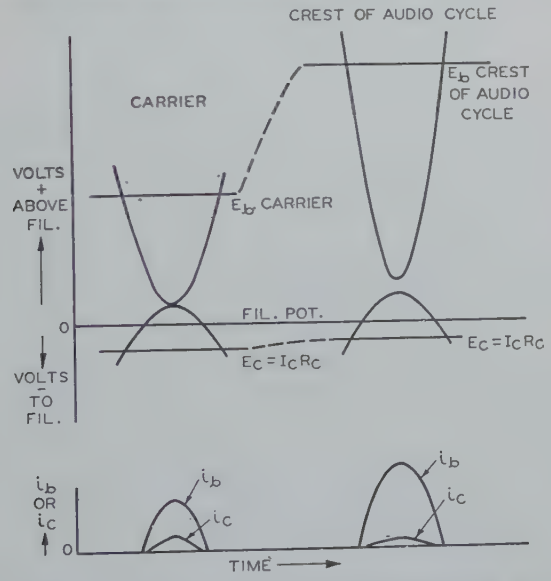

Fig. 9—Typical tube voltages and currents developed in a plate modulated class C radio-frequency power amplifier.

their maximum. These relations are shown in Fig. 9 for the carrier and crest conditions. In this maximum modulation state, the ratio of audio-frequency signal crest amplitude to direct plate voltage supply (E_b) is 1.0. This ratio is the modulation factor.

In order to obtain distortionless modulation, we must have a linear relationship between currents and voltages. Thus, as the plate supply voltage (E_b) is doubled, the radio-frequency output voltage and current must double. Likewise, as E_b is driven to zero, the input and output currents and voltages must fall to zero. Averaged over an audio cycle, however, the direct supply voltage and current (E_b and I_b) remain constant because the superimposed audio variations are symmetrical about the direct-current values. For a modulation factor

of 1.0, the superimposed audio-frequency crest voltage and crest current become equal to the direct supply voltage and current (E_b and I_b). Hence, their root-mean-square values are equal to $E_b/\sqrt{2}$ and $I_b/\sqrt{2}$ and the audio-frequency modulating power required is $1/2\, E_b\, I_b$. Thus, when a tube is being modulated with a modulation factor of 1.0, the total input power is the sum of the direct-current input and audio-frequency input, or $E_b\, I_b + 1/2\, E_b\, I_b$ or $3/2\, E_b\, I_b$. The radio-frequency modulated carrier power also goes up 50 per cent with complete modulation because the energy in the side bands is then 50 per cent of the carrier energy. Since the tube efficiency remains almost constant, the tube plate dissipation losses rise 50 per cent. In order to allow for this level of dissipation, it is necessary for the carrier losses to equal two thirds of the maximum rated dissipation of the tube. These factors have usually been considered in specifying the maximum rated values of a transmitting tube type for different services.

Plate modulated service usually requires a higher grid bias voltage than the unmodulated class C service. This will be seen readily at the completion of the calculations which show that the bias must change with the modulation in the plate circuit. This variation is more easily obtained where it is not too large a fraction of the total bias, and hence it is well to assume a large bias voltage. Such values reduce the total angle of plate current flow and the cutoff angle to less than that for the usual class C telegraph service. Calculations may be made by assuming initially either an operating angle (θ) or a specific value of bias. To demonstrate the latter type of calculation and to assure the large value of bias voltage, these calculations will be made on the basis of an assumed grid bias voltage.

As a plate modulated radio-frequency power amplifier, the type 203-A has the following maximum ratings at the carrier:

Direct plate voltage, $E_b = 1000$ volts
Direct plate current, $I_b = 175$ milliamperes
Direct-current plate power input, $P.I. = 175$ watts
Direct grid current, $I_c = 60$ milliamperes
Plate dissipation = 65 watts (two thirds of telegraph rating)

Let us take the following conditions for the computations:

$E_b = 1000$ volts, $I_b = 175$ milliamperes, and $E_c = -200$ volts

With the bias stipulated, it is necessary to make first an appoximation of θ in order to establish the voltages involved. These voltages will then permit θ to be calculated to a sufficiently correct final value.

Say $\theta = 60$ degrees. From Fig. 5, $i_{b_{max}}/I_b = 4.6$. Hence,

$$i_{b_{max}} = 4.6 \times 175 = 805 \text{ milliamperes.}$$

Assume that the maximum current point is on the line of equal grid and plate voltages. Then, from the i_b vs. e_b curves of Fig. 8, $e_{c_{max}} = +160$ volts and $e_{b_{min}} = 160$ volts. Therefore,

$$E_g = 200 + 160 = 360 \text{ volts}$$
$$E_p = 1000 - 160 = 840 \text{ volts}$$

$$\cos\theta = \frac{-\left(-200 + \frac{1000}{25}\right)}{360 - \frac{840}{25}} = 0.50$$

and,

$$\theta = 60 \text{ degrees}.$$

The original estimate of θ is seen to have been satisfactory.

At 60 degrees, from Fig. 5, $I_p/I_b = 1.79$. Therefore,

$$I_p = 1.79 \times 175 = 313 \text{ milliamperes}$$
$$\text{P.O.} = 1/2 \times 0.313 \times 840 = 131 \text{ watts}$$
$$\text{P.I.} = 0.175 \times 1000 = 175 \text{ watts}$$
$$\text{Plate dissipation} = 44 \text{ watts}$$
$$\text{Efficiency} = 75 \text{ per cent.}$$

At the audio signal maximum (modulation factor of 1.0), the values become for no distortion:

$$E_b = 2 \times 1000 = 2000 \text{ volts}$$
$$E_p = 2 \times 840 = 1680 \text{ volts}$$
$$I_p = 2 \times 313 = 626 \text{ milliamperes.}$$

These values must be attained with the same load circuit impedance and usually with the same grid circuit radio-frequency driving voltage. It is then desirable for the grid bias voltage to be permitted to vary over the audio cycle in order to attain this linear modulation.

At the crest, a trial value of θ is found to be 78 degrees. From Fig. 5, $I_p/I_b = 1.67$, and $i_{b_{max}}/I_b = 3.5$. Therefore,

$$I_b = \frac{I_p}{1.67} = \frac{626}{1.67} = 375 \text{ milliamperes}$$

and,

$$i_{b_{max}} = 3.5 \times 375 = 1310 \text{ milliamperes}.$$

From the crest values, we have

$$e_{b_{min}} = 2000 - 1680 = 320 \text{ volts}.$$

From the i_b vs. e_b curves for $i_{b_{max}} = 1310$ and $e_{b_{min}} = 320$, it is found that $+e_{c_{max}}$ must be 220 volts.

Because E_g is the same as for the carrier condition, the bias voltage (E_c) must be reduced to have $e_{c\max}$ shift from +160 volts at the carrier to +220 volts at the crest of the audio cycle. Therefore, $E_g = 360$ volts $= -E_c + 220$ volts, and $E_c = -140$ volts.

Practically this variation may be obtained quite well by the use of a grid leak resistor to develop the bias voltage. Let us compare the carrier and crest conditions of the grid circuit to see how the bias shifts can occur. The maximum current points to attain this with a given value of grid resistor (E_c) have been found and are given below:

	Carrier	*Crest*	
E_g	360	360	volts
$e^c_{\max}$	+160	+220	volts
E_c	−200	−140	volts
From Fig. 8 at the maximum current point and from Fig. 5			
$i_{c\max}$	220	133	milliamperes
θ_{grd}	56.5	67	degrees
$i_{c\max}/I_c$	6.0	5.2	
I_c	36.6	25.6	milliamperes
R_c	5460	5460	ohms
I_cR_c	−200	−140	volts
Driving power	11.9	8.3	watts

It is seen that as $e_{b\min}$ rises, it must pull away from $e_{c\max}$ so that the peak grid current is reduced; hence, the direct grid current may develop less bias in the grid resistor. It is thus seen that a poor regulation source of bias is desirable for plate modulated telephony. This bias may preferably be a combination of fixed and grid leak bias as is discussed in an article on this subject by I. E. Mouromtseff and H. N. Kozanowski.[4]

(*c*). *Class C Telephony, Grid Modulated.*

In the grid modulated radio-frequency power amplifier, the grid excitation is an unmodulated radio-frequency voltage and the direct-current grid bias has an audio-frequency signal superimposed on it. Thus, for the analysis of a single radio-frequency cycle, the grid bias may be considered to have been shifted by the audio-frequency signal. The analysis is similar to that for class *C* amplifiers except that the carrier maximum current point must be chosen so that sufficient operating leeway is allowed to permit the plate circuit radio-frequency voltage to double at the crest of an audio cycle. In order to assure that the tube will be fully utilized, it is best to make the initial calculations at the crest of the audio cycle.

Fig. 10 shows the developed radio-frequency voltages and the plate and grid circuit current pulses. It should be noted that the direct plate

voltage is the same at both the carrier and crest conditions, and hence the developed plate voltage swing (E_p) at the carrier can utilize only about half the direct voltage. Then, at the crest of the audio cycle when the radio-frequency voltages and currents must be doubled, the plate voltage swing can approach the full direct plate voltage amplitude without driving e_{bmin} down below the instantaneous positive peak grid voltage. The limited plate voltage swing at the carrier means that the radio-frequency output is low and that the plate circuit efficiency is only about half that of a class C telegraph amplifier.

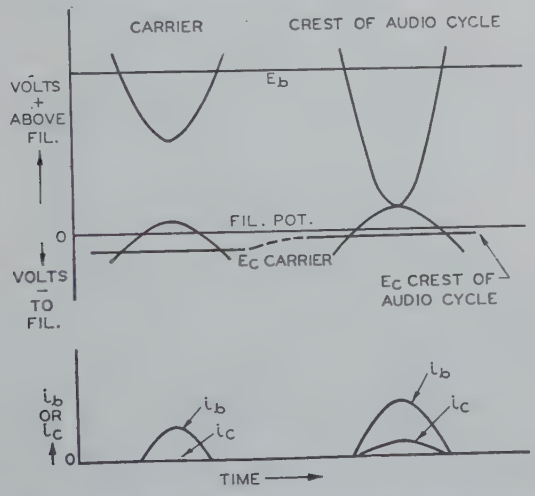

Fig. 10—Typical tube voltages and currents developed in a grid modulated class C radio-frequency power amplifier.

At the crest of the audio cycle, the grid bias (E_c) has been reduced in magnitude to raise the peak grid voltage and to drive a much greater peak plate current through the tube. Let us assume the cutoff angle at this point has increased to 90 degrees. At the crest of the audio cycle, I_b rises to a little more than double.

In class C radio-frequency power amplifier service with grid modulation, the maximum ratings are the same as in class B radio-frequency power amplifier telephony service where the modulation also appears in the grid circuit. For the 203-A, the maximum ratings at the carrier are:

Direct plate voltage, E_b = 1250 volts
Direct plate current, I_b = 150 milliamperes
Direct-current plate power input, P.I. = 150 watts
Plate dissipation = 100 watts.

For 150 watts input, let us take $E_b = 1250$ volts and $I_b = 120$ milliamperes. As I_b more than doubles at the crest of the audio cycle, assume $I_{b\text{crest}} = 270$ milliamperes.

Thus, at the crest, $E_b = 1250$ volts, $I_b = 270$ milliamperes, and $\theta = 90$ degrees. From Fig. 5, $i_{b\max}/I_b = \pi$, and $I_p/I_b = 1.57$. Therefore,

$$i_{b\max} = \pi \times 270 = 848 \text{ milliamperes}$$
$$I_p = 1.57 \times 270 = 424 \text{ milliamperes.}$$

Taking the maximum current point of 848 milliamperes on the line of equal grid and plate voltages from Fig. 8, we have $e_{c\max} = e_{b\min} = 165$ volts. Then,

$$E_p = 1250 - 165 = 1085 \text{ volts}$$
$$E_c = \frac{-E_b}{\mu} \text{ at 90 degrees} = -50 \text{ volts}$$
$$E_g = 50 + 165 = 215 \text{ volts}$$
$$\text{P.O.} = 1/2 I_p E_p = 1/2 \times 0.424 \times 1085$$
$$= 230 \text{ watts at crest of audio cycle.}$$

At the carrier, E_p and I_p must be cut to half values. Therefore, $I_p = 424/2 = 212$ milliamperes, and $E_p = 1085/2 = 542$ volts.

Say $\theta = 65$ degrees as an approximation to determine voltages. From Fig. 5, $i_{b\max}/I_b = 4.2$, and $I_p/I_b = 1.76$. Then,

$$I_b = 212/1.76 = 120 \text{ milliamperes}$$
$$i_b = 4.2 \times 120 = 504 \text{ milliamperes}$$
$$e_{b\min} = E_b - E_p = 1250 - 542 = 708 \text{ volts.}$$

From the i_b vs. e_b curves of Fig. 8, in order to attain $i_{b\max}$ at $e_{b\min} = 708$ volts, $e_{c\max}$ must be $+80$ volts, and $i_{c\max}$ is found to be 25 milliamperes.

Since the radio-frequency grid voltage is constant, $E_g = 215$ volts and since $E_c = -(215 - 80) = -135$ volts, we have

$$\cos\theta = \frac{-(-135) + \dfrac{1250}{25}}{215 - \dfrac{542}{25}} = 0.44$$

and,

$$\theta = 64 \text{ degrees.}$$

This value of θ is in satisfactory agreement with the assumed value.

Then,

$$\text{P.O.} = 1/2 \times 0.212 \times 542 = 57.2 \text{ watts}$$
$$\text{P.I.} = 0.120 \times 1250 = 150 \text{ watts}$$
$$\text{Efficiency} = 38 \text{ per cent}$$
$$\text{Plate dissipation} = 92.5 \text{ watts}$$
$$\cos \theta_{grid} = 135/215 = 0.627$$

and,

$$\theta_{grid} = 51 \text{ degrees.}$$

From Fig. 5, $i_{cmax}/I_c = 6.6$. Therefore,

$$I_c = 25/6.6 = 3.8 \text{ milliamperes.}$$

This current, however, does not indicate the peak driving condition. At the crest, $e_{cmax} = 165$ volts, $e_{bmin} = 165$ volts, and from Fig. 8, $i_{cmax} = 200$ milliamperes. We also find $\cos \theta_{grid} = 50/215 = 0.232$ and $\theta_{grid} = 76.5$ degrees. From Fig. 5, $i_{cmax}/I_c = 4.6$. Therefore,

$$I_c = 200/4.6 = 43.5 \text{ milliamperes.}$$

and,

$$\text{driving power} = 0.9 \times 0.0435 \times 215$$
$$= 8.4 \text{ watts at crest of audio cycle.}$$

Since the bias at the crest is -50 volts, and at the carrier is -135 volts, the audio voltage peak swing must be the difference, or 85 volts. The audio supply must be capable of supplying 43.5 milliamperes of current at the peak and of not distorting under the varying load throughout the remainder of the cycle. The radio-frequency excitation must be 215 volts and capable of good regulation under the varying load. Similarly, the source of carrier bias of -135 volts must be of good regulation because it must pass this same varying grid current.

Over an audio cycle, the direct plate current from the supply rises and falls almost linearly so that the direct-current average is practically equal to the direct plate current drawn at the carrier. Thus, the input power to the plate circuit is practically constant. As modulation occurs, the power in the radio-frequency output increases by the amount of the side-band energy. Since the plate dissipation is the difference of the direct-current input power and the radio-frequency output power, the plate loss is maximum at zero modulation, or under carrier conditions.

(d). Class B Telephony.

This case is very similar to the grid modulated class C power amplifier except that θ is maintained close to 90 degrees. The bias is practically constant at the cutoff point, and the radio-frequency exci-

tation is a modulated carrier whose amplitude varies about the carrier level with the changes in the audio signal. The currents and voltages acting in the tube throughout a radio-frequency cycle are pictured in Fig. 11 and show that the carrier efficiency must be low since only half the available plate voltage swing can be developed at the carrier. Calculations should be made at the crest of the audio cycle to assure that the tube is fully utilized.

This mode of operation is freer from distortion than the grid modulated case since the angle (θ) does not change appreciably throughout the audio cycle. The bias and direct plate voltage remain practically

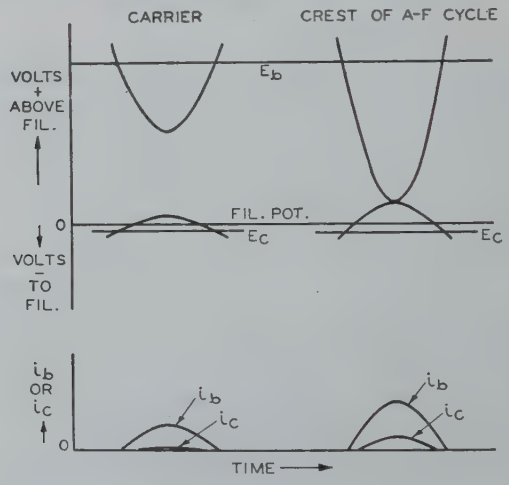

Fig. 11—Typical tube voltages and currents developed in a class B radio-frequency power amplifier (telephony).

constant at values that reduce the effective direct component voltage in the basic equation to approximately zero. Hence, any variation of the alternating-current component cannot change the angle much from 90 degrees.

In this service the maximum ratings for the 203-A at the carrier are:

Direct plate voltage, E_b = 1250 volts
Direct plate current, I_b = 150 milliamperes
Direct-current plate power input, P.I. = 150 watts
Plate dissipation = 100 watts.

Let us take $I_{b\text{at the carrier}} = 120$ milliamperes, and $E_b = 1250$ volts for a carrier input of 150 watts. At the crest, the tube output currents are doubled, and since θ is constant, the input current is also doubled.

At the crest, then, $I_b = 240$ milliamperes, $E_b = 1250$ volts, and $\theta = 90$ degrees. From Fig. 5, $i_{b\max}/I_b = \pi$, and $I_p/I_b = 1.57$. Therefore,

$$i_{b\max} = \pi \times 240 = 755 \text{ milliamperes.}$$

From the i_b vs. e_b curves of Fig. 8, take the maximum current point on the limiting line of $e_c = e_b$. For $i_b = 755$ milliamperes, $e_{c\max} = e_{b\min} = 155$ volts. Then,

$$E_p = 1250 - 155 = 1095 \text{ volts.}$$

At the carrier, $I_b = 120$ milliamperes, $E_b = 1250$ volts, and $\theta = 90$ degrees. So

$$i_{b\max} = \pi \times 120 = 377 \text{ milliamperes.}$$

but,

$$E_p = 1/2 \times 1095 = 547 \text{ volts.}$$

Therefore,

$$e_{b\min} = 1250 - 547 = 703 \text{ volts.}$$

From Fig. 8, at $i_{b\max} = 377$ milliamperes and $e_{b_{\min}} = 703$ volts,

$$e_{c\max} = +60 \text{ volts.}$$

If E_c is adjusted to the cutoff point at the carrier, $E_c = -50$ volts and $E_g = 60 + 50 = 110$ volts. At the crest, E_g must be double and, therefore, $E_g = 2 \times 110 = 220$ volts.

However, it has already been shown that for the required plate current at the crest, $e_{c_{\max}}$ must be $+155$ volts. Thus, $E_c = -(220 - 155) = -65$ volts. This small change in bias from the carrier point is usually made up in the regulation of the bias or excitation sources, since the grid current loading varies greatly over the audio cycle. The resulting crest angle will vary only slightly from 90 degrees.

A tabulation of the grid circuit calculations follows:

	Carrier	*Crest*	
E_g	110	220	volts
E_c	−50	−65	volts
$i_{c_{\max}}$ (from Fig. 8)	20	190	milliamperes
$\cos \theta_{grid}$	$\frac{50}{110} = 0.455$	$\frac{65}{220} = 0.295$	
θ_{grid}	63	73	degrees
$i_{c_{\max}}/I_c$ (from Fig. 5)	5.5	4.8	
I_c	3.6	39.5	milliamperes
R_c (assumed)	420	420	ohms
$I_c R_c$	−1.5	−16.5	volts
$E_{c_{fixed}}$	−48.5	−48.5	volts
$E_{c_{total}}$	−50	−65	volts
Driving power	—	$0.9 \times 0.0395 \times 220 = 7.8$	watts

It should be noted that a very small degree of regulation (due to $R_c = 420$ ohms) in the grid bias supply aids the linearity of performance.

Finally, we have

$I_{p_{\text{carrier}}} = 1.57 \times 120 = 188.5$ milliamperes
P.O. $= 1/2 \times 0.1885 \times 547 = 51.5$ watts
P.I. $= 0.120 \times 1250 = 150$ watts
Efficiency $= 34.4$ per cent
Plate dissipation $= 98.5$ watts.

As in the case of the grid modulated class C amplifier, the plate dissipation is maximum at the carrier, and the direct plate current averaged over the audio-frequency cycle remains constant.

2. Calculation of Class B Audio-Frequency Power Amplifier.

In class B service the operating angle is 90 degrees, and hence a tube carries plate current for 2θ or 180 degrees of the cycle. By using two tubes, one for each half of the cycle, it is possible to obtain the complete sine wave of current. However, the analysis of each individual tube can be made in the manner that has been presented.

At maximum signal, the maximum ratings for each 203-A in this service are:

Direct plate voltage, $E_b = 1250$ volts
Direct plate current, $I_b = 175$ milliamperes
Direct plate power input, $P.I. = 220$ watts
Plate dissipation $= 100$ watts

Let us take $E_b = 1250$ volts, $I_b = 175$ milliamperes, and $E_c = -45$ volts. From Fig. 5, $\theta = 90$ degrees, $i_{b\max}/I_b = \pi$, and $i_{b\max} = \pi \times 175 = 550$ milliamperes. Arbitrarily take $e_{b\min} = 200$ volts. Then, $E_p = 1250 - 200 = 1050$ volts.

Proceeding as for radio-frequency circuits, we have from Fig. 5, $I_p/I_b = 1.57$, and $I_p = 275$ milliamperes. Therefore,

$$\text{P.O.} = 1/2 \times 0.275 \times 1050 = 144.5 \text{ watts}$$

and,

$$\text{P.O.}_{\text{two tubes}} = 2 \times 144.5 = 289 \text{ watts}$$

A simpler and more direct method, however, is to calculate the power output from the sine waves of voltage and current present. The maximum plate current ($i_{b_{\max}}$) calculated above is the amplitude of the full sine wave of current from the two tubes. Since the developed amplitude of the alternating voltage in the plate circuits of the two tubes is a full alternating-current sine wave, the usual alternating-current power computations may be applied. Hence,

$$\text{P.O.} = 1/2\ i_{b_{\max}} \times E_p$$
$$\text{P.O.}_{\text{two tubes}} = 1/2 \times 0.550 \times 1050 = 289 \text{ watts}$$

and the total power input is

$$\text{P.I.}_{\text{two tubes}} = 2 \times 0.175 \times 1250 = 438 \text{ watts.}$$

Therefore,

$$\text{efficiency} = 66 \text{ per cent.}$$

Some confusion is apt to occur in the detailed analysis of two tubes operating in class B due to the fact that they are not operated at complete cutoff with zero signal and to the fact that the tubes interact through the common magnetic circuit of the output transformer. Thus, for small signals the tubes operate as push-pull class A amplifiers, with large signals as class AB push-pull amplifiers, and with very large signals almost as pure class B amplifiers.

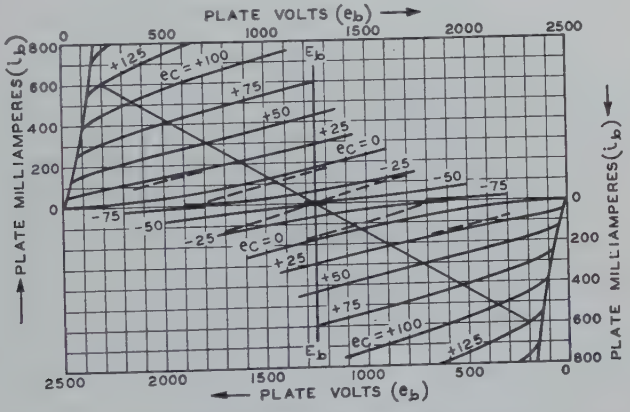

Fig. 12—Composite plate characteristic for combined tubes and transformer as used in class B audio-frequency power amplifier under the following conditions: $E_b = 1250$ volts, $E_c = -25$ volts, and $I_b = 175$ milliamperes.

This confusion can be completely dispelled by referring to the graphical method outlined by B. J. Thompson.[7] In this method the static i_b vs. e_b curves of the two tubes are placed so as to form a composite plate circuit characteristic curve of the combined tubes and transformer, as reproduced in Fig. 12. Operation of the 203-A's at $E_c = -25$ volts has been chosen for the illustration. Because the plate currents from the two tubes flow through opposite halves of the output transformer, their magnetizing forces cancel and only their differences act usefully in the secondary output. Hence, the composite plate circuit curves for corresponding signal grid voltages are formed from the differences of the plate currents and are shown as broken lines.

[7] B. J. Thompson, "Graphical determination of performance of push-pull audio amplifiers," Proc. I.R.E., vol. 21, pp. 591–600; April, (1933).

Thus, the analysis of the output from the standpoint of two tubes is complete when the operating load line is a straight line drawn on these composite curves. The analysis of the currents in a single tube must be taken from the single tube curves with the voltages obtained from the composite curves.

From the composite curves, it is easily seen that the required load resistance value for each tube is

$$\frac{E_b - e_{b_{\min}}}{i_{b_{\max}} - 0} = \frac{E_p}{i_{b_{\max}}}.$$

Hence, for this case,

$$R_{p_{\text{per tube}}} = \frac{1050}{0.550} = 1910 \text{ ohms}.$$

On the per tube basis again, and from Fig. 8, we find $e_{c_{\max}} = +115$ volts, and $i_{c_{\max}} = 80$ milliamperes. Then,

$$E_g = -(E_c) + e_{c_{\max}} = 45 + 115 = 160 \text{ volts}$$
$$\cos \theta_{\text{grid}} = 45/160 = 0.272$$
$$\theta_{\text{grid}} = 74 \text{ degrees}.$$

From Fig. 5, $i_{c_{\max}}/I_c = 4.8$. Therefore,

$$I_c = 80/4.8 = 16.7 \text{ milliamperes}.$$

We have, then,

$$\text{average driving power}_{\text{ per tube}} = 0.9 \times 0.0167 \times 160$$
$$= 2.4 \text{ watts}$$
$$\text{average driving power}_{\text{ two tubes}} = 4.8 \text{ watts}.$$

In order to understand the grid circuit requirements, it is advisable to plot a curve of instantaneous i_c values. This curve for the 203-A analysis is shown in Fig. 13. On this curve are also shown the values of plate output, power input, and plate dissipation averaged over a full audio cycle and plotted against peak signal amplitude. It is essential to note that the maximum plate dissipation occurs at a signal less than the maximum.

VIII. Conclusion

In conclusion it is seen that the performance of vacuum tubes in power amplifier service can be computed in a straightforward manner. The requirements for linear modulation have been indicated and the application of these requirements demonstrate why in grid modulation

the plate efficiency of the tube must inherently be low. From a study of the conditions to be met at the carrier and at the crest of the audio cycle, the importance of the amount of regulation of the various voltages and power supplies can be seen.

The results of these simplified computations should indicate what items are important in obtaining the most satisfactory results from transmitting tubes. Of course, the best way to study the practical overall modulation characteristics of a power amplifier system is to use an

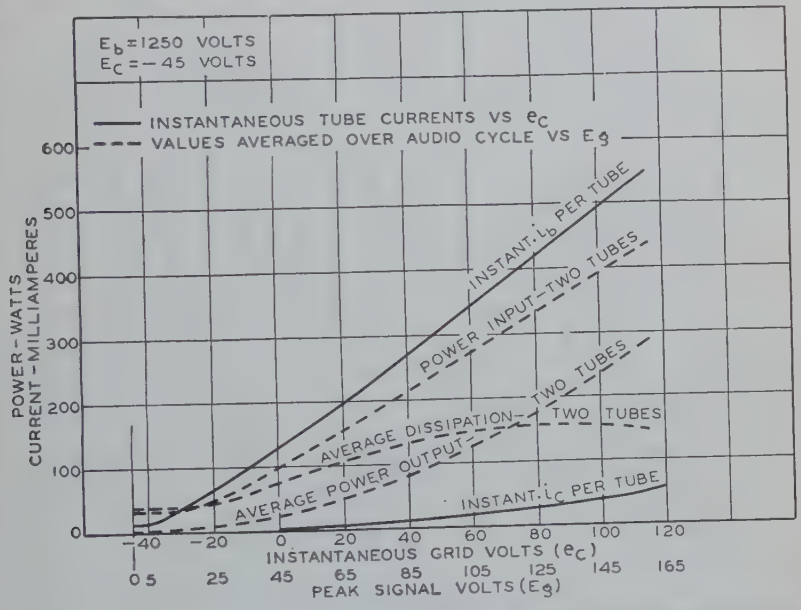

Fig. 13—Instantaneous current curves of a class B alternating-frequency power amplifier and power performance curves vs. signal amplitude.

indicating device such as a cathode-ray oscillograph. To interpret and control the results, however, it is always well to be able to estimate the relative importance and effects of the factors influencing performance.

Appendix

1. Results of Fourier Analysis of Simple Pulses.

(a). Sine Wave Pulse.

$$\text{Current pulse} = i = \cos \omega t - \cos \theta$$

where positive current flows during each cycle between $\omega t = -\theta$ and $\omega t = +\theta$.

$$\text{Direct-current component} = 1/\pi\ (\sin\theta - \theta\cos\theta)$$

$$\text{First harmonic} = 1/\pi\ (\theta - 1/2\sin 2\theta)\cos\omega t$$

$$n\text{th harmonic} = \frac{1}{\pi}\left[\frac{\sin(n+1)\theta}{n+1} + \frac{\sin(n-1)\theta}{n-1} - \frac{2}{n}\cos\theta\sin n\theta\right]\cos n\omega t.$$

(*b*). *Squared Sine Wave Pulse.*

$$\text{Current pulse} = i = (\cos\omega t - \cos\theta)^2$$

where positive current flows during each cycle between $\omega t = -\theta$ and $\omega t = +\theta$.

$$\text{Direct-current component} = 1/2\pi\ (\theta - (3/2)\sin 2\theta + 2\theta\cos^2\theta).$$

$$\text{First harmonic} = 1/\pi\ (-2\theta\cos\theta + 3/2\sin\theta + 1/6\sin 3\theta)\cos\omega t$$

$$\text{Second harmonic} = 1/\pi\left[1/4(1 + 6\cos^2\theta)\sin 2\theta - 2(\sin\theta + 1/3\sin 3\theta)\cos\theta + \theta/2\right]\cos 2\omega t$$

$$n\text{th harmonic} = 1/\pi\left\{2/n\ (1/2 + \cos^2\theta)\sin n\theta - \cos\theta\left[\frac{2\sin(n-1)\theta}{n-1} + \frac{2\sin(n+1)\theta}{n+1}\right] + \frac{\sin(n-2)\theta}{2(n-2)} + \frac{\sin(n+2)\theta}{2(n+2)}\right\}\cos n\omega t.$$

2. Extrapolation of Vacuum Tube Static Curves.

It sometimes happens that the static curves of a vacuum tube need to be extended to aid in making the computations. With certain requirements maintained, this can be done quite well by using the three-halves power law relating currents and voltages. Provided the relative magnitudes of all electrode voltages are not changed, but are each varied by the same percentage, the distribution of total current to the electrodes will not be altered, and all currents will rise and fall as the three-halves power of the voltage changes.

This follows from the fact that the shape of the voltage fields within the tube is not disturbed. Thus, the magnitudes of the currents are affected and not the distribution to the different electrodes. The application of this rule is limited to regions that do not approach the limit of cathode emission. The accuracy may also be adversely affected somewhat by high secondary emission currents.

Proceedings of the Institute of Radio Engineers
Volume 25, Number 1, Part 1 *January, 1937*

DIRECTIONAL ANTENNAS*

By

G. H. Brown

(RCA Manufacturing Company Inc., RCA Victor Division, Camden, New Jersey)

Summary—*The object of this paper is to develop analytical methods which are readily applicable to the general problems that arise in array design and to provide design curves that may be used without reference to the field theory underlying the problem.*

The cases of both driven and parasitic arrays have been treated. Where possible, the results have been tested by comparison with experimental results.

The field and circuit conditions are treated for the case of multielement driven arrays. The effective impedance and the total radiated power, as well as the power radiated by each antenna, are determined. Expressions are given for the radiation patterns of the arrays. Examples are treated which show how these arrays are used to protect the service areas of other stations operating on the same frequency assignment.

In the case of a single parasitic reflector, it is found that spacings less than a quarter wave length are desirable in both the transmitting and receiving case. It is seen that the parasitic antenna functions equally well as a director or a reflector.

The case of an antenna parallel to an infinite sheet acting as a reflector is treated. It is shown that it is desirable to space the antenna very much less than a quarter wave length from the sheet.

A method of measuring the mutual impedance between antennas is advanced.

A systematic method of adjusting a complicated array is outlined.

Appendix I shows a method of computing the mutual impedance between a tower and a T antenna.

Other appendixes give the derivation of the expressions for the electromagnetic field in the vicinity of a straight wire, end-loaded, and of arbitrary length, and the extension of these expressions to yield the vertical radiation characteristics at great distances.

I. Introduction

THE multielement or directional antenna is becoming of increasing importance throughout the spectrum of radio frequencies. Various forms of directive arrays have been used for many years for short-wave use. In the past few years, arrays have become important in the so-called "broadcast" band of frequencies. The purpose of the arrays used in this range of frequencies has been twofold. In some cases, the energy is directed into a desirable or densely populated territory at the expense of a decrease in the energy sent out into thinly populated territory, waste land, or large bodies of water. By far the greatest use of the directive array has been to prevent energy from going out in such directions which point toward the service areas of

* Decimal classification: R325. Original manuscript received by the Institute, October 5, 1936.

stations on the same or adjacent channels. The use of such arrays allows stations to increase their power without increasing the amount of interference they cause to another station.

In designing an array, it is desirable to determine several quantities. The shape of the space distribution curve of the electric intensity (or magnetic flux density) at a distance from the array is determined by the relative phase and magnitude of the currents in the elements making up the array. The next step is to place the scale factor on this diagram. This is usually done by integrating the flow of power through the surface of a large sphere whose center lies at the array. For an array consisting of more than two elements, this process is very tedious. By reducing the field relations to a study of self- and mutual impedances, the problem becomes that of analyzing a coupled circuit. This process has the added advantage of yielding relations of importance in designing the feeding and matching circuits. The amount of power contributed by each element is then known, as well as the effective resistance and reactance which each element will offer to its respective transmission line. With a complete knowledge of the phenomena occuring in the system, the adjustment becomes merely a correction of second order effects instead of the usual "cut-and-try" procedure which must be followed when the action of the system is not thoroughly understood.

It is the purpose of this report to develop analytical methods which are readily applicable to the general problems that arise in array design and to provide design curves which may be used without reference to the field theory underlying the problem. The theory will be applied to a number of important cases. It is realized that some of the work closely parallels that of other authors. In fact, a certain amount may seem a duplication of previous work,[1] but this was done for completeness and continuity of treatment. Furthermore, the report has been prepared with the idea of utility predominating over that of presenting entirely new material.

II. The Fields in the Vicinity of a Transmitting Antenna

In order to predict effects occuring at the antenna itself, it is necessary to have available expressions for the electromagnetic field in the vicinity of a radiating element. In particular, let us examine the top-loaded antenna shown in Fig. 1. This antenna consists of a vertical wire with a nonradiating capacity area at the top so that the current

[1] P. S. Carter, "Circuit relations in radiating systems and applications to antenna problems," Proc. I.R.E., vol. 20, pp. 1004–1041; June, (1932).

distribution is as shown. Then b is the length of the portion of sine wave suppressed by the capacity area. We define the quantities.

$$B = 2\pi b/\lambda \text{ radians} = 360\ b/\lambda \text{ degrees}$$
$$A = 2\pi a/\lambda \text{ radians} = 360\ b/\lambda \text{ degrees}$$
$$G = A + B.$$

The current on this antenna is then distributed according to the relation

$$i_y = \frac{I_0 \sin (G - ky)}{\sin G} \tag{1}$$

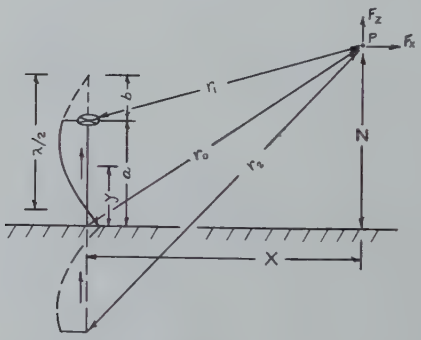

Fig. 1

where y = the distance from the surface of the earth to the point at which the current, i_y, is being determined.

I_0 = current at the base of the antenna
λ = operating wave length
$k = 2\pi/\lambda$.

The components of electric intensity at point, P, are[2]

$$F_x = +j\frac{30I_0}{x \sin G}\left[\frac{(z-a)}{r_1}\epsilon^{-jkr_1}\cos B + \frac{(z+a)}{r_2}\epsilon^{-jkr_2}\cos B\right.$$
$$-\frac{2z}{r_0}\epsilon^{-jkr_0}\cos G - \frac{x^2}{kr_1^3}\epsilon^{-jkr_1}\sin B + \frac{x^2}{kr_2^3}\epsilon^{-jkr_2}\sin B$$
$$\left.+j\frac{(z-a)^2}{r_1^2}\epsilon^{-jkr_1}\sin B - j\frac{(z+a)^2}{r_2^2}\epsilon^{-jkr_2}\sin B\right] \tag{2}$$

[2] Appendix III.

and,

$$F_z = -j\frac{30I_0}{\sin G}\left[\frac{\epsilon^{-jkr_1}}{r_1}\cos B + \frac{\epsilon^{-jkr_2}}{r_2}\cos B - \frac{2\epsilon^{-jkr_0}}{r_0}\cos G\right.$$
$$+ j\frac{(z-a)}{{r_1}^2}\epsilon^{-jkr_1}\sin B - j\frac{(z+a)}{{r_2}^2}\epsilon^{-jkr_2}\sin B$$
$$\left. + \frac{(z-a)}{k{r_1}^3}\epsilon^{-jkr_1}\sin B - \frac{(z+a)}{k{r_2}^3}\epsilon^{-jkr_2}\sin B\right] \tag{3}$$

where,

$$r_0 = \sqrt{x^2+z^2}$$
$$r_1 = \sqrt{x^2+(z-a)^2}$$
$$r_2 = \sqrt{x^2+(z+a)^2}.$$

The magnetic flux density lies in horizontal circles, with the center of the circles lying on the vertical axis of the antenna. The magnetic flux density is

$$B_\phi = j\frac{10^{-9}I_0}{x\sin G}\left[\epsilon^{-jkr_1}\cos B + \epsilon^{-jkr_2}\cos B - 2\epsilon^{-jkr_0}\cos G\right.$$
$$\left. + j\frac{(z-a)}{r_1}\epsilon^{-jkr_1}\sin B - j\frac{(z+a)}{r_2}\epsilon^{-jkr_2}\sin B\right]. \tag{4}$$

When there is no loading at the top of the antenna, the field components become

$$F_x = +j\frac{30I_0}{x\sin G}\left[\frac{(z-a)}{r_1}\epsilon^{-jkr_1} + \frac{(z+a)}{r_2}\epsilon^{-jkr_2}\right.$$
$$\left. - \frac{2z}{r_0}\epsilon^{-jkr_0}\cos G\right] \tag{5}$$

$$F_z = -j\frac{30I_0}{\sin G}\left[\frac{\epsilon^{-jkr_1}}{r_1} + \frac{\epsilon^{-jkr_2}}{r_2} - \frac{2\epsilon^{-jkr_0}}{r_0}\cos G\right] \tag{6}$$

and,

$$B_\phi = j\frac{10^{-9}I_0}{x\sin G}\left[\epsilon^{-jkr_1} + \epsilon^{-jkr_2} - 2\epsilon^{-jkr_0}\cos G\right]. \tag{7}$$

At times, the sectionalized arrangement (Fig. 2) is used instead of top loading. The coil is placed some distance from the top of the antenna.

The total antenna height is d, while a is the distance from the earth to the coil. The length of sine wave which would be above the coil point if the coil and top section of antenna were replaced by a straight wire is b. Then we define

$$D = 2\pi d/\lambda \text{ radians} = 360d/\lambda \text{ degrees}$$
$$A = 2\pi a/\lambda \text{ radians} = 360a/\lambda \text{ degrees}$$
$$B = 2\pi b/\lambda \text{ radians} = 360b/\lambda \text{ degrees.}$$

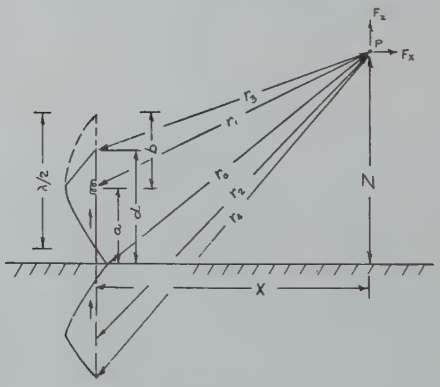

Fig. 2

The antenna current is given by

$$i = \frac{I_0 \sin (G - ky)}{\sin G} \tag{8}$$

when y is less than a. When y is greater than a, the distribution is

$$i = \frac{I_0 \sin B \cdot \sin (D - ky)}{\sin G \cdot \sin (D - A)}. \tag{9}$$

The components of the electromagnetic field become

$$F_x = +j \frac{30 I_0}{\sin G}\left[\frac{(z-a)}{r_1}\epsilon^{-jkr_1}\cos B + \frac{(z+a)}{r_2}\epsilon^{-jkr_2}\cos B - \frac{2z}{r_0}\epsilon^{-jkr_0}\cos G + \frac{\sin B}{\sin (D-A)}\left\{\frac{(z-d)}{r_3}\epsilon^{-jkr_3} + \frac{(z+d)}{r_4}\epsilon^{-jkr_4} - \frac{(z-a)}{r_1}\epsilon^{-jkr_1}\cos (D-A) - \frac{(z+a)}{r_2}\epsilon^{-jkr_2}\cos (D-A)\right\}\right] \tag{10}$$

$$F_z = -j\frac{30I_0}{\sin G}\left[\frac{\epsilon^{-jkr_1}}{r_1}\cos B + \frac{\epsilon^{-jkr_2}}{r_2}\cos B - \frac{2\epsilon^{-jkr_0}}{r_0}\cos G + \frac{\sin B}{\sin (D-A)}\left\{\frac{\epsilon^{-jkr_3}}{r_3} + \frac{\epsilon^{-jkr_4}}{r_4} - \frac{\epsilon^{-jkr_1}}{r_1}\cos (D-A) - \frac{\epsilon^{-jkr_2}}{r_2}\cos (D-A)\right\}\right] \tag{11}$$

and,

$$B_\phi = \frac{j\cdot 10^9 I_0}{x\sin G}\left[\epsilon^{-jkr_1}\cos B + \epsilon^{-jkr_2}\cos B - 2\epsilon^{-jkr_0}\cos G + \frac{\sin B}{\sin (D-A)}\left\{\epsilon^{-jkr_3} + \epsilon^{-jkr_4} - \epsilon^{-jkr_1}\cos (D-A) - \epsilon^{-jkr_2}\cos (D-A)\right\}\right] \tag{12}$$

where,

$$r_0 = \sqrt{x^2 + z^2}$$
$$r_1 = \sqrt{x^2 + (z-a)^2}$$
$$r_2 = \sqrt{x^2 + (z+a)^2}$$
$$r_3 = \sqrt{x^2 + (z-d)^2}$$
$$r_4 = \sqrt{x^2 + (z+d)^2}.$$

All the above fields have been computed on the assumption that the earth beneath the antenna is a perfect conductor.

The above expressions are essential in computing the mutual impedances between antennas. They are also of use in investigating earth currents near transmitting antennas,[3] in adjusting top-loaded or sectionalized antennas,[4] and in estimating the effects of supporting guys.

III. The Mutual Impedance Between Antennas

The classical method of calculating the power radiated from an antenna was to integrate the Poynting vector over the surface of a sphere whose radius was very large compared to the antenna dimensions and to the wave length. This process then gave the radiation resistance of the antenna. Several years ago, Pistolkors[5] moved the

[3] G. H. Brown, "The phase and magnitude of earth currents near radio transmitting antennas," Proc. I.R.E., vol. 23, pp. 168–181; February, (1935).

[4] G. H. Brown, "A simple method of adjusting sectionalized and top-loaded broadcast antennas," *Broadcast News*, No. 19, p. 14; April, (1936).

[5] A. A. Pistolkors, "The radiation resistance of beam antennas," Proc. I.R.E., vol. 17, pp. 562–628; March, (1929).

surface of the integration so that this surface coincided with the surface of the antenna. This method yields the reactance as well as the resistance of the antenna. This procedure has been elaborated upon by other workers.[6]

The Poynting vector in this case becomes the product of the current flowing in an element of conductor and the component of electric intensity at the surface of the conductor and parallel to the direction of current flow. The component of electric intensity is found by letting the point, P, of Fig. 1 approach the surface of the antenna. Then the distance, z, assumes the value, y, which is the elevation of the cur-

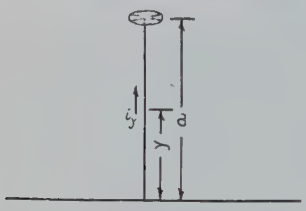

Fig. 3

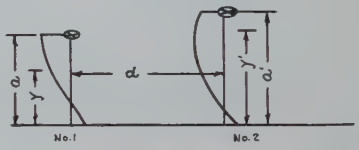

Fig. 4

rent element we are examining, and x approaches the radius of the conductor. The total power passing outward from the surface of the conductor (Fig. 3) is

$$p \text{ (watts)} = -\int_{y=0}^{y=a} F_y i_y dy. \tag{13}$$

Here i_y is the current in the antenna element and F_y is the vertical component of electric intensity at the elevation, y, where this electric intensity is due to the current (and charge) of the entire antenna. The notation F_y has been used instead of F_z to agree with the current notation and to indicate that the field is to be taken at the surface of the conductor. This electric intensity is computed from (3), (6), or (11), depending on the type of antenna used. Equation (13) consists of a real term and an imaginary term, each of which is proportional to I_0^2. Thus the real coefficient of I_0^2 is identified as the radiation resistance and the imaginary factor as the reactance of the antenna.

Let us now turn to the situation of Fig. 4. Two antennas of heights a and a' are separated a distance, d. The self-resistance and reactance of either antenna may be found by equation (13). At the same time, antenna No. 2 produces a field at the surface of No. 1 which yields a Poynting term of power. Thus the power flowing out of No. 1 due to the presence of No. 2 is

[6] J. Labus, "Recherische Ermittlung der Impedanz von Antennan," *Hochfrequenz. und Elektroakustik*, p. 17, January, (1933).

$$p_m = -\int_{y=0}^{y=a} F_y i_y dy \tag{14}$$

where i_y is the current in No. 1 and F_y is the electric intensity at the surface of No. 1 due to No. 2 [$x=d$ in (3), (6), or (11)]. This power term splits into a real and an imaginary part, multiplied by the product, $I_0 I_0'$. We have thus arrived at a definition and a means for computing the mutual impedance between two antennas. We shall denote this complex mutual impedance as

$$\overline{Z}_m = R_m + jX_m = |Z_m| \angle + \theta_m \tag{15}$$

where,

$$|Z_m| = \sqrt{R_m^2 + X_m^2} \tag{16}$$

and,

$$\tan \theta_m = X_m/R_m. \tag{17}$$

Likewise, the power flowing from No. 2 due to No. 1 is

$$p_m' = \int_{y'=0}^{y'=a'} F_{y'} i_{y'} dy' \tag{18}$$

where $i_{y'}$ is the current in No. 2 and $F_{y'}$ is the electric intensity at the surface of No. 2 due to No. 1.

Because of the reciprocal relation existing between (14) and (18), ($p_m = p_m'$), either may be used to evaluate the mutual impedance. When one antenna is top-loaded or sectionalized and the other is a straight vertical wire with no loading, it is generally simpler to integrate along the top-loaded or sectionalized antenna since the expression for the field due to the simple antenna is less cumbersome to handle.

In general, it is desirable to plot the integrand of (14) or (18) and perform a mechanical integration. The actual integration yields very cumbersome formulas[7] which involve a large amount of arithmetic before a numerical answer is obtained. Experience with both methods has proved that the graphical method is less tedious as well as less time-consuming.

The special case where the two antennas are of equal heights is of great importance. Fig. 5 shows the value, $|Z_m|$ for height, a, ($G = 2\pi a/\lambda$) and spacing, d, for a number of values of G. The antennas are straight vertical unloaded antennas over a perfect earth. Fig. 6 shows the phase angle, θ_m.

[7] G. H. Brown and Ronold King, "High-frequency models in antenna investigations," Proc. I.R.E., vol. 22, 471, equations (7) and (8); April, (1934).

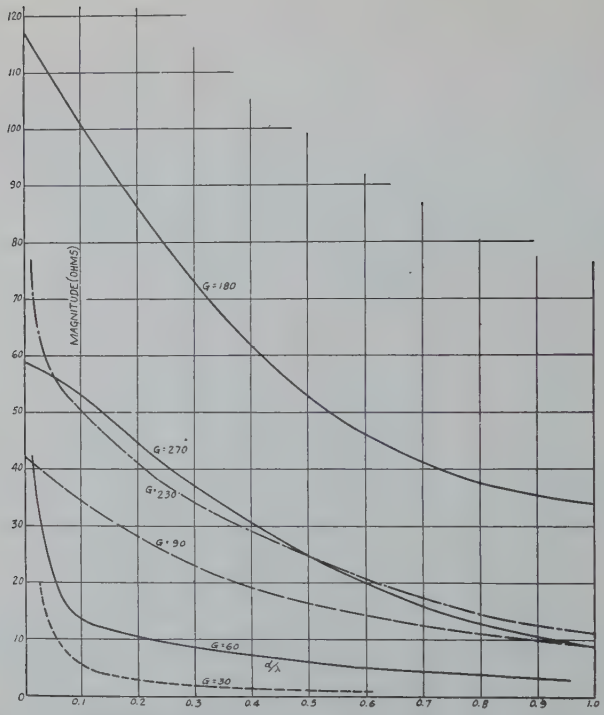

Fig. 5—Magnitude of the mutual impedance between identical vertical antennas.

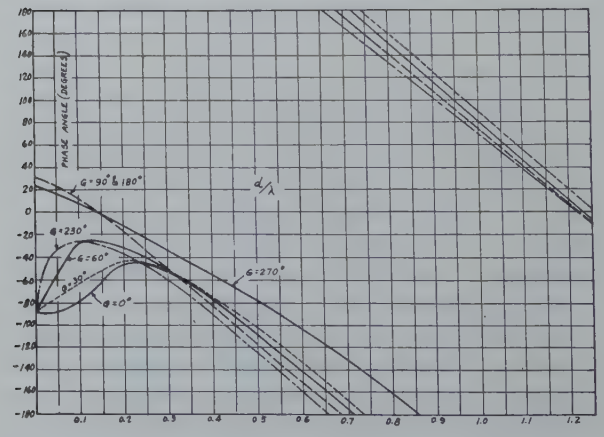

Fig. 6—The phase angle of the mutual impedance between identical vertical antennas.

These mutual impedances are referred to the current at the base of the antenna except in the case, $G = 180$ degrees, where the reference is made to the current loop at the center of the antenna.

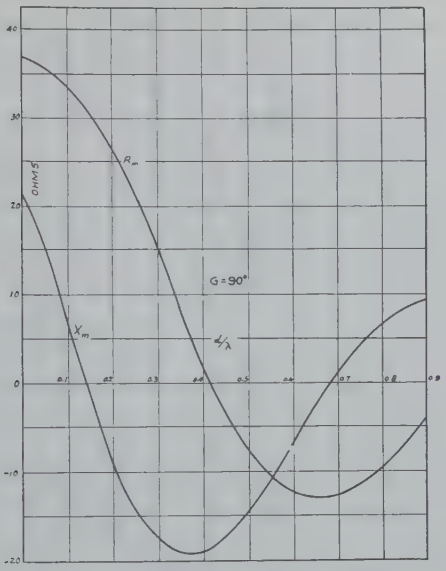

Fig. 7—The resistive and reactive components of the mutual impedance between two one-quarter wave antennas.

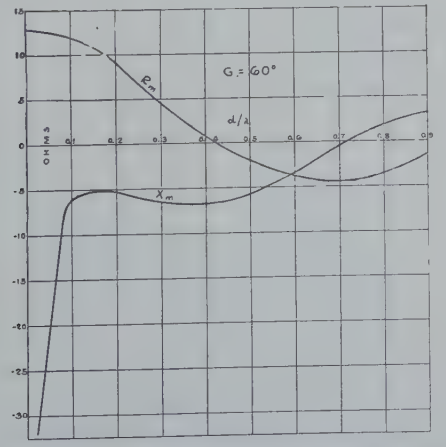

Fig. 8—The resistive and reactive components of the mutual impedance between two one-sixth wave antennas. ($G = 60$ degrees.)

It is to be noted that, as $d = 0$, the mutual impedance between two identical antennas approaches the self-impedance of each antenna.

Fig. 7 shows the components, R_m and X_m, as a function of d/λ for $G=90$ degrees.

Fig. 8 is a similar set of curves when $G=60$ degrees.

It is seen that for $d>0.15\lambda$, the curves of mutual reactance are almost identical in shape, differing only in scale. When $d<0.15\lambda$, the reactances depart greatly in character. The similarity between the mutual resistance curves holds for all values of d. Table I shows the ratio R_m/R_0 as a function of d/λ for a number of values of G, where R_0 is the value of mutual resistance when $d/\lambda=0$. R_0 is then the self-resistance of a single antenna. We see that, for a given d/λ, R_m/R_0 is substantially constant for all values of G less than 180 degrees. This fact is of importance in the work that follows.

TABLE I

d/λ / G	0 degrees	R_m/R_0		
		90 degrees	180 degrees	230 degrees
0.0	1.0	1.0	1.0	1.0
0.05	0.955	0.967	0.999	0.931
0.10	0.9195	0.918	0.990	0.900
0.15	0.831	0.848	0.936	0.777
0.20	0.710	0.735	0.837	0.640
0.25	0.569	0.582	0.722	0.493
0.30	0.412	0.412	0.598	0.328
0.40	0.1036	0.0532	0.335	−0.0199

The above values of mutual impedance have been calculated for antennas located directly above a perfectly conducting earth. (Fig. 9(a)).

When the conducting earth is replaced by a wire exactly like the antenna already in use (Fig. 9(b)), the values of mutual impedance given above should be doubled in magnitude.

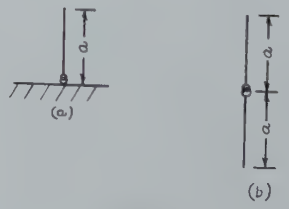

Fig. 9

IV. Two Driven Antennas

First we shall examine the case of two driven antennas.

The term "driven antennas" will be used to apply to antennas so fed by transmission lines that any current ratio and phase relation between the various antenna currents may be obtained.

The antennas are spaced a distance, d. In the arrangement of Fig.

10, the point, P, at which we shall calculate the field intensity, is so far from the antennas, 0 and 1, that $r_1 \gg d$, $r_0 \gg d$.

$$r_1 \doteq r_0 + d \cos \psi. \tag{19}$$

The projection of r_1 on the X axis is $r_1 \cos \psi$. The same projection is also $r_1 \sin \theta \cos \phi$, so that $\cos \psi = \sin \theta \cos \phi$. Then,

$$r_1 \doteq r_0 + d \sin \theta \cos \phi. \tag{20}$$

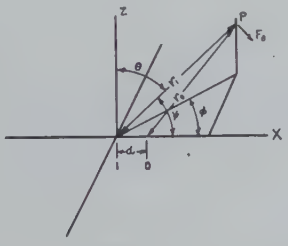

Fig. 10

The electric intensity at P due to antenna 0 is

$$(F_\theta)_0 = j \frac{60 \bar{I}_0}{r_0} \epsilon^{-j2\pi r_0/\lambda} K_0 f_0(\theta) \tag{21}$$

where K is the form factor of the antenna and $f(\theta)$ is the vertical radiation characteristic.[8]

The electric intensity at the same point due to antenna 1 is

$$(F_\theta)_1 = j \frac{60 \bar{I}_1}{r_1} \epsilon^{-j2\pi r_1/\lambda} K_1 f_1(\theta). \tag{22}$$

Since $1/r_1 \doteq 1/r_0$, the total field is

$$F_\theta = j \frac{60 \epsilon^{-j2\pi r_0/\lambda}}{r_0} \left[\bar{I}_0 K_0 f_0(\theta) + \bar{I}_1 K_1 f_1(\theta) \epsilon^{-j(2\pi d/\lambda) \sin \theta \cos \phi} \right]. \tag{23}$$

When the currents are related by the relation

$$\bar{I}_1 = M \bar{I}_0 \angle + \alpha \tag{24}$$

the total field becomes

$$F_\theta = j \frac{60 \bar{I}_0}{r_0} K_0 f_0(\theta) \epsilon^{-j2\pi r_0/\lambda} \left[1 + \frac{M K_1 f_1(\theta)}{K_0 f_0(\theta)} \angle \alpha - \frac{2\pi d}{\lambda} \sin \theta \cos \phi \right]. \tag{25}$$

[8] G. H. Brown, "A critical study of the characteristics of broadcast antennas as affected by antenna current distribution," PROC. I.R.E., vol. 24, p. 49, equations (2) and (3); January, (1936).

When the antennas are identical,

$$F_\theta = j\frac{60\bar{I}_0}{r_0} Kf(\theta)\epsilon^{-j2\pi r_0/\lambda}\left[1 + M \angle \alpha - \frac{2\pi d}{\lambda}\sin\theta\cos\phi\right]. \quad (26)$$

Let us turn for the moment to the circuit relations at the antennas themselves. Kirchoff's law for the two circuits becomes

$$\bar{V}_0 = \bar{I}_0\bar{Z}_{00} + \bar{I}_1\bar{Z}_m \quad (27)$$

$$\bar{V}_1 = \bar{I}_0\bar{Z}_m + \bar{I}_1\bar{Z}_{11} \quad (28)$$

where,

$\bar{Z}_{00} = R_{00} + jX_{00}$ = self-impedance of antenna 0.
$\bar{Z}_{11} = R_{11} + jX_{11}$ = self-impedance of antenna 1.
$\bar{V}$ = driving voltage at the terminals of the antenna.

Then,

$$\bar{V}_0 = \bar{I}_0[R_{00} + jX_{00} + M|Z_m| \angle \alpha + \theta_m] \quad (29)$$

and,

$$\bar{V}_1 = \bar{I}_1\left[R_{11} + jX_{11} + \frac{1}{M}|Z_m| \angle -\alpha + \theta_m\right]. \quad (30)$$

Expanding, we obtain

$$\bar{V}_0/\bar{I}_0 = R_{00} + M|Z_m|\cos(\alpha + \theta_m) + j\{X_{00} + M|Z_m|\sin(\alpha + \theta_m)\} \quad (31)$$

and,

$$\bar{V}_1/\bar{I}_1 = R_{11} + \frac{1}{M}|Z_m|\cos(-\alpha + \theta_m) + j\left\{X_{11} + \frac{1}{M}|Z_m|\sin(-\alpha + \theta_m)\right\}. \quad (32)$$

Equations (31) and (32) show quantitatively the change in resistance and reactance of an antenna when another element is brought into operation. These relations are of importance in designing antenna coupling circuits for directional arrays.

When the array is in operation, with the currents obeying the relation

$$\bar{I}_1 = M\bar{I}_0 \angle +\alpha$$

the resistance at the terminals of antenna 0 will no longer be R_{00} but will assume the value

$$R_0 = R_{00} + M|Z_m|\cos(\alpha + \theta_m) \quad (33)$$

while the resistance at the terminals of antenna 1 becomes

$$R_1 = R_{11} + \frac{1}{M} | Z_m | \cos (- \alpha + \theta_m). \tag{34}$$

Thus, the values R_0 and R_1 will only be equal when $M = 1$, and then only when $\alpha = 0$ or 180 degrees.

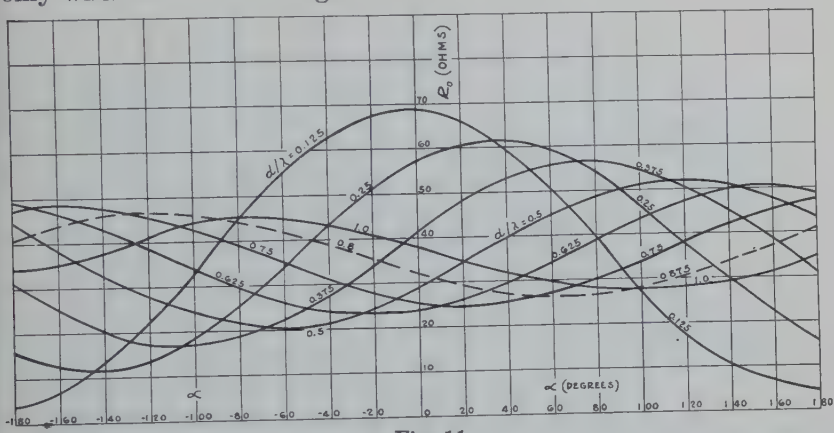

Fig. 11

Fig. 11 shows the variation of R_0 as a function of the phase angle, α, for a number of antenna spacings. These values are for the special case where $M = 1$ and $G = 90$ degrees.

Fig. 12 shows a similar curve for R_1.

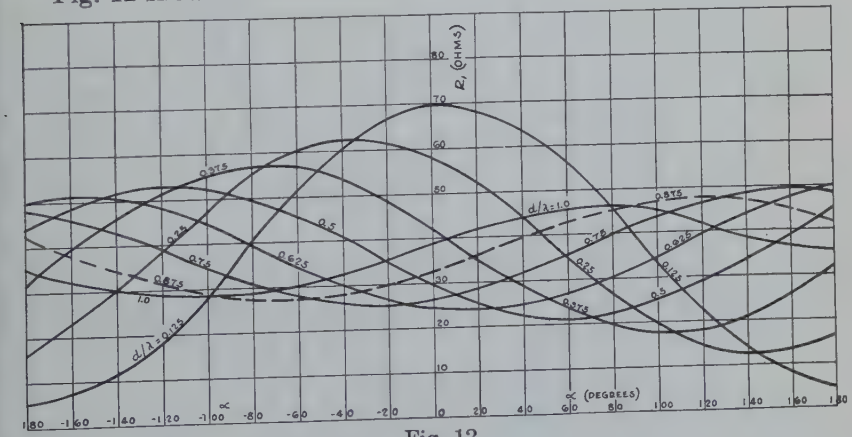

Fig. 12

The new reactance of each antenna is

$$X_0 = X_{00} + M | Z_m | \sin (\alpha + \theta_m) \tag{35}$$

and,

$$X_1 = X_{11} + \frac{1}{M} | Z_m | \sin (- \alpha + \theta_m). \tag{36}$$

Figs. 13 and 14 show the quantities,

$X_0 - X_{00}$ and $X_1 - X_{11}$ for $M = 1$ and $G = 90$ degrees.

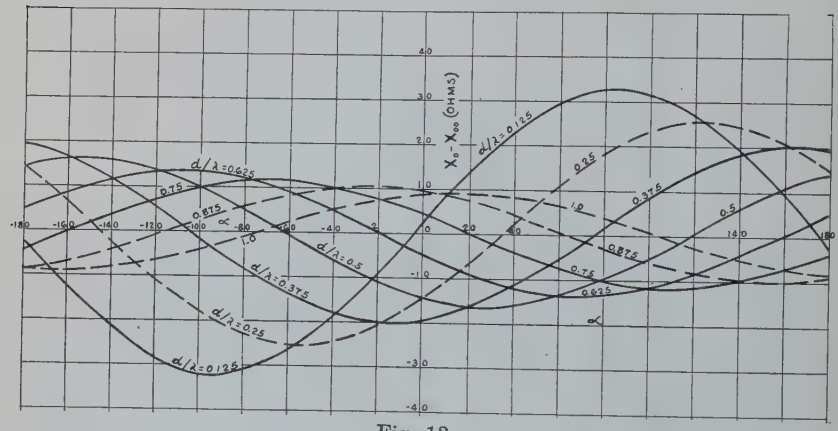

Fig. 13

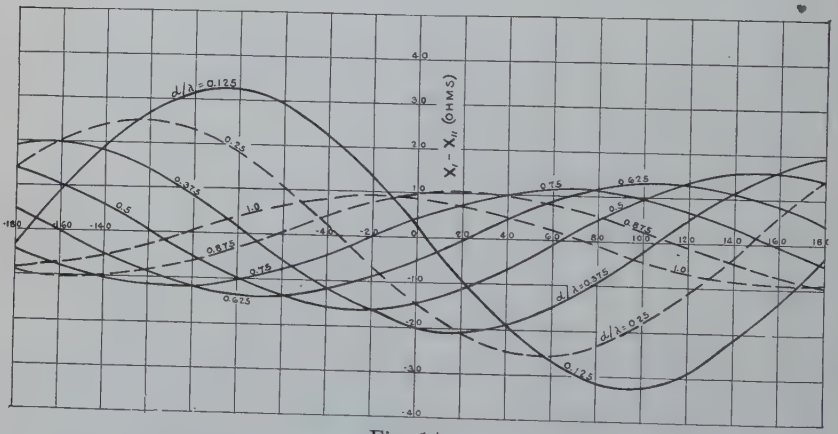

Fig. 14

Figs. 11 to 14 may be utilized to determine the values when $M \neq 1$ from the following relations

$$(R_0)_M = M[(R_0)_{M=1} - R_{00}] + R_{00} \tag{37}$$

$$(X_0)_M = M \cdot (X_0 - X_{00})_{M=1} + X_{00} \tag{38}$$

$$(R_1)_M = \frac{1}{M}[(R_1)_{M=1} - R_{11}] + R_{11} \tag{39}$$

$$(X_1)_M = \frac{1}{M} \cdot (X_1 - X_{11})_{M=1} + X_{11}. \tag{40}$$

The power delivered to antenna 0 is

$$P_0 = I_0^2 R_0 = I_0^2 [R_{00} + M \mid Z_m \mid \cos (\alpha + \theta_m) \tag{41}$$

while,

$$P_1 = I_1^2 R_1 = I_1^2 \left[R_{11} + \frac{1}{M} \mid Z_m \mid \cos (- \alpha + \theta_m) \right]. \tag{42}$$

The total power is

$$\begin{aligned} P_T &= I_0^2 \left[R_{00} + M \mid Z_m \mid \cos (\alpha + \theta_m) \right. \\ &\quad \left. + M^2 \left\{ R_{11} + \frac{1}{M} \mid Z_m \mid \cos (- \alpha + \theta_m) \right\} \right] \\ &= I_0^2 [R_{00} + M^2 R_{11} + 2MR_m \cos \alpha]. \end{aligned} \tag{43}$$

Thus, for a given power input to the antenna array, (43) gives a convenient method of evaluating I_0.

The magnitude of I_1 is $M \cdot I_0$.

We are now prepared to return to the field intensity relations. In particular, let us examine the case of two identical antennas, with equal self-resistances.

For a given input power

$$F_\theta = j \frac{60Kf(\theta)}{r_0} \epsilon^{-jkr_0} \frac{[1 + M \angle \alpha - kd \sin \theta \cos \phi] \sqrt{P}}{\sqrt{R_{00}(1 + M^2) + 2MR_m \cos \alpha}}. \tag{44}$$

When $\theta = 90$ degrees

$$F_{\theta=90^\circ} = j \frac{60K}{r_0} \epsilon^{-jkr_0} \frac{[1 + M \angle \alpha - kd \cos \phi] \sqrt{P}}{\sqrt{R_{00}(1 + M^2) + 2MR_m \cos \alpha}}. \tag{45}$$

This relation gives the distribution in the horizontal plane (as a function of ϕ). If a single antenna were fed with the same power, the field on the horizontal plane would be

$$F_0 = j \frac{60K}{r_0} \epsilon^{-jkr_0} \sqrt{\frac{P}{R_{00}}}. \tag{46}$$

It is then convenient to express the horizontal field intensity distribution in terms of the field intensity of a single antenna

$$\frac{F_{\theta=90^\circ}}{F_0} = \frac{\sqrt{R_{00}} [1 + M \angle \alpha - kd \cos \phi]}{\sqrt{R_{00}(1 + M^2) + 2MR_m \cos \alpha}} \tag{47}$$

or,

$$\frac{F_{\theta=90^\circ}}{F_0} = \frac{1 + M \angle\alpha - kd\cos\phi}{\sqrt{1 + M^2 + 2M\frac{R_m}{R_{00}}\cos\alpha}} \tag{48}$$

$$\left|\frac{F_{\theta=90^\circ}}{F_0}\right| = \sqrt{\frac{1 + M^2 + 2M\cos(\alpha - kd\cos\phi)}{1 + M^2 + 2M\frac{R_m}{R_{00}}\cos\alpha}}. \tag{49}$$

From our previous discussion, we learned that R_m/R_{00} was substantially independent of the antenna heights, provided both antennas remained equal in height. Thus, for a fixed current ratio and phase angle, we see that the gain of two similar antennas over one of these antennas is essentially independent of the antenna height.

When the currents become equal in magnitude, $(M=1)$

$$\left|\frac{F_{\theta=90^\circ}}{F_0}\right| = \frac{\sqrt{2}\cos\left(\frac{\alpha}{2} - \frac{kd}{2}\cos\phi\right)}{\sqrt{1 + \frac{R_m}{R_{00}}\cos\alpha}}. \tag{50}$$

The above equation as a function of ϕ, d/λ, and α is illustrated by Fig. 15. Diagrams similar to Fig. 15 have been published elsewhere.[9] However, these diagrams have merely been plots of the factor,

$$\cos\left(\frac{\alpha}{2} - \frac{kd}{2}\cos\phi\right)$$

so that the effect of mutual coupling is not present.

Since it is difficult to scale values from Fig. 15, maximum values of (50) have been plotted in Fig. 16 as a function of α for a number of values of d/λ. We see it is possible to increase the field about 75 per cent with reasonable spacings between elements.

It is interesting to attempt to maximize (49) by adjusting M and α. Suppose we wish to maximize the field in the direction making an angle ϕ with the line of antennas.

[9] G. C. Southworth, "Certain factors affecting the gain of directive antennas," Proc. I.R.E., p. 1507, Fig. 3; September, (1930); A. James Ebel, "Directional radiation patterns," *Electronics*, vol. 9, p. 29; April, (1936).

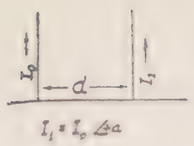

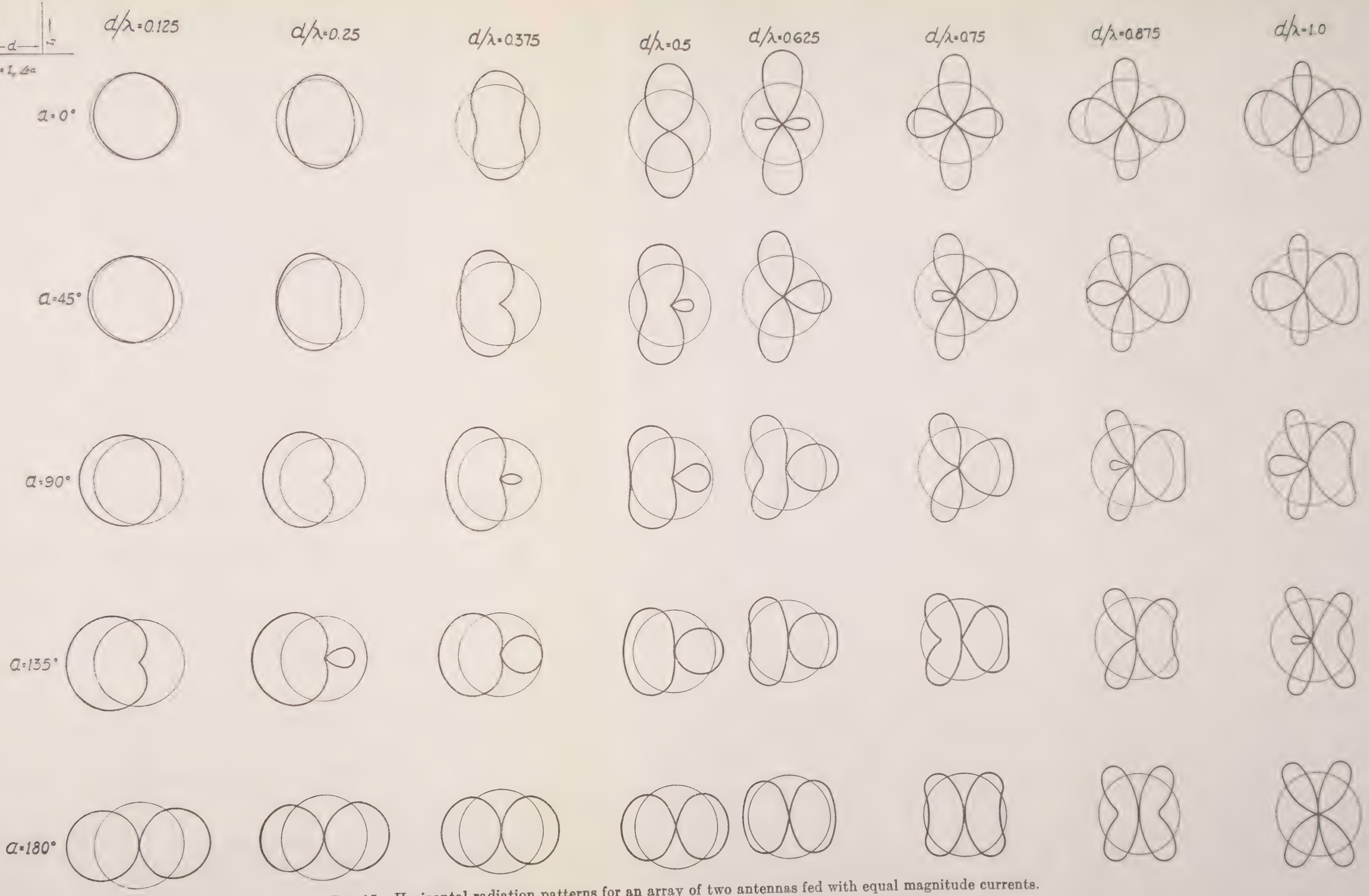

Fig. 15—Horizontal radiation patterns for an array of two antennas fed with equal magnitude currents.

Squaring (49)

$$\left|\frac{F_{\theta=90^\circ}}{F_0}\right|^2 = \frac{1 + M^2 + 2M\cos(\alpha - kd\cos\phi)}{1 + M^2 + 2M\dfrac{R_m}{R_{00}}\cos\alpha}. \tag{51}$$

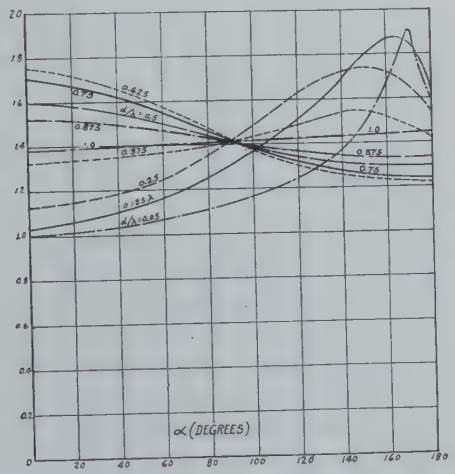

Fig. 16—The maximum increase in field intensity possible from an array of two antennas.

Differentiating with respect to M and setting equal to zero

$$\left[1 + M^2 + 2M\frac{R_m}{R_{00}}\cos\alpha\right][2M + 2\cos(\alpha - kd\cos\phi)]$$
$$- [1 + M^2 + 2M\cos(\alpha - kd\cos\phi)]\left[2M + \frac{2R_m}{R_{00}}\cos\alpha\right] = 0 \tag{52}$$

or,

$$M^2\left[\frac{R_m}{R_{00}}\cos\alpha - \cos(\alpha - kd\cos\phi)\right]$$
$$-\left[\frac{R_m}{R_{00}}\cos\alpha - \cos(\alpha - kd\cos\phi)\right] = 0. \tag{53}$$

Then $M^2 = 1$ and $M = \pm 1$.

Since we have used M merely as a ratio, with the angle α to indicate phase, we are interested only in the value $M = +1$. Thus we see that maximum fields are obtained when the currents are equal in magnitude. We could differentiate (51) to find the optimum phase angle. It is simpler to obtain this information from an inspection of Fig. 15.

It now seems desirable to discuss a numerical example in order to illustrate the theory we have outlined. Let us suppose we are confronted with the following problem. The service area of a certain radio station is split into two parts. The most important part of the service area lies due south of the transmitter site, while the area of secondary importance lies due north. It is desired to operate on a power of 500 watts with a directional antenna which will do three things; namely, suppress the radiation in the direction of another station on the same frequency assignment lying 500 miles due east of our station, send as much signal as possible to the south in a broad beam, and give a signal at least equivalent to 500 watts in the northern direction. We wish to know the electrical constants of the array as well as the radiation characteristics.

Then, by various devious means, we decide to use an array of two antennas, one-quarter wave tall, and separated a quarter wave length. The antennas lie on a line which runs due north and south. Antenna 0 is the northernmost antenna. The antennas are to be so excited that the current in the south antenna is 67.0 per cent of the current in the north antenna. The current in the south antenna lags the current in the north antenna by 160 electrical degrees. Then, from (24),

$$\bar{I}_1 = M\bar{I}_0 \angle + \alpha = 0.67\bar{I}_0 \angle - 160 \text{ degrees} \tag{54}$$

$$M = 0.67 \tag{55}$$

$$\alpha = -160 \text{ degrees.} \tag{56}$$

The self-resistance of each antenna is 36.6 ohms while the reactance is +21.25 ohms.

To determine the reactance which will appear at the terminals of each antenna when the array is in correct adjustment, we turn to Figs. 13 and 14 and find

$$(X_0 - X_{00})_{M=1} = +6.5$$

$$(X_1 - X_{11})_{M=1} = +20.2.$$

From (38) and (40),

$$X_0 = 0.67 \times 6.5 + 21.25 = +25.6 \text{ ohms}$$

$$X_1 = +\frac{20.2}{0.67} + 21.25 = +51.35 \text{ ohms.}$$

Thus we see that it would not be proper to resonate the antennas individually without due consideration to the coupling effects.

In the same fashion, from Figs. 11 and 12,

$$(R_0)_{M=1} = 12.5 \text{ ohms}$$
$$(R_1)_{M=1} = 22.5 \text{ ohms}.$$

Then from (37) and (39),

$$R_0 = 0.67\,[12.5 - 36.6] + 36.6 = +20.5 \text{ ohms}$$
$$R_1 = \frac{1}{0.67}\,[22.5 - 36.6] + 36.6 = +15.5 \text{ ohms}.$$

The total power (500 watts) is

$$20.5 I_0^2 + 15.5 I_1^2 = 500.$$

Since $|I_1| = 0.67 |I_0|$

$$I_0^2[20.5 + 15.5 \times 0.67^2] = 27.45 I_0^2 = 500$$
$$I_0 = \sqrt{\frac{500}{27.45}} = 4.27 \text{ amperes}$$
$$I_1 = 2.86 \text{ amperes}.$$

The power fed to each antenna is,

$$P_0 = 4.27^2 \times 20.5 = 373.0 \text{ watts}$$
$$P_1 = 2.86^2 \times 15.5 = 127.0 \text{ watts}.$$

We are now ready to calculate the distribution patterns by means of (26). In (26), the electric intensity is given in volts per centimeter when the distance, r_0, is measured in centimeters. If we measure r_0 in miles and change the constant, 60, to 37.25, our answer is then expressed in millivolts per meter. Then when r_0 is one mile, (26) becomes

$$F_\theta = 37.25 I_0 K f(\theta) \left[1 + M \angle\alpha - \frac{2\pi d}{\lambda} \sin\theta \cos\phi\right]. \qquad (57)$$

But,

$$I_0 = 4.27 \text{ amperes}$$
$$K = 1.0 \text{ for a quarter-wave antenna}$$
$$f(\theta) = \cos(90° \cos\theta)/\sin\theta$$
$$M = 0.67$$
$$\alpha = -160°$$
$$\frac{2\pi d}{\lambda} = \frac{\pi}{2} \text{ radians} = 90°.$$

Then (57) becomes

$$F_\theta(mv/m) = \frac{159.0 \cos (90 \cos \theta)}{\sin \theta} [1 + 0.67 \angle -160^\circ - 90 \sin \theta \cos \phi] \quad (58)$$

$$F_\theta(mv/m) = \frac{159.0 \cos (90 \cos \theta)}{\sin \theta \sqrt{1.449 + 1.34 \cos (160 + 90 \sin \theta \cos \phi)}}. \quad (59)$$

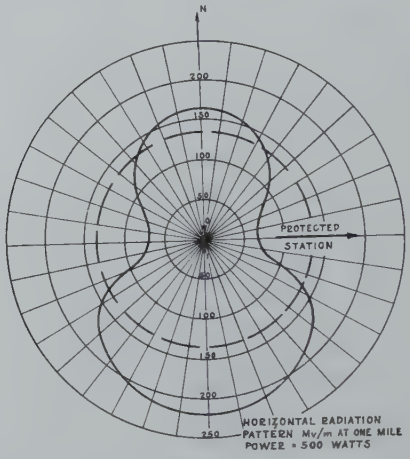

Fig. 17

Fig. 17 shows the horizontal plane distribution characteristic obtained from (59) by setting $\theta = 90$ degrees, and letting ϕ take on values from zero to 360 degrees. The broken circle indicates the value that would be obtained with a power of 500 watts in a single quarter-wave antenna.

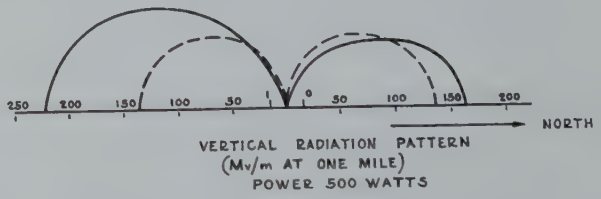

Fig. 18

Fig. 18 shows the vertical radiation patterns in a vertical plane which coincides with the line of antennas. The broken curves are again the values obtained from a single antenna operating under the same power. It is interesting to see that the ground signal is increased with the directional array, while the high angle radiation, which causes fading, remains equal to or less than that obtained from a single antenna.

Fig. 19 is the vertical radiation pattern in the direction of the station to be protected. It is to be noted that the signal in this direction is the same as would be obtained with 125 watts in a nondirectional antenna.

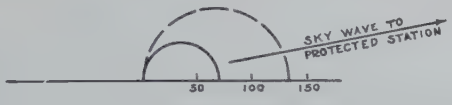

VERTICAL RADIATION PATTERN
(MV/m AT ONE MILE)
POWER = 500 WATTS

Fig. 19

In (57), the shape of the diagram is determined by the term

$$\left[1 + M \angle \alpha - \frac{2\pi d}{\lambda} \sin\theta \cos\phi\right] = \sqrt{1 + M^2 + 2M \cos(\alpha - kd \sin\theta \cos\phi)}. \quad (60)$$

The scale is determined by the magnitude of I_0. From (43), I_0 is given as

$$I_0 = \frac{\sqrt{P}}{\sqrt{36.6(1 + M^2) + 2MR_m \cos\alpha}}. \quad (61)$$

The shape and size of the diagram is determined by the product of (60) and (61).

Let us now choose a new current ratio, M', of such a value that

$$M' = \frac{1}{M}. \quad (62)$$

Then (60) becomes

$$\sqrt{1 + (M')^2 + 2M' \cos(\alpha - kd \sin\theta \cos\phi)} \quad (63)$$

and (61) becomes

$$I_0' = \frac{\sqrt{P}}{\sqrt{36.6(1 + M'^2) + 2M'R_m \cos\alpha}}. \quad (64)$$

Substituting (62) in (64),

$$I_0' = \frac{\sqrt{P}}{\sqrt{36.6\left(1 + \frac{1}{M^2}\right) + \frac{2R_m}{M} \cos\alpha}} = \frac{M\sqrt{P}}{\sqrt{36.6(1 + M^2) + 2R_m M \cos\alpha}}. \quad (65)$$

Making the same substitution in (63) yields

$$\frac{1}{M}\sqrt{1 + M^2 + 2M \cos (\alpha - kd \sin \theta \cos \phi)}. \tag{66}$$

Thus the product of (65) and (66) is identical with the product of (60) and (61). We thus arrive at the conclusion that the radiation pattern will be unaltered in size or shape when the current ratios are interchanged. That is, the condition

$$\bar{I}_1 = M\bar{I}_0 \angle + \alpha$$

will yield the same result as the condition

$$\bar{I}_1 = \frac{1}{M} \cdot \bar{I}_0 \angle + \alpha.$$

Let us now see how our terminal conditions are altered in the example we have been considering.

From (65) we see that now

$$I_0 = 2.86 \text{ amperes}$$

and,

$$I_1 = 4.27 \text{ amperes.}$$

Then,

$$R_1 = 0.67[22.5 - 36.6] + 36.6 = 27.18 \text{ ohms}$$

and,

$$P_1 = 4.27^2 \times 27.18 = 495.0 \text{ watts}$$

while,

$$R_0 = \frac{1}{0.67}[12.5 - 36.6] + 36.6 = 0.61 \text{ ohms}$$

and,

$$P_0 = 2.86^2 \times 0.61 = 5.0 \text{ watts.}$$

Thus we see that a very small amount of power will be fed to antenna 0. In fact, it is so small that we need not feed this antenna at all but can simply operate it as a parasitic reflector by properly tuning it.

V. Multielement Driven Arrays

The two-element arrays are limited in use since the horizontal space pattern is symmetrical about the line of antennas. Furthermore, we saw that it was not possible to increase the field strength more than ninety per cent over that obtainable with a single antenna. It is often desirable to use more than two antennas to distort the pattern in a

variety of ways when more than one station is to be protected. In short-wave practice, a number of elements are used to concentrate the energy in narrow beams.

The method of attack will be illustrated by an example. Suppose that a station, at present operating on a power of 500 watts, contemplates increasing the power to 1000 watts. The main service area lies west of the station, with areas of secondary importance lying east and south of the station. Three other stations, on the same or adjacent channels must be protected. Station A lies due north, while Station

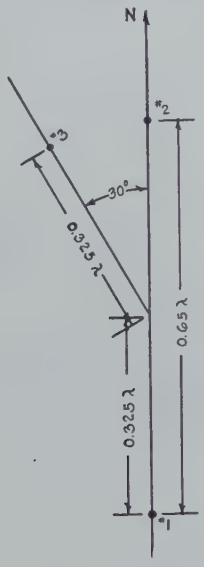

Fig. 20

B is located forty degrees south of west, with Station C forty-five degrees south of east. The array which gives the desired results, consists of three one-quarter wave antennas disposed as shown in Fig. 20.

The currents are related as follows:

$$\left.\begin{aligned} \bar{I}_1 &= \bar{I}_2 \\ \bar{I}_3 &= +0.5 \cdot \bar{I}_1 \angle -90^\circ \end{aligned}\right\}. \tag{67}$$

The mutual impedances are

$$\left.\begin{aligned} \bar{Z}_{12} &= 13.2 \angle -168^\circ \\ \bar{Z}_{13} &= 12.0 \angle -152^\circ \\ \bar{Z}_{23} &= 30.0 \angle -8^\circ \\ \bar{Z}_{11} &= \bar{Z}_{22} = \bar{Z}_{33} = 36.6 + j21.25 \end{aligned}\right\}. \tag{68}$$

Then the three circuit equations become

$$\left.\begin{aligned} \bar{V}_1 &= \bar{I}_1\bar{Z}_{11} + \bar{I}_2\bar{Z}_{21} + \bar{I}_3\bar{Z}_{31} \\ \bar{V}_2 &= \bar{I}_1\bar{Z}_{12} + \bar{I}_2\bar{Z}_{22} + \bar{I}_3\bar{Z}_{32} \\ \bar{V}_3 &= \bar{I}_1\bar{Z}_{13} + \bar{I}_2\bar{Z}_{23} + \bar{I}_3\bar{Z}_{33} \end{aligned}\right\}. \tag{69}$$

Substituting (67) and (68) in (69),

$$\left.\begin{aligned} \bar{V}_1 &= \bar{I}_1[36.6 + j21.25 + 13.2 \angle -168^\circ \\ &\qquad + 0.5 \times 12.0 \angle -242^\circ] \\ \bar{V}_2 &= \bar{I}_2[36.6 + j21.25 + 13.2 \angle -168^\circ \\ &\qquad + 0.5 \times 30.0 \angle -98^\circ] \\ \bar{V}_3 &= \bar{I}_3\left[36.6 + j21.25 + \frac{30.0}{0.5} \angle +82^\circ + \frac{12.0}{0.5} \angle -62^\circ\right] \end{aligned}\right\} \tag{70}$$

or,

$$\left.\begin{aligned} \bar{V}_1 &= \bar{I}_1[20.89 + j23.845] \\ \bar{V}_2 &= \bar{I}_2[21.61 + j3.72] \\ \bar{V}_3 &= \bar{I}_3[56.2 + j59.55] \end{aligned}\right\}. \tag{71}$$

We thus see that the resistance and reactance of each antenna is greatly affected by the neighboring elements. The total power is

$$P_T = 20.89 \cdot I_1^2 + 21.61 \cdot I_2^2 + 56.2 \cdot I_3^2 \tag{72}$$

or,

$$P_T = [20.89 + 21.61 + 0.5^2 \times 56.2]I_1^2 = 56.55 \cdot I_1^2. \tag{73}$$

When the power is 1000 watts,

$$I_1 = I_2 = \sqrt{\frac{1000}{56.55}} = 4.21 \text{ amperes}$$

and $I_3 = 2.105$ amperes.
Then the power in each antenna is

$$\left.\begin{aligned} P_1 &= 4.21^2 \times 20.89 = 370 \text{ watts} \\ P_2 &= 4.21^2 \times 21.61 = 383 \text{ watts} \\ P_3 &= 2.105 \times 56.2 = 247 \text{ watts} \end{aligned}\right\}. \tag{74}$$

The horizontal pattern is given by

$F(mv/m \text{ at one mile})$

$$= 37.35[2 \mid I_1 \mid \cos(117^\circ \cos\phi) + \mid I_3 \mid \angle -90^\circ + 117^\circ \cos(\phi - 30^\circ)]$$

$$= 312.0[\cos(117^\circ \cos\phi) + 0.25 \angle -90^\circ + 117^\circ \cos(\phi - 30^\circ)] \tag{75}$$

where ϕ is measured counterclockwise from north. The horizontal polar diagram is shown by Fig. 21.

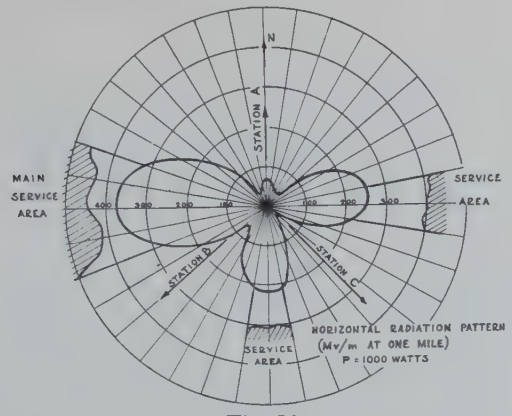

Fig. 21

VI. A Single Parasitic Reflector

(*a*). *The Transmitting Case*

We will next consider the case of an antenna with a single parasitic element. In Fig. 22, 0 denotes the antenna driven by the transmitter while No. 1 is the parasitic element excited by radiation coupling. This element is grounded through a reactance. For simplicity, we will consider each antenna to be one-quarter wave tall.

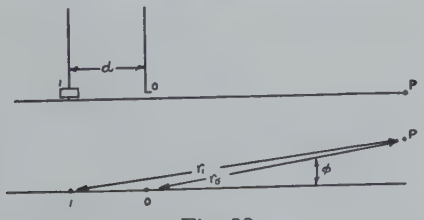

Fig. 22

Writing Kirchoff's law for the two circuits involved,

$$\left.\begin{aligned} \bar{V}_0 &= \bar{I}_0\bar{Z}_{00} + \bar{I}_1\bar{Z}_{01} \\ 0 &= \bar{I}_0\bar{Z}_{01} + \bar{I}_1\bar{Z}_{11} \end{aligned}\right\}. \tag{76}$$

The parasitic current is expressed in terms of the main antenna current, thus,

$$\bar{I}_1 = -\frac{\bar{I}_0\bar{Z}_{01}}{\bar{Z}_{11}} = -\frac{\bar{I}_0|\,Z_{01}\,|}{|\,Z_{11}\,|}\angle\,\theta_m - \tau = \bar{I}_0|\,Z_{01}\,|\angle + \beta \tag{77}$$

where,

θ_m = phase angle of the mutual impedance

$\tau = \tan^{-1}\dfrac{X_{11}}{R_{11}}$

X_{11} = reactance of the reflector antenna proper plus the grounding reactor.

β = angle by which I_1 leads $I_0 = 180° + \theta_m - \tau$.

The field at a point, P, is

$$F = +j\frac{60}{r_0}\left[\bar{I}_0 + \bar{I}_1 \angle -\frac{2\pi d}{\lambda}\cos\phi\right] \angle -2\pi r_0/\lambda$$

$$= +j\frac{60\bar{I}_0}{r_0}\left[1 + \frac{|\bar{Z}_{01}|}{|\bar{Z}_{11}|} \angle \beta - kd\cos\phi\right] \angle -\frac{2\pi r_0}{\lambda}. \qquad (78)$$

The resistance and reactance of the main antenna is given by

$$\bar{V}_0 = \bar{I}_0\left[\bar{Z}_{00} - \frac{\bar{Z}_{01}^2}{\bar{Z}_{11}}\right] \qquad (79)$$

or,

$$\bar{V}_0 = \bar{I}_0\left[R_{00} - \frac{|Z_{01}|^2}{|Z_{11}|}\cos(2\theta_m - \tau) + j\left\{X_{00} - \frac{|Z_{01}|^2}{|Z_{11}|}\sin(2\theta_m - \tau)\right\}\right]. \qquad (80)$$

Then the resistance of the main antenna with the parasitic element present is

$$R_0 = R_{00} - \frac{|Z_{01}|^2}{|Z_{11}|}\cos(2\theta_m - \tau). \qquad (81)$$

The reactance of the main antenna changes from X_{00} to

$$X_{00} - \frac{|Z_{01}|^2}{|Z_{11}|}\sin(2\theta_m - \tau).$$

Thus, to tune the main antenna to resonance, we must assign a value to X_{00} so that

$$X_{00} = \frac{|Z_{01}|^2}{|Z_{11}|}\sin(2\theta_m - \tau). \qquad (81a)$$

For a constant power, P_0, the antenna current is

$$I_0 = \sqrt{\frac{P_0}{R_0}}. \tag{82}$$

The field intensity expressed as a fraction of that obtained with the same power into a single antenna is

$$\frac{F}{F_0} = \sqrt{\frac{R_{00}}{R_0}}\left[1 + \frac{|Z_{01}|}{|Z_{11}|} \angle \beta - kd \cos \phi\right]. \tag{83}$$

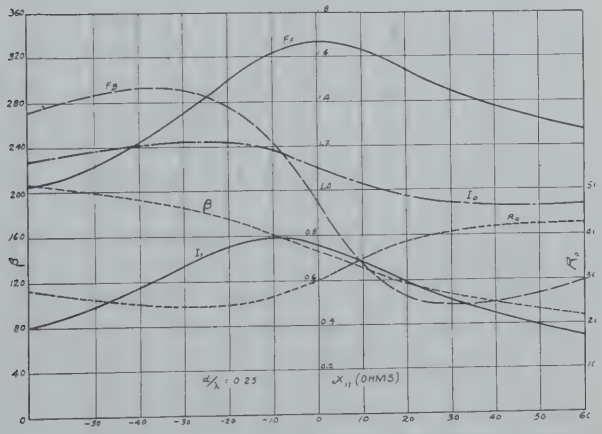

Fig. 23—The effect on the circuit conditions of tuning a parasitic reflector. (Spacing between antenna and reflector = 0.25λ.)

When $\phi = 0$, (83) yields the field in a forward direction

$$\frac{F_F}{F_0} = \sqrt{\frac{R_{00}}{R_0}}\left[1 + \frac{|Z_{01}|}{|Z_{11}|} \angle \beta - kd\right]. \tag{84}$$

When $\phi = 180$ degrees, the field in the backward direction becomes

$$\frac{F_B}{F_0} = \sqrt{\frac{R_{00}}{R_0}}\left[1 + \frac{|Z_{01}|}{|Z_{11}|} \angle \beta + kd\right]. \tag{85}$$

Fig. 23 shows F_F, F_B, I_0, I_1, R_0, and β as a function of X_{11} for a spacing $d = 0.25\lambda$. The currents and electric intensities are expressed in terms of the values which would obtain if a single antenna were operated at the same power. We see that as the parasitic reflector is detuned by making X_{11} large in magnitude, the quantities in question approach the values obtained with a single antenna.

Fig. 24 shows the same quantities for a spacing, $d = 0.1\lambda$.

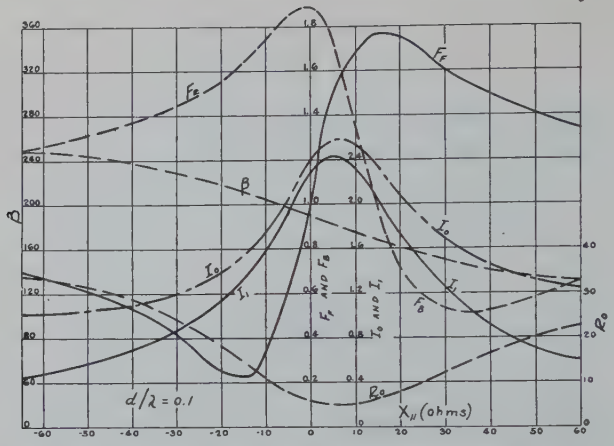

Fig. 24—Similar to Fig. 23, except that spacing is 0.1λ.

From Figs. 23 and 24, as well as similar diagrams for other spacings, it is possible to find the maximum F_F and F_B that may be obtained for each spacing. The result of such a procedure is shown by Fig. 25. The corresponding values of X_{11}, the reactance of the parasitic element, are

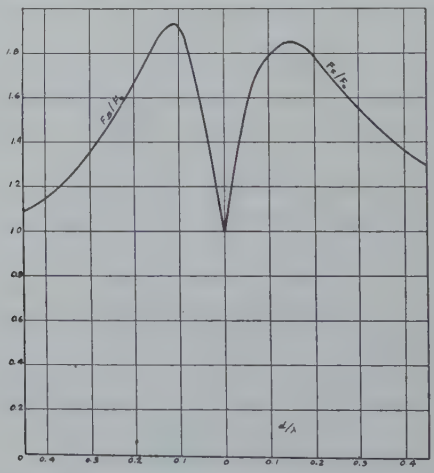

Fig. 25—The maximum increase in forward and backward signal as a function of spacing between the antenna and the reflector.

given by Fig. 26, while Fig. 27 illustrates the values of resistance as measured at the terminals of the driven antenna when maximum forward or backward field is being obtained.

An inspection of Fig. 25 shows that a spacing of one-quarter wave is not an optimum value for either maximum forward or backward radiation. Much smaller spacings are preferable.

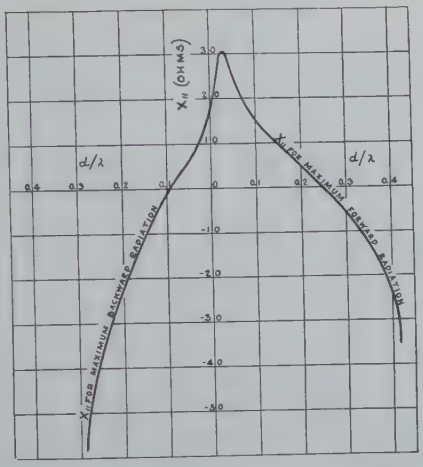

Fig. 26—The tuning condition for maximum forward or backward radiation.

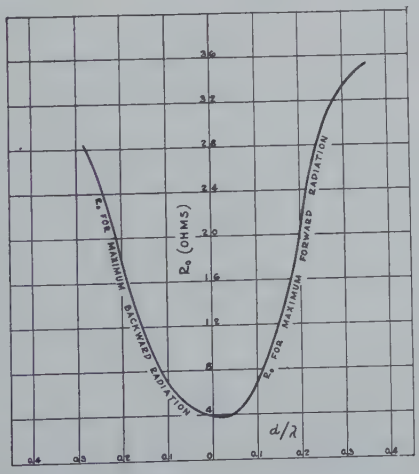

Fig. 27—The radiation resistance measured at the main antenna terminals when the reflector is adjusted for maximum forward or backward radiation.

Fig. 28 shows horizontal polar diagrams for a number of spacings and tunings of the parasitic element. The circles indicate the value of field intensity obtained from a nondirectional antenna operated at the same power.

Another case of interest is that in which the parasitic antenna is self-resonanted so that $X_{11}=0$.

Then,

$$R_{11} = 36.6 \text{ ohms}$$
$$\tau = 0$$
$$\beta = 180 + \theta_m$$

$$R_0 = R_{00} - \frac{|Z_{01}|^2}{R_{11}} \cos(2\theta_m) \tag{86}$$

$$\frac{F_F}{F_0} = \sqrt{\frac{R_{00}}{R_0}}\left[1 - \frac{|Z_{01}|}{R_{11}} \angle \theta_m - kd\right] \tag{87}$$

$$\frac{F_B}{F_0} = \sqrt{\frac{R_{00}}{R_0}}\left[1 - \frac{|Z_{01}|}{R_{11}} \angle \theta_m + kd\right]. \tag{88}$$

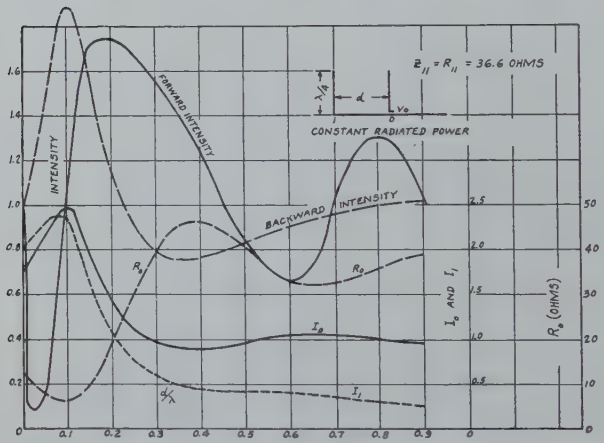

Fig. 29—The circuit conditions when the reflector is self-resonant.

The various pertinent quantities are shown in Fig. 29 as a function of d/λ.

(*b*). *The Receiving Case*

Before proceeding with the analysis of a receiving antenna with a parasitic reflector, we must examine the case of a single receiving antenna. Let us suppose that in the transmitting case (Fig. 22), the parasitic reflector is moved away from the main antenna a great distance, many miles if we wish. However, equations (76) are still valid. They are rewritten here for ease of reference.

$$\bar{V}_0 = \bar{I}_0\bar{Z}_{00} + \bar{I}_1\bar{Z}_{01} \tag{89}$$

$$0 = \bar{I}_0\bar{Z}_{01} + \bar{I}_1\bar{Z}_{11}. \tag{90}$$

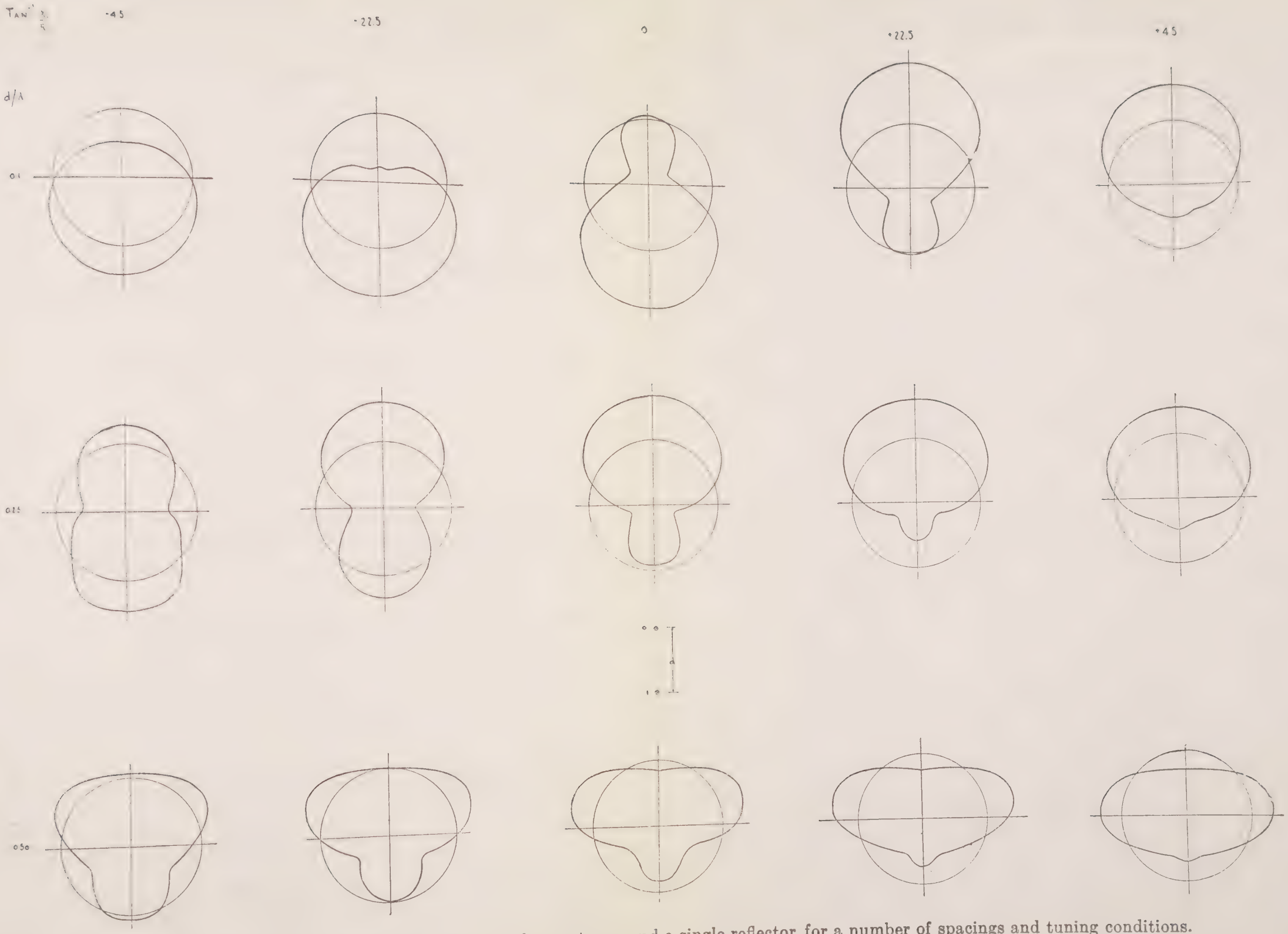

Fig. 28—The horizontal radiation patterns of an antenna and a single reflector, for a number of spacings and tuning conditions.

With this large separation, we have no trouble in visualizing antenna 0 as the transmitter and antenna 1 as the receiving antenna. The current in antenna 1 is so weak that the reaction back into antenna 0 is negligible so that (89) becomes

$$\bar{V}_0 = \bar{I}_0 \bar{Z}_{00}. \tag{91}$$

Thus I_0 remains independent of anything that transpires in the circuit of antenna 1.

From (90),

$$-\bar{I}_0 \bar{Z}_{01} = \bar{I}_1 \bar{Z}_{11}. \tag{92}$$

The term $-\bar{I}_0 \bar{Z}_{01}$ may then be regarded as a voltage induced in antenna 1. This voltage is constant in magnitude.

Let us now turn to the definition of Z_{01} as given by (14)

$$\bar{I}_0 \bar{I}_1 \bar{Z}_{01} = p_m = -\int_{y=0}^{y=a} F_y i_y dy. \tag{93}$$

Then,

$$-\bar{I}_0 \bar{Z}_{01} = \frac{1}{I_1} \int_{y=0}^{y=a} F_y i_y dy. \tag{94}$$

Here F_y is the electric intensity along antenna 1 due to the current in antenna 0. Because of the large separation between antennas, this intensity is essentially constant over the antenna length. Then

$$-\bar{I}_0 \bar{Z}_{01} = \frac{F}{I_1} \int_{y=0}^{y=a} i_y dy. \tag{95}$$

Then,

$$E_i = -\bar{I}_0 \bar{Z}_{01} = Fh \tag{96}$$

where,

E_i = the induced voltage

$h = \frac{1}{I_1} \int_{y=o}^{y=a} i_y dy$ = the effective height, which is a function of configuration, only.

For the top-loaded antenna of Fig. 1,

$$h = \frac{\lambda}{2\pi} \frac{\cos B - \cos G}{\sin G}. \tag{97}$$

For a simple quarter-wave antenna with no top loading, the effective height is simply

$$h = \frac{\lambda}{2\pi}. \tag{98}$$

We are now ready to attack the case of a receiving antenna and a parasitic reflector. The receiving case may be divided into two distinct classes. First, if we have available a detecting device which requires no power for its operation and the antennas themselves have only slight losses, we are primarily interested in getting as large a current as possible in the main antenna element. With no losses, all of the energy absorbed by the wave is reradiated. In the second case, however, where the detector has a finite resistance, we are interested in absorbing in the detector resistance as much power as possible. For the present, we will examine a few cases which fall under the first class.

We shall first consider two antennas placed broadside to the wave front (Fig. 30).

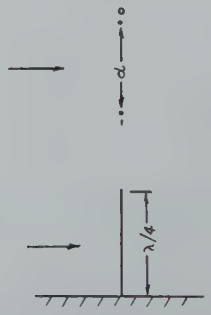

Fig. 30

Then,

$$\bar{E}_0 = \bar{I}_0\bar{Z}_{00} + \bar{I}_1\bar{Z}_{10} \tag{99}$$

$$\bar{E}_1 = \bar{I}_0\bar{Z}_{10} + \bar{I}_1\bar{Z}_{11} \tag{100}$$

where $\bar{E}_0$ and $\bar{E}_1$ are the voltages induced by the impinging wave. Let us next assume that each antenna is self-resonanted so that $X_{00} = X_{11} = 0$.

Since,

$$\bar{E}_0 = \bar{E}_1, \qquad \bar{I}_0 = \bar{I}_1,$$

so that,

$$\bar{I}_0 = \frac{\bar{E}_0}{R_{00} + \bar{Z}_{10}}. \tag{101}$$

The current in a single antenna with the other antenna absent is

$$\bar{I}_0' = \frac{\bar{E}_0}{R_{00}} \tag{102}$$

and,

$$\bar{I}_0/\bar{I}_0' = \frac{1}{1 + \bar{Z}_{01}/R_{00}}. \tag{103}$$

The absolute value of this ratio is shown by Fig. 31. The experimental points are those given by C. R. Fountain.[10]

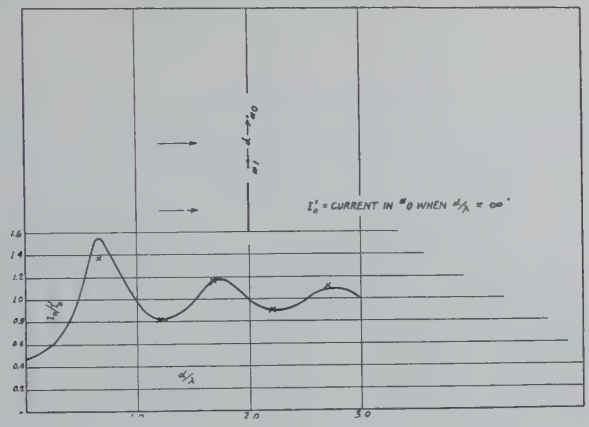

Fig. 31—Two receiving antennas in broadside.

The experimental values shown on Fig. 31 are obtained by taking the square root of Fountain's measurements, since he apparently used a square-law indicator.

Suppose the antennas are placed in the line of propagation of the wave. (Fig. 32.) Then the induced voltages are related thus:

$$\bar{E}_1 = \bar{E}_0 \angle -2\pi d/\lambda. \tag{104}$$

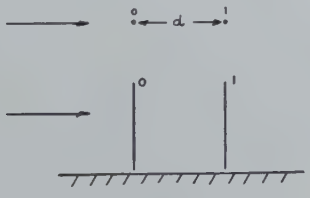

Fig. 32

Then we assume that $X_{00}=X_{11}=0$, and the current in antenna 0 becomes

$$\bar{I}_0 = \frac{\bar{E}_0[R_{11} - \bar{Z}_{10} \angle -2\pi d/\lambda]}{R_{00}R_{11} - \bar{Z}_{10}^2}. \tag{105}$$

As shown in (102), the current in a single antenna with the other antenna absent is

$$\bar{I}_0' = \frac{\bar{E}_0}{R_{00}}. \tag{106}$$

[10] C. R. Fountain, *Phys. Rev.*, ser. 2, vol. 43, p. 384; March 1, (1933).

Dividing (105) by (106) and noting that $R_{00}=R_{11}$,

$$\frac{\bar{I}_0}{\bar{I}_0'}=\frac{1-\dfrac{\bar{Z}_{10}}{R_{00}}\angle -2\pi d/\lambda}{1-Z_{10}^2/R_{00}^2}. \tag{107}$$

Fig. 33 shows the mode of variation of (107) as a function of spacing. The results shown on the left side of the figure, where antenna

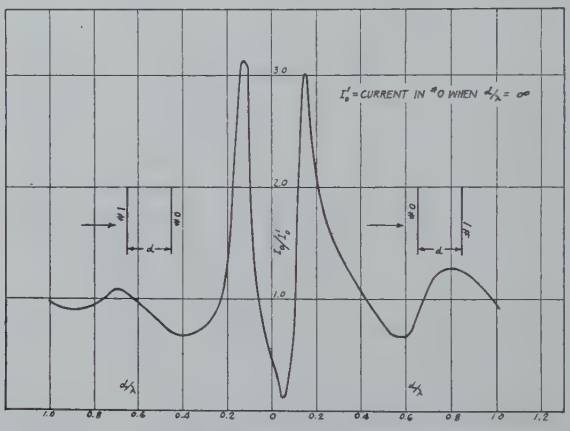

Fig. 33—"End-on" array of a receiving antenna and a single reflector. Both antennas are self-resonant.

1 is in front of antenna 0 with respect to the impinging wave, were obtained by changing $-2\pi d/\lambda$ to $+2\pi d/\lambda$ in (107).

The results of Fig. 33 were verified experimentally in the following manner. Two half-wave rods were arranged as shown by Fig. 34, many wave lengths from a transmitting antenna. A series circuit consisting

Fig. 34

of an inductance and a capacitance were placed at the middle of each rod. A vacuum tube voltmeter was connected across the coil in antenna 0. Since the coil was fixed, the reading of the voltmeter was proportional to the antenna current. The condition, $X_{00}=X_{11}=0$, was achieved by tuning each antenna to maximum response with the other antenna removed.

The value, I_0', was found by removing antenna 1. The experimental results, which bear a striking resemblance to the theoretical curve of Fig. 33, are illustrated in Fig. 35.

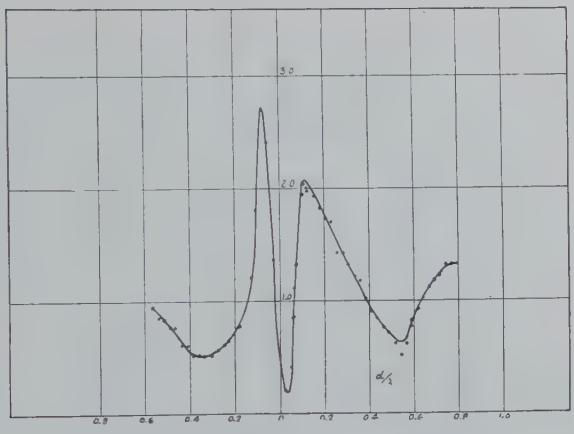

Fig. 35—An experimental verification of Fig. 33.

If the wave is arriving at an angle, ϕ, Fig. 36, and the antennas are not self-resonated, the current in antenna 0 becomes

$$\frac{\bar{I}_0}{\bar{I}_0'} = \frac{R_{00}\left[R_{11} + jX_{11} - \bar{Z}_{01} \angle -\frac{2\pi d}{\lambda}\cos\phi\right]}{(R_{00}R_{11} - X_{00}X_{11}) + j(R_{00}X_{11} + R_{11}X_{00}) - \bar{Z}_{10}^2}. \quad (108)$$

In the transmitting case, we achieved maximum fields when X_{00} and X_{11} were not equal to zero. We shall now attempt to maximize (108). In the first step we shall assume that $R_{00} = R_{11} = 36.6$ ohms, and

Fig. 36

that X^{11} is fixed. Since the spacing is fixed, the only variable is X_{00}. We see that the numerator of (108) is independent of X_{00}. Thus we need find only the condition which makes the denominator a minimum. The denominator is

$$\begin{aligned} D = {} & R_{00}R_{11} - X_{00}X_{11} - |Z_{01}|^2 \cos(2\theta_m) \\ & + j\{R_{00}X_{11} + R_{11}X_{00} - |Z_{01}|^2 \sin(2\theta_m)\} \end{aligned} \quad (109)$$

or,

$$D/R_{00}R_{11} = 1 - \frac{|Z_{10}|^2}{R_{11}^2}\cos(2\theta_m) - \frac{X_{00}}{R_{11}}\cdot\frac{X_{11}}{R_{11}} + j\left\{\frac{X_{11}}{R_{11}} + \frac{X_{00}}{R_{11}} - \frac{|Z_{10}|^2}{R_{11}^2}\sin(2\theta_m)\right\}. \tag{110}$$

Let,

$$a = 1 - \frac{|Z_{10}|^2}{R_{11}^2}\cos(2\theta_m)$$

$$c = X_{11}/R_{11}$$

$$b = \frac{X_{11}}{R_{11}} - \frac{|Z_{10}|^2}{R_{11}^2}\sin(2\theta_m).$$

Then,

$$\left(\frac{D}{R_{00}R_{11}}\right)^2 = \left(a - c\,\frac{X_{00}}{R_{11}}\right)^2 + \left(b + \frac{X_{00}}{R_{11}}\right)^2. \tag{111}$$

Differentiating (111) and setting equal to zero yields

$$\frac{X_{00}}{R_{11}} = \frac{ac - b}{c^2 + 1} \tag{112}$$

or,

$$\frac{X_{00}}{R_{11}} = \frac{\dfrac{X_{11}}{R_{11}}\left(1 - \dfrac{|Z_{01}|^2}{R_{11}^2}\cos(2\theta_m)\right) - \dfrac{X_{11}}{R_{11}} + \dfrac{|Z_{01}|^2}{R_{11}^2}\sin(2\theta_m)}{\dfrac{X_{11}^2}{R_{11}^2} + 1}. \tag{113}$$

This becomes

$$X_{00} = \frac{|Z_{01}|^2}{\sqrt{R_{11}^2 + X_{11}^2}} \times \frac{R_{11}\sin(2\theta_m)}{\sqrt{R_{11}^2 + X_{11}^2}} - \frac{|Z_{10}|^2}{\sqrt{R_{11}^2 + X_{11}^2}} \times \frac{X_{11}\cos(2\theta_m)}{\sqrt{R_{11}^2 + X_{11}^2}}. \tag{114}$$

Let,

$$\tau = \tan^{-1}\frac{X_{11}}{R_{11}} \tag{115}$$

and (114) becomes

$$X_{00} = \frac{|Z_{10}|^2}{|Z_{11}|}\left[\sin(2\theta_m)\cos\tau - \sin\tau\cos(2\theta_m)\right] = \frac{|Z_{10}|^2}{|Z_{11}|}\sin(2\theta_m - \tau). \tag{116}$$

Thus X_{00} must have the same value as that given by (81a) for the transmitting case. The value assigned to X_{00} is independent of the angle of arrival of the wave. Fig. 37 shows the value X_{00}, for maximum current, plotted as a function of X_{11}, when the spacing, d, is 0.25λ.

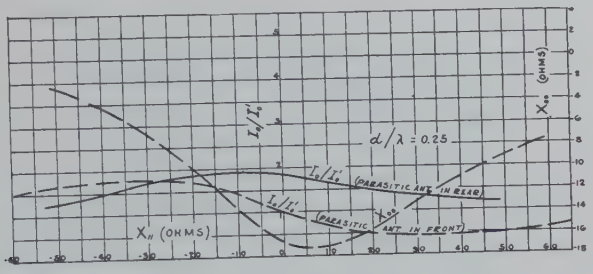

Fig. 37

When the parasitic antenna 1 is farther from the transmitter than antenna 0, we shall say it is in the rear of the main antenna, while in the reverse position we shall say it is in front. When in the rear, $\phi = 0$ degrees in (108), while $\phi = 180$ degrees corresponds to placing antenna

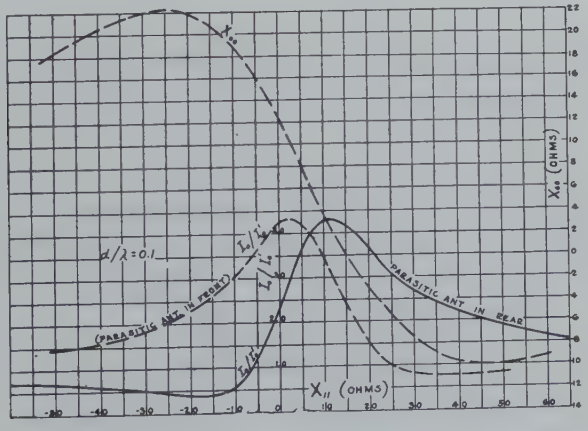

Fig. 38

1 in front. Fig. 37 shows the results of substituting the values of (116) in (108) with $\phi = 0$ degrees and $\phi = 180$ degrees. Fig. 38 is similar to Fig. 37 except that $d = 0.1\lambda$.

From Figs. 37 and 38, and similar diagrams, it is possible to pick off values of the maximum current obtainable for each spacing. The

results of such procedure are shown by Fig. 39. The circles on this diagram were obtained experimentally using the arrangement of Fig. 34. For each spacing, the capacitors in each antenna were juggled simultaneously to obtain maximum deflection on the voltmeter.

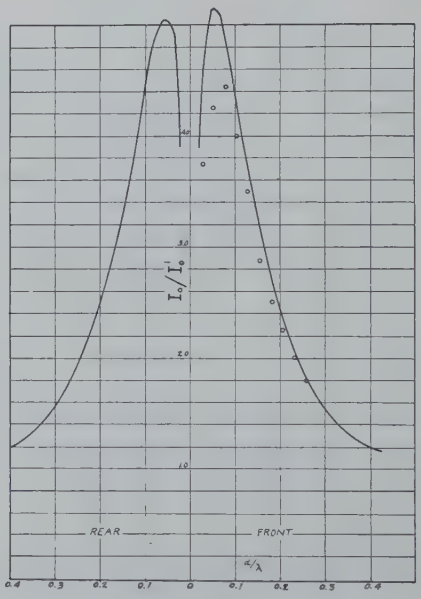

Fig. 39—The maximum increase available from a receiving antenna and a single tuned reflector.

Fig. 40 shows the horizontal polar diagram for a number of cases. In each case, the signal was maximized with the parasitic antenna in front of the main antenna. The left-hand figure is calculated for the following conditions:

$$d/\lambda = +0.1$$
$$X_{00} = +10.3 \text{ ohms}$$
$$X_{11} = +25.0 \text{ ohms.}$$

The figure in the center corresponds to the conditions below

$$d/\lambda = 0.05$$
$$X_{00} = +19.1 \text{ ohms}$$
$$X_{11} = +10.0 \text{ ohms}$$

while the figure on the extreme right is an experimentally determined curve for $d = 0.075\lambda$.

Let us next assume that our receiving device has a finite resistance so that it is necessary to abstract as much power as possible from the

wave. Then to get the proper energy transfer, our detector will be connected to antenna 0 through an impedance matching network. This circuit will then offer a resistance R to the circuit of antenna 0. Then the total resistance R_{00} of this antenna will be the sum of the radiation

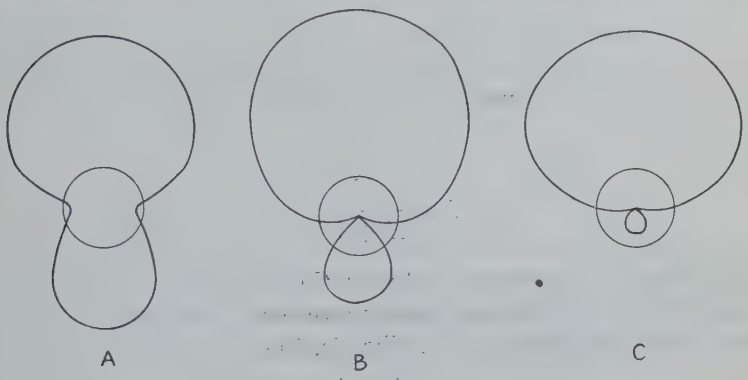

Fig. 40—A. $d/\lambda = 0.1$
$X_{00} = +10.3$ ohms
$X_{11} = +25.0$ ohms
B. $d/\lambda = 0.05$
$X_{00} = +19.1$ ohms
$X_{11} = +10.0$ ohms
C. $d/\lambda = 0.075$ (experimental)

resistance, $R_r = 36.6$, and the load resistance, R. The resistance, R_{11}, will be only that of radiation. The equivalent circuit is shown by Fig. 41. The object is to adjust, in order, X_{00} and R to give maximum power in R for a fixed spacing and a fixed value of X_{11}.

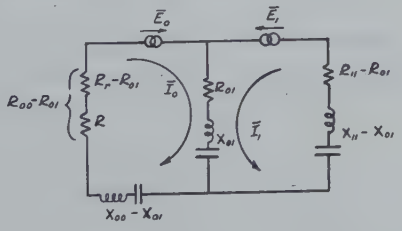

Fig. 41

When antenna 1 is removed the power dissipated in R, located at the center of antenna 0, is

$$P_0' = \frac{E_0^2 R}{(R_r + R)^2} \text{ watts.} \tag{117}$$

The power dissipated is maximum when $R = R_r$ so that

$$P_0' \text{ (maximum)} = E_0^2/4R_r. \tag{118}$$

The power dissipated in R when the parasitic reflector is present is I_0^2R. We shall obtain the current by means of Thevenin's theorem, which may be stated in its steady-state form as follows:[11]

"If an impedance Z be connected between any two points of a circuit, the resulting (steady-state) current I through the impedance is the ratio of the potential difference V between the two points, prior to the connection, and the sum of the values of (1) the connected impedance and (2) the impedance of the circuit, measured between the two points."

That is,

$$I = \frac{V}{Z + Z'}.$$

The impedance Z' measured between the two terminals is given by (81) and (81a). Then for maximum power extraction, the impedance, Z, must be the conjugate of Z'. That is, the added resistance will be

$$R = R_0 = R_r - \frac{|Z_{01}|^2}{|Z_{11}|} \cos(2\theta_m - \tau)$$

while enough reactance must be added to cancel the self-reactance of the antenna itself and the transfer reactance,

$$-\frac{|Z_{01}|^2}{|Z_{11}|} \sin(2\theta_m - \tau).$$

Then,

$$I_0 = \frac{V}{2R_0}. \tag{119}$$

When antenna 0 is open-circuited, the voltage V is

$$\bar{V} = \bar{E}_0 - \bar{I}_1\bar{Z}_{10} \tag{120}$$

where,

$$\bar{E}_1 = \bar{E}_0 \angle -\frac{2\pi d}{\lambda} \cos\phi = \bar{I}_1\bar{Z}_{11}. \tag{121}$$

Then,

$$\begin{aligned} \bar{V} &= \bar{E}_0\left[1 - \frac{\bar{Z}_{10}}{Z_{11}} \angle -\frac{2\pi d}{\lambda}\cos\phi\right] \\ &= \bar{E}_0\left[1 + \frac{|Z_{10}|}{|Z_{11}|} \angle \beta - kd\cos\phi\right] \end{aligned} \tag{122}$$

[11] T. E. Shea, "Transmission Networks and Wave Filters," D. van Nostrand, Inc., Chapter II, p. 55.

where,

$$\beta = 180° + \theta_m - \tau$$
$$\tau = \tan^{-1} X_{11}/R_{11}.$$

Then the power dissipated in R is

$$P_0 = I_0^2 R = \left(\frac{V}{2R_0}\right)^2 R_0$$
$$= \frac{E_0^2}{4R_0}\left| 1 + \frac{|Z_{10}|}{|Z_{11}|} \angle \beta - kd\cos\phi \right|^2. \tag{123}$$

The power gain over a single antenna is found by dividing (123) by (118).

$$\frac{P_0}{P_0'} = \frac{R_r}{R_0}\left| 1 + \frac{|Z_{10}|}{|Z_{11}|} \angle \beta - kd\cos\phi \right|^2. \tag{124}$$

Comparison of (124) and (83) shows that the voltage gain across the detector in the receiving case is identical with the field intensity gain in the transmitting case. We can then use the information of Section VI(*a*) to supply the story of the receiving antenna operating into a detector of finite resistance.

Another case of some practical importance will be treated. The main antenna is so detuned (or has so much impedance in its base that the current flowing in this antenna is very small compared to that in the parasite). This condition may be met where a high impedance detector is inserted directly into the antenna circuit or when the antenna feeds directly into a transmission line.

The voltage induced in antenna 0 by the wave alone is E_0'. The voltage induced by the current in the adjacent antenna is $-\bar{I}_1\bar{Z}_{10}$ so that the total induced voltage is

$$\bar{E}_0 = \bar{E}_0' - \bar{I}_1\bar{Z}_{10}. \tag{125}$$

But,

$$\bar{E}_1 = \bar{E}_0' \angle -\frac{2\pi d}{\lambda}\cos\phi = \bar{I}_1\bar{Z}_{11} \tag{126}$$

so that (125) becomes

$$\frac{E_0}{E_0'} = 1 - \frac{\bar{Z}_{10}}{Z_{11}} \angle -\frac{2\pi d}{\lambda}\cos\phi. \tag{127}$$

Fig. 42 shows the voltage gain as a junction of d/λ for $\phi = 0$ degrees and $\phi = 180$ degrees.

At each d/λ, X_{11} is adjusted to give the maximum voltage gain. This reactance is also shown on Fig. 42.

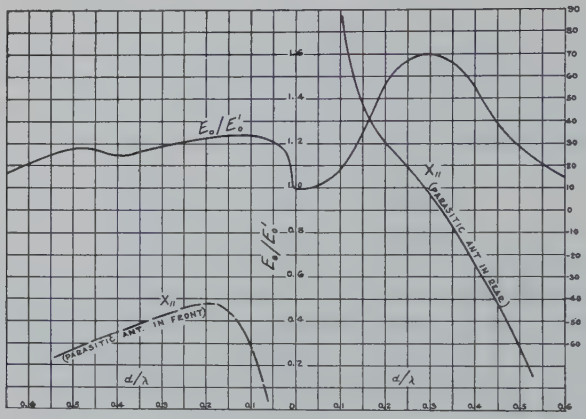

Fig. 42

VII. A Transmitting Antenna With a Number of Parasitic Elements

The foregoing procedure is readily applicable to the analysis of a system containing more than one parasitic element. The treatment is carried through simply as a number of coupled circuits with complex mutual impedances. Let us attack a specific example. Nagy[12] gives the

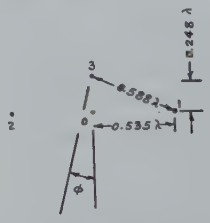

Fig. 43

horizontal polar diagram of an antenna and three parasitic reflectors arranged as shown in Fig. 43. The circuit equations are

$$\left.\begin{aligned} \bar{E}_0 &= \bar{I}_0\bar{Z}_{00} + \bar{I}_1\bar{Z}_{10} + \bar{I}_2\bar{Z}_{20} + \bar{I}_3\bar{Z}_{30} \\ 0 &= \bar{I}_0\bar{Z}_{01} + \bar{I}_1\bar{Z}_{11} + \bar{I}_2\bar{Z}_{21} + \bar{I}_3\bar{Z}_{31} \\ 0 &= \bar{I}_0\bar{Z}_{02} + \bar{I}_1\bar{Z}_{12} + \bar{I}_2\bar{Z}_{22} + \bar{I}_3\bar{Z}_{32} \\ 0 &= \bar{I}_0\bar{Z}_{03} + \bar{I}_1\bar{Z}_{13} + \bar{I}_2\bar{Z}_{23} + \bar{I}_3\bar{Z}_{33} \end{aligned}\right\}. \qquad (128)$$

[12] A. Wheeler Nagy, "An experimental study of parasitic wire reflectors on 2.5 meters," Proc. I.R.E., vol. 24, p. 240, Fig. 8; February, (1936).

From symmetry,

$$\left.\begin{aligned} \bar{I}_1 &= \bar{I}_2 \\ \bar{Z}_{01} &= \bar{Z}_{02} \\ \bar{Z}_{13} &= \bar{Z}_{23} \end{aligned}\right\} \tag{129}$$

so that (128) becomes

$$\left.\begin{aligned} \bar{E}_0 &= \bar{I}_0\bar{Z}_{00} + 2\bar{I}_1\bar{Z}_{01} + \bar{I}_3\bar{Z}_{03} \\ 0 &= \bar{I}_0\bar{Z}_{01} + \bar{I}_1[\bar{Z}_{11} + \bar{Z}_{12}] + \bar{I}_3\bar{Z}_{13} \\ 0 &= \bar{I}_0\bar{Z}_{03} + 2\bar{I}_1\bar{Z}_{13} + \bar{I}_3\bar{Z}_{33} \end{aligned}\right\}. \tag{130}$$

In this case

$$\begin{aligned} \bar{Z}_{00} &= 36.6 \\ \bar{Z}_{01} &= 15.3 \angle -129^\circ \\ \bar{Z}_{03} &= 25.7 \angle -33^\circ \\ \bar{Z}_{13} &= 14.3 \angle -147^\circ \\ \bar{Z}_{12} &= 10.4 \angle +51^\circ. \end{aligned}$$

Placing these numerical values in (130) and solving,

$$\begin{aligned} \bar{I}_1/\bar{I}_0 &= \bar{I}_2/\bar{I}_0 = +0.307 \angle +95^\circ \\ \bar{I}_3/\bar{I}_0 &= +0.929 \angle +142.5^\circ. \end{aligned}$$

When these values are placed in the first equation of (130), we find the impedance measured at the terminals of antenna 0 to be

$$\frac{\bar{E}_0}{\bar{I}_0} = [\bar{Z}_{00} + 0.614 \times 15.3 \angle -34^\circ + 0.929 \times 25.7 \angle +109.5^\circ].$$

The resistance is then

$$R_0 = 36.6 + 7.8 - 7.95 = 36.45 \text{ ohms}$$

and the reactance is +17.15 ohms.

Then the current in antenna 0, for the same power, will be practically unchanged whether the parasitic elements are present or not. The horizontal diagram, expressed in terms of the field of a single nondirectional antenna, is

$$\begin{aligned} F/F_0 = 1 &+ 0.929 \angle +142.5^\circ - 89.5^\circ \cos\phi \\ &+ 0.614 \cos(192.8^\circ \sin\phi) \angle +95^\circ. \end{aligned}$$

When $\phi = 0$ degrees,

$$F_F/F_0 = 2.02$$

while $\phi = 180$ degrees gives

$$F_B/F_0 = 0.41.$$

Fig. 44 shows $(F/F_0)^2$ plotted as a function of ϕ. The field intensity was squared so that it could be compared directly with the results of

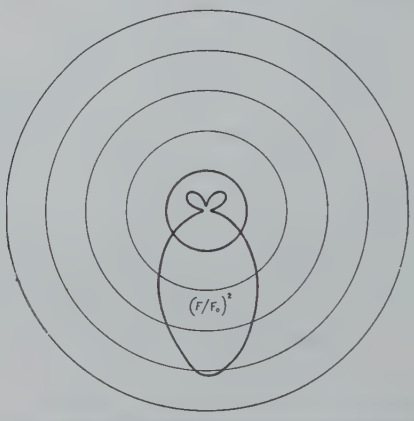

Fig. 44—The horizontal pattern of the array shown in Fig. 43.

Nagy. His measurements were made using a square-law detector. Fig. 45 is a tracing of Nagy's Fig. 8. His curve shows a value of $(F/F_0)^2 = 3$ compared to 4.08 from a theoretical standpoint.

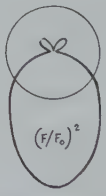

Fig. 45—Nagy's measurements for the array shown in Fig. 43.

VIII. Flat Sheet Reflectors

(a). *The Transmitting Case*

We shall next examine the action of the antenna shown in Fig. 46. The flat sheet is considered to be a perfect conductor, infinite in extent. Then the sheet may be replaced in effect by an image antenna as shown, where the current in the image is equal to the main antenna current and in phase opposition. The field at P due to the antenna is

$$\overline{F}' = j\frac{60\bar{I}_0}{r_0}\epsilon^{-jkr_0}. \qquad (131)$$

The image contributes

$$\bar{F}'' = j\frac{60\bar{I}_1}{r_1}\epsilon^{-jkr_1} = -j\frac{60\bar{I}_0}{r_1}\epsilon^{-jkr_1}. \tag{132}$$

The total field is then

$$\bar{F}_T = j\frac{60\bar{I}_0}{r}\epsilon^{-jkr}\left[\epsilon^{+jkx} - \epsilon^{-jkx}\right] \tag{133}$$

or,

$$|F_T| = \frac{60I_0}{r}(2\sin kx). \tag{134}$$

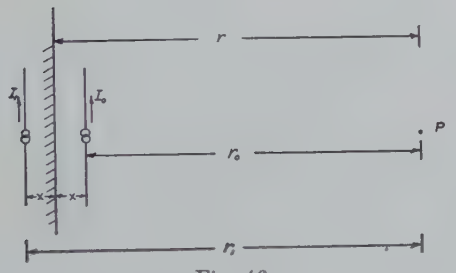

Fig. 46

At the terminals of the antenna

$$\bar{V}_0 = \bar{I}_0\bar{Z}_{00} + \bar{I}_1\bar{Z}_m = \bar{I}_0[\bar{Z}_{00} - \bar{Z}_m]. \tag{135}$$

The resistance of the antenna is then

$$R_0 = R_{00} - R_m \tag{136}$$

while the reactance is

$$X_0 = X_{00} - X_m. \tag{137}$$

For a power, P_1 watts,

$$F_T = \frac{60}{r}\sqrt{\frac{P_1}{R_{00} - R_m}}(2\sin kx). \tag{138}$$

With the sheet absent, and the same power, the antenna produces a field

$$F_0 = \frac{60}{r}\sqrt{\frac{P_1}{R_{00}}} \tag{139}$$

so that the gain ratio is

$$|F_T/F_0| = \frac{2\sin kx}{\sqrt{1 - R_m/R_{00}}}. \tag{140}$$

On Fig. 47, F_T/F_0 is plotted as a solid curve while the two broken curves show the quantities, 2 sin kx and $1\sqrt{1-R_m/R_{00}}$. It is interesting to note that nothing particularly exciting happens when the spacing is one-quarter wave length.

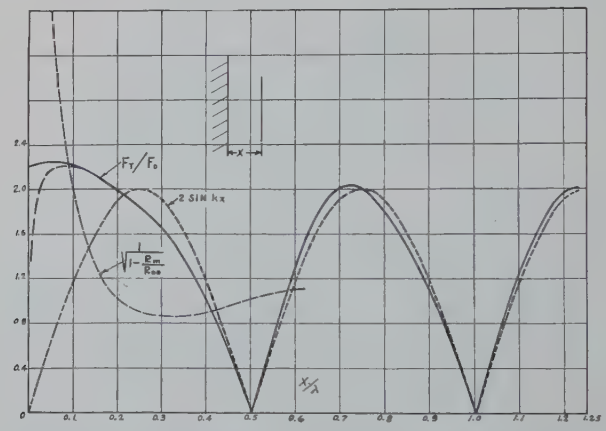

Fig. 47—A transmitting antenna in front of a flat sheet.

The broken curve at the extreme left of Fig. 47 shows the effect of slight losses. We have assumed the antenna to consist of a metallic conductor with an effective loss resistance of 0.5 ohm so that R_{00} is $73.2+0.5=73.7$ ohms.

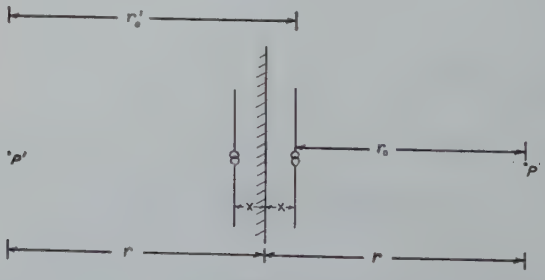

Fig. 48

The value of R_m as obtained from Fig. 7 must be doubled since the present antenna is one-half wave long. Also d/λ on Fig. 7 is $2x/\lambda$ in our present calculations.

The shape of the horizontal polar diagrams are found by inspecting the lower row of figures on Fig. 15. The flat sheet reflector of course yields a unidirectional pattern.

(*b*). *The Receiving Case*

Let us now suppose that the antenna in front of the sheet is a receiving antenna. A transmitter is placed at P. The field at the receiving antenna due to the transmitter at P is

$$\frac{A}{r_0} \angle -kr_0 \doteq \frac{A}{r} \angle -kr \angle +kx. \tag{141}$$

The field at the receiving antenna due to the transmitter image is

$$-\frac{A}{r_0'} \angle -kr_0' \doteq -\frac{A}{r} \angle -kr \angle -kx. \tag{142}$$

Then the total induced voltage due to the impinging wave and its reflection component is

$$\bar{E}_i = 2j \frac{A\lambda}{2\pi} \frac{\sin kx}{r} \angle -kr. \tag{143}$$

But,

$$\bar{E}_i = \bar{I}_0\bar{Z}_{00} + \bar{I}_1\bar{Z}_m = \bar{I}_0[R_{00} - R_m + jX_{00} - jX_m]. \tag{144}$$

X_{00} is made equal to X_m so

$$E_i = \bar{I}_0[R_{00} - R_m] \tag{145}$$

or,

$$\bar{I}_0 = \frac{\bar{E}_i}{R_{00} - R_m} = j \frac{A\lambda}{2\pi} \frac{\angle -kr}{r} \cdot \frac{2 \sin kx}{R_{00} - R_m}. \tag{146}$$

When the sheet is absent,

$$\bar{I}_0' = \frac{A\lambda}{2\pi r} \frac{\angle -kr}{R_{00}} \tag{147}$$

so that,

$$\bar{I}_0/\bar{I}_0' = \frac{2 \sin kx}{1 - R_m/R_{00}}. \tag{148}$$

Fig. 49 shows the ratio, I_0/I_0', as a function of spacing from the sheet. The broken curve is again computed for a loss resistance of 0.5 ohm.

It should be noted that the above treatment applies only to the condition where the detector does not introduce appreciable loss into the system so that practically all of the power taken into the antenna system is reradiated. For the case of a detector of appreciable resist-

ance, where we wish to absorb a maximum amount of power, we may again turn to the transmitting case, just as we did for a parasitic array. Fig. 47 then applies.

IX. Measurement of Mutual Impedance

In the discussion of driven arrays, the consequences of certain current ratios and phase relations were discussed. It was assumed that these relations could be attained. In short-wave work, where the arrays are usually used for the purpose of beaming the energy to furnish point-to-point communication, the correct phases are easily obtained by adjusting the lengths of certain transmission line feeders. In the

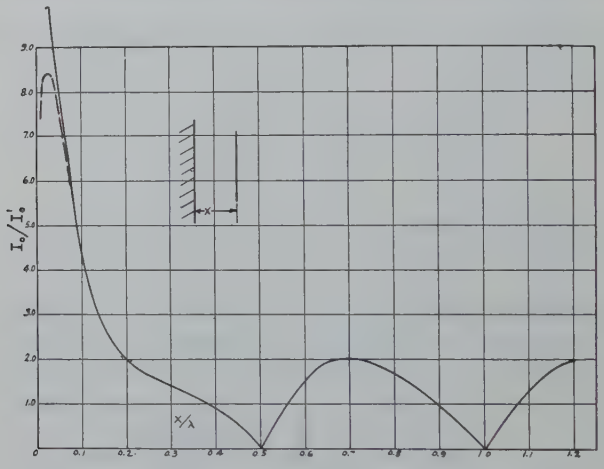

Fig. 49—A receiving antenna in front of a flat sheet.

broadcast range, where the pattern is distorted in numerous odd ways to furnish protection to other stations on the same channel, it is necessary to divide power and shift phase with lumped constant networks. The remainder of this paper will be devoted to methods of design and adjustment of these associated circuits. It will be assumed that the engineer who is adjusting the array is equipped to measure resistance and reactance.

The first step in the adjustment of an array is the determination of the mutual impedance between each pair of antennas in the array. A knowledge of the mutual impedances is necessary not only to assist in the adjustment but also to enable us to measure the power fed into the antenna when the array is in adjustment.

Let us suppose that we wish to measure the mutual impedance between a pair of antennas, 0 and 1. We first isolate antenna 1 from

ground so that no current flows in it. (If it is of such a height that it will resonate when floating, the antenna should be grounded.) Then we proceed to measure the self resistance and reactance of antenna 0, obtaining the values R_{00} and X_{00}. Antenna 0 is then isolated and R_{11} and X_{11} determined at antenna 1. We next connect antenna 1 to ground through a reactance equal to $-X_{11}$, so that this antenna is resonant. We then measure the resistance and reactance at the terminals of antenna 0, and obtain new values, R_0 and X_0. This arrangement is nothing more than the case of a single parasitic reflector, tuned to resonance. Then from (80),

$$R_0 = R_{00} - \frac{|Z_m|^2}{R_{11}} \cos 2\theta_m \tag{149}$$

$$X_0 = X_{00} - \frac{|Z_m|^2}{R_{11}} \sin 2\theta_m. \tag{150}$$

Eliminating between these two equations, we find

$$|Z_m| = \sqrt{R_{11}}[(R_0 - R_{00})^2 + (X_0 + X_{00})^2]^{1/4} \tag{151}$$

and,

$$\theta_m = \tfrac{1}{2} \tan^{-1} \frac{(X_{00} - X_0)}{R_{00} - R_0} \tag{152}$$

where R_{00} and X_{00} are measured with antenna 1 isolated, while R_0 and X_0 are measured with antenna 1 resonated. The components of mutual impedance are

$$R_m = |Z_m| \cos \theta_m \tag{153}$$

and,

$$X_m = |Z_m| \sin \theta_m. \tag{154}$$

Due regard should be given the signs of the reactances in (152) since it is possible for θ_m to lie in any one of the four quadrants. It will be seen that an ambiguity of 180 degrees may arise in using (152). The correct choice may be made by using Fig. 6 as a guide.

In some instances, it will be found desirable to have a certain amount of reactance in antenna 1. The mutual impedance may be of such a phase angle that either $R_0 - R_{00}$ or $X_0 - X_{00}$ is close to zero. To increase the magnitude of the small term, the reactance in antenna 1 is adjusted so that the antenna is no longer resonant. Then X_{11} represents the antenna reactance plus the grounding reactor. Then (151) becomes

$$|Z_m| = (\sqrt{R_{11}^2 + X_{11}^2})^{1/2}[(R_0 - R_{00})^2 + (X_0 - X_{00})^2]^{1/4} \tag{151a}$$

and (152) changes to

$$\theta_m = \frac{1}{2}\tan^{-1}\frac{X_{11}}{R_{11}} + \frac{1}{2}\tan^{-1}\frac{(X_{00} - X_0)}{R_{00} - R_0}. \qquad (152a)$$

X. Means of Adjusting and Feeding a Multielement Array

In Section IV, it was shown that the effective resistance and reactance present at the terminals of an antenna which formed part of an array were generally much different than the resistance and reactance measured when the antenna stood alone.

Let us suppose that an engineer who is adjusting an array first resonates one antenna and adjusts the coupling circuit to the trans-

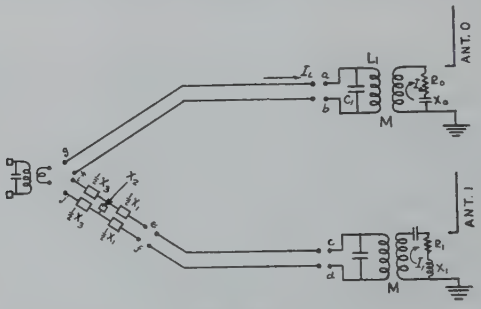

Fig. 50

mission line so that the standing waves on the line are eliminated. This adjustment is made with the other antennas in the array detuned and inoperative. The same adjustment is then made on a second antenna. Then, when both antennas receive power simultaneously it will be found that the coupling circuits are no longer in tune and the lines no longer terminated so that the standing waves are eliminated.

The coupling circuit of the first antenna must then be readjusted. But on readjusting the second antenna, the first will again be thrown out of tune, so that the process of adjustment assumes the characteristics of an endurance contest. If a three- or four-element array is used, this "cut-and-try" method becomes rather hopeless. In searching for a more scientific method, we find that the theory of mutual impedances offers a powerful tool.

Before the adjustment of an array has been started, the relative magnitudes of the antenna currents, as well as the phase relations, have been stipulated. The self-resistance and reactance of each antenna and the mutual impedance between antennas is measured, in accordance with Section IX. From (33), (34), (35), and (36), the impedance offered to the driving circuit by each antenna when the array is in ad-

justment is calculated. Then the terminating circuits are connected to dummy impedances which have these values. (Fig. 50). We shall use parallel wire transmission lines for illustration.

The circuit containing R_0 and X_0 is decoupled from the line tank circuit and loosely coupled to a local oscillator set at the operating frequency of the station. This circuit is then tuned to resonance. Then when the antenna circuit and the line tank circuits are coupled together, the antenna circuit introduces a pure resistance in the branch L_1. Then if C_1 is fixed, as it usually is, L_1 must be varied until the impedance between $a-b$ is equal to Z_c ohms of resistance, where Z_c is the characteristic impedance of the transmission line. This adjustment is made by removing L_1 and C_1 from the circuit and tuning them alone to a frequency, F, where F is determined from the relation

$$F = \frac{f}{\sqrt{1 - \frac{1}{1 + [2\pi f C_1 Z_c]^2}}} \tag{155}$$

where,

f = operating frequency (cycles per second)
C_1 = capacitance of tank condenser (farads)
Z_c = characteristic impedance of line (ohms)
F = tuning frequency (cycles per second).

The elements are then returned to their positions in the circuit and the system is returned to operating frequency. The remaining adjustment is the mutual coupling. This coupling is increased until the condition

$$(\omega M)^2 = \frac{R_0 Z_c}{1 + [2\pi f C_1 Z_c]^2} \tag{156}$$

is fulfilled. This condition is known to be attained when

$$\left| I_{\text{line}}/I_0 \right| = \sqrt{R_0/Z_c} \tag{157}$$

and,

$$\left| I_{c_1}/I_{\text{line}} \right| = 2\pi f C_1 Z_c \tag{158}$$

where I_{c_1} is the current through C_2 and I_{line} is the line current flowing into the tank circuit. A further check may be made to see that all traces of standing waves are removed from the transmission line. The same procedure is then followed in adjusting the dummy load of antenna 1 to its transmission line.

The phase shift between the antenna current and the line current will be a small angle equal to the $\cot^{-1}(2\pi f C_1 Z_c)$.

In usual practice, $2\pi f C_1 Z_c$ is greater than 10 so that the phase shift is less than six degrees. In any event, the phase shift between antenna and line current may be made the same at each antenna by using equal values of $2\pi f C_1 Z_c$. The current in the transmission line at g will lead the current at a by an angle, $2\pi x/\lambda$, where x is the length of the transmission line to antenna 0. Likewise the current in the line at e will lead the current at c by an angle, $2\pi y/\lambda$, where y is the length of the transmission line to antenna 1. Thus if the points, $g-h$ and $e-f$ were paralleled, the two dummy loads would receive equal power, and the currents in the dummy loads would differ in phase by an angle, $2\pi(x-y)/\lambda$. It is hardly ever convenient to make the lengths of the transmission lines such that $2\pi(x-y)/\lambda$ equals the desired angle, α. We have also seen that in general, the two antennas do not receive equal powers, even though the antenna currents may be equal. The proper condition may be achieved by inserting a network between $e-f$ and $i-j$, as shown. This network must offer the proper resistance at $i-j$ to take the correct amount of power. At the same time, the network must shift the phase between its input and output currents an amount, ρ, where

$$\rho = \alpha - \frac{2\pi(x-y)}{\lambda}.$$

The details of the network are shown in Fig. 51. ρ is then the angle by which $I_{e,f}$ leads $I_{i,j}$. It may assume negative values, depending on the

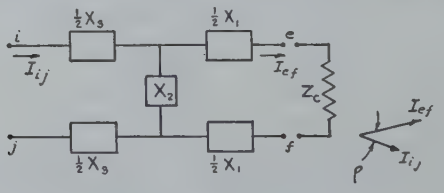

Fig. 51

relative sizes of α, x, and y. The elements of the network are inductive or capacitive reactances determined from the following equations:

$$X_1 = -\sqrt{Z_c R_{i,j}}\left[1 - \sqrt{\frac{Z_c}{R_{i,j}}}\cos\rho\right]/\sin\rho \qquad (159)$$

$$X_2 = +\sqrt{Z_c R_{i,j}}/\sin\rho \qquad (160)$$

$$X_3 = -\sqrt{Z_c R_{i,j}}\left[1 - \sqrt{\frac{R_{i,j}}{Z_c}}\cos\rho\right]/\sin\rho \qquad (161)$$

where $R_{i,j}$ is determined from

$$R_{i,j}/Z_c = P_0/P_1 \tag{162}$$

where P_0 and P_1 are the powers fed to antenna 0 and antenna 1, respectively, as determined from (41) and (42), Section IV.

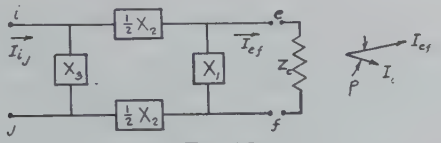

Fig. 52

A π network may be substituted for the T network of Fig. 51. This network is shown in Fig. 52. Then

$$X_1 = \frac{\sqrt{Z_c R_{i,j}} \sin \rho}{1 - \sqrt{\frac{R_{ij}}{Z_c}} \cos \rho} \tag{163}$$

$$X_2 = -\sqrt{Z_c R_{i,j}} \sin \rho \tag{164}$$

$$X_3 = \frac{\sqrt{Z_c R_{i,j}} \sin \rho}{1 - \sqrt{\frac{Z_c}{R_{i,j}}} \cos \rho} \tag{165}$$

With these conditions fulfilled, we may then replace the dummy loads by their respective antennas, and excite the entire system with the main transmitter. If normal care has been exercised, the system should be in close adjustment.

Ammeters in each antenna indicate whether or not the desired current ratio has been obtained.

An indication of phase relationship is a little more difficult. Auxiliary transmission lines are run from each antenna to a point which is preferably equidistant from the antennas. The line is fed by a coil, which is loosely coupled to the antenna. The far end of each line is terminated in a resistance equal to the characteristic impedance of the line. The voltage across the terminating resistor is then impressed on a pair of plates of a cathode-ray oscillograph. The voltage across the terminating resistor of another test line is then impressed on the remaining pair of plates of the oscillograph. The figure on the oscillograph is elliptical. Then the voltage on plate 2 (Fig. 53) leads the voltage on plate 1 by $\sin^{-1}(OA/OB)$. The point, O, is the spot location when no voltage is applied to any plate. The dimensions OA and OB

are easily measured if a piece of ruled celluloid is placed over the end of the cathode-ray tube.

The final test of adjustment is the measurement of the horizontal pattern with field intensity equipment.

A peculiar condition sometimes arises which is apt to puzzle one who is not aware of it. This is the condition where the current ratios are such that one antenna induces more than enough voltage in another antenna to set up the proper current. This condition may often arise in pattern-distorting arrays using three or more antennas. We shall illustrate with an example which utilizes only two antennas. Sup-

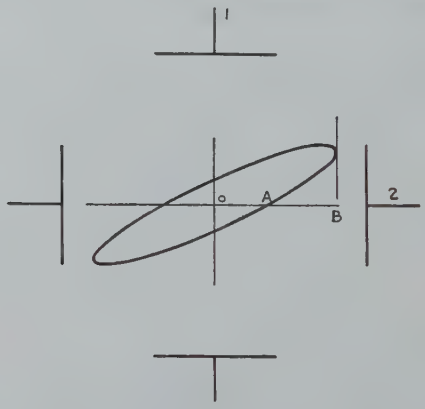

Fig. 53

pose that for some reason it is desirable to use an array in which the antennas are spaced 0.14λ, with a current ratio of 0.5, and a phase angle of 150 degrees between the currents. Then,

$$\begin{aligned} \bar{I}_1 &= M\bar{I}_0\angle + \alpha \\ M &= 0.5 \\ \alpha &= 150^\circ \\ |Z_m| &= 31.8 \\ \theta_m &= 0^\circ \quad \text{from Figs. 5 and 6.} \end{aligned}$$

$$\begin{aligned} R_{00} &= R_{11} = 36.6 \text{ ohms} \\ X_{00} &= X_{11} = +21.25 \text{ ohms} \\ P_T &= \text{total radiated power} = 1000 \text{ watts.} \end{aligned}$$

From (43),

$$1000 = I_0^2[36.6 + (1/2)^2 \cdot 36.6 + 2 \times 1/2 \times 31.8 \cos(150^\circ)]$$

or,

$$I_0 = \sqrt{\frac{1000}{18.1}} = 7.43 \text{ amperes.}$$

Then, from (41),

$$P_0 = 7.43^2[36.6 + 1/2 \times 31.8 \cos (150°)]$$
$$= 7.43^2 \times 22.8 = 1258.0 \text{ watts.}$$

From (42),

$$P_1 = 3.715^2 \left[36.6 + \frac{31.8}{0.5} \cos (-150°)\right]$$
$$= -3.715^2 \times 18.6 = -258.0 \text{ watts.}$$

Thus we see that the transmitter delivers 1000 watts to the system, 1258 watts are passed along one transmission line to antenna 0, and

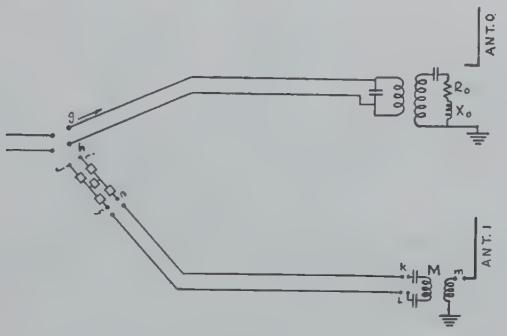

Fig. 54

258 watts come back along the transmission line from antenna 1. Then the termination which eliminates the standing wave on this last transmission line must be on the end of the line nearest the transmitter.

The coupling circuit at antenna 0 may now be adjusted with a dummy load just as we did before in an orthodox array.

The condition of reversal of the direction of power flow in antenna 1 changes the procedure in this part of the system. The coupling system is modified as shown in Fig. 54.

Let us suppose for the moment that the network at the transmitter end is so adjusted that the line is terminated in its characteristic impedance. Then at the antenna end of the line, the impedance between the terminals, $k-l$, looking towards the transmitter, is Z_c, the characteristic impedance of the line. The series capacitors are provided to tune out the reactance of the coil, L_2. This circuit then transfers a resistance into the antenna circuit of $(\omega M)^2/Z_c$ ohms. Then the total impedance of the antenna circuit becomes

$$R_1 + jX_1 = 36.6 + \frac{(\omega M)^2}{Z_c} + j(21.25 + \omega L_1).$$

Since 258 watts were to flow back into the system when the antenna current was 3.715 amperes,

$$258 = 3.715^2(\omega M)^2/Z_c$$

or,

$$(\omega M)^2/Z_c = 18.6 \text{ ohms}$$

so that,

$$R_1 + jX_1 = 55.2 + j(21.25 + \omega L_1).$$

But,

$$\bar{I}_1 = -\frac{I_0\bar{Z}_m}{R_1 + jX_1}.$$

To make

$$\bar{I}_1/\bar{I}_0 = 0.5 \angle +150°$$

we can control X_1.

$$\bar{I}_1/\bar{I}_0 = 0.5 \angle +150° = -\frac{\bar{Z}_m}{R_1 + jX_1} = \frac{31.8 \angle +180°}{R_1 + jX_1}$$

so that,

$$R_1 + jX_1 = 63.6 \angle +30°$$

or,

$$R_1 + jX_1 = 55.2 + j31.8.$$

Then,

$$21.25 + \omega L_1 = 31.8$$

or,

$$\omega L_1 = 10.55 \text{ ohms}.$$

We turn now to the conditions at the other end of the transmission line. The currents in the primary and secondary of the antenna coupling system of antenna 1 (L_1 and L_2) are in quadrature. Then, if the

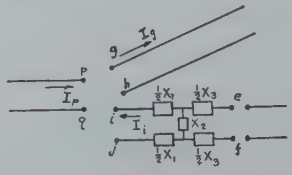

Fig. 55

transmission lines are of the same length, the network at the transmitter end must shift the phase of its entering and leaving currents by 60 degrees to attain a 150-degree relation between antenna currents. The points, i, p, and g (Fig. 55) are to be connected together, while h, j, and q are also joined. Therefore the voltage across any pair of

terminals must be equal. The impedance looking into terminals, $g-h$, is Z_c. Then the voltage is determined from

$$E_{gh}I_g = 1258 \text{ watts}$$

or,

$$E^2_{gh}/Z_c = 1258 \text{ watts}.$$

$$E_{gh} = \sqrt{1258Z_c}.$$

The voltage, E_{pq}, is equal to this same value. The power passing into the system through terminals, $p-q$, is 1000 watts so that

$$E_{pq}I_p = 1000$$

or,

$$I_p = \frac{1000}{\sqrt{1258Z_c}}$$

then,

$$\frac{E_{pq}}{I_p} = \frac{1258}{1000}Z_c = 1.258Z_c.$$

Thus the transmitter looks into $1.258Z_c$ ohms. Likewise,

$$E_{ij} = E_{g,h}$$

so that, .

$$E_{ij}I_i = 258$$

or,

$$I_i = \frac{258}{\sqrt{1258Z_c}}$$

and the effective termination of the network is

$$\frac{E_{ij}}{I_i} = R_{ij} = \frac{1258}{258}Z_c = 4.86Z_c \text{ ohms}.$$

To determine the values of reactance in the network, we may use the relations of (159), (160), and (161), with the provision that R_{ij} and Z_c must be interchanged in these expressions.

$$R_{ij} = 4.86Z_c.$$

Then,

$$\sqrt{Z_cR_{ij}} = 2.205Z_c$$

and,

$$\left(\sqrt{\frac{Z_c}{R_{ij}}}\right)_{(159)} = \sqrt{\frac{R_{ij}}{Z_c}} = 2.205.$$

If,

$$\rho = -60°$$

$$X_1 = \frac{-2.205}{-0.866} Z_c[1 - 2.205 \times 0.5] = -0.26Z_c \text{ ohms}$$

$$X_2 = \frac{+2.205}{-0.866} Z_c = -2.548Z_c \text{ ohms}$$

$$X_3 = \frac{-2.205Z_c\left[1 - \frac{0.5}{2.205}\right]}{-0.866} = +1.97Z_c \text{ ohms.}$$

When the radio station using a directional array is allowed to determine the input power by the "direct method," two procedures are possible. First the resistance and current may be measured at some point between the common junction of the transmission lines and the transmitter. The power supplied at this point includes the power dissipated in all the coupling and tuning equipment as well as the power fed to the antennas themselves. However, the resistance of each antenna and the mutual impedance have already been measured. The antenna currents are measured by meters inserted in each antenna. Then the power pumped into each antenna is given by (41) and (42), while (43) yields the total power sent into the antenna system. This method of power determination may seem indirect and complicated. The writer believes that, in view of the fact that an array in itself is more complicated than a single antenna, some degree of indirectness must be tolerated. In fact, many quantities used in engineering practice are determined by methods more devious than the above plan.

It has been suggested to the writer a number of times that the total antenna power may be measured in the following manner. The resistance of each antenna alone, with the other antennas detuned, is measured. Then when the array is in operation, the current in each antenna is measured. The power fed into a particular antenna is the square of the antenna current in this antenna multiplied by the resistance previously measured for this antenna. The total power is the sum of terms determined in this manner. The error involved in determining power in this fashion is usually great. For illustration, we will consider two quarter-wave antennas, separated a distance, d. The antennas are fed with equal currents so that

$$I_1 = I_0 \angle +\alpha.$$

Also $R_{00} = R_{11} =$ the self-resistance of each antenna. From (43), the actual antenna power is

$$P_{\text{actual}} = 2I_0^2[R_{00} + R_m \cos \alpha].$$

The apparent power, measured by the method described in the above paragraph is

$$P_{\text{apparent}} = I_0^2 R_{00} + I_1^2 R_{11} = 2I_0^2 R_{00}$$

so that,

$$\frac{P_{\text{actual}}}{P_{\text{apparent}}} = 1 + \frac{R_m}{R_{00}} \cos \alpha.$$

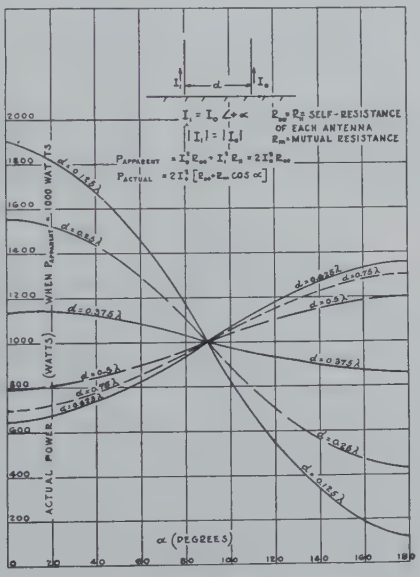

Fig. 56

Fig. 56 shows the actual power as a function of α, for a number of values of d/λ, when the apparent power is 1000 watts.

XI. Conclusion

In the preceding discussion, we have treated the cases of both driven and parasitic arrays. Where possible, the results have been tested by comparison with experimental results.

The field and circuit conditions are treated for the case of multi-element driven arrays. For a given current ratio and phase relation, the effective impedance of each antenna and the total radiated power,

as well as the power radiated by each antenna, are readily found. The radiation pattern of the array is easily calculated. These arrays are often used to protect the service areas of other stations operating on the same frequency assignment.

In the case of a single parasitic reflector, it is found that the mysterious something that is supposed to happen when the spacing is one-quarter wave length fails to materialize. Closer spacings are found to be desirable in both the transmitting and receiving case. It is found that the parasitic antenna functions equally well as a director or a reflector.

The case of an antenna parallel to an infinite sheet acting as a reflector is treated. It is shown that it is desirable to space the antenna very much less than a quarter wave length from the sheet. A similar treatment of parabolic and hyperbolic reflectors will be published at a later date.

A method of measuring the mutual impedance between antennas is advanced. A systematic method of adjusting a complicated array is outlined.

Appendix I

The Calculation Of Mutual Impedance Between a Tower and a T Antenna

In a number of cases where directional arrays were desired, the stations were already equipped with a T antenna supported between two towers. When the line of towers happened to be right, the desired array was formed by using the T antenna and one or both supporting towers as the array. In some cases, it was necessary to reconstruct the T so that it did not stand midway between the towers. In cases of this sort, it is desirable to be able to calculate the mutual impedance between the T antenna and a tower. This mutual impedance is also of value in predicting the effect of the supporting towers on the field pattern when the T antenna alone is fed, while the towers are supposedly only supporting structures.[7]

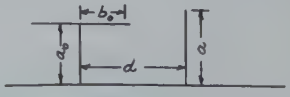

Fig. 57

We shall assume the antenna and tower to be located as shown in Fig. 57. The sag in the horizontal section is neglected. The following symbolism will be used:

[7] G. H. Brown and Ronold King, *loc. cit.*, pp. 477–479.

λ = wave length
$k = 2\pi/\lambda$
a = height of the tower
$G = ka$ radians $= 360 \cdot a/\lambda$ degrees
a_0 = height of vertical section of the T.
b_0 = half length of horizontal section of the T.
d = distance from tower to vertical downlead of the T
b_0' = equivalent half length of horizontal section where $\tan(kb_0') = 2\tan(kb_0)$
$B_0 = kb_0$ radians
$B_0' = kb_0'$ radians
$G_0' = k(a + b_0')$ radians

The mutual impedance is found by forming (13) over the entire T antenna. This impedance is then given as the sum of three integrals. Then

$$\overline{Z}_m = J_1 + J_2 + J_3. \text{ (loop)} \tag{166}$$

The first integral sums the energy over the vertical portion of the T antenna. Then

$$J_1 = 30 \int_{y=0}^{y=a_0} \sin(G_0' - ky) \left[\left\{ \frac{\sin kr_1}{r_1} + \frac{\sin kr_2}{r_2} - 2\cos G \frac{\sin kr_0}{r_0} \right\} + j \left\{ \frac{\cos kr_1}{r_1} + \frac{\cos kr_2}{r_2} - 2\cos G \frac{\sin kr_0}{r_0} \right\} \right] dy \tag{167}$$

where,

$$\left. \begin{aligned} r_1 &= \sqrt{(a-y)^2 + d^2} \\ r_2 &= \sqrt{(a+y)^2 + d^2} \\ r_0 &= \sqrt{y^2 + d^2} \end{aligned} \right\}. \tag{168}$$

The second integral takes account of the energy flow from the half of the flat top nearest the tower, so that

$$J_2 = \frac{15 \sin B_0'}{\sin B_0} \int_{y=0}^{y=b_0} \frac{\sin(B_0 - ky)}{(d-y)} \left[\frac{(a_0 - a)}{r_3} \sin kr_3 + \frac{(a_0 + a)}{r_4} \sin kr_4 - \frac{2a_0}{r_5} \cos G \sin kr_5 \right\} + j \left\{ \frac{(a_0 - a)}{r_3} \cos kr_3 + \frac{(a_0 + a)}{r_4} \cos kr_4 - \frac{2a_0}{r_5} \cos G \cos kr_5 \right\} \right] dy \tag{169}$$

where,

$$\left.\begin{aligned} r_3 &= \sqrt{(a_0 - a)^2 + (d - y)^2} \\ r_4 &= \sqrt{(a_0 + a)^2 + (d - y)^2} \\ r_5 &= \sqrt{a_0^2 + (d - y)^2} \end{aligned}\right\}. \tag{170}$$

The remaining term, which takes account of the half of the horizontal section farthest removed from the tower is

$$\begin{aligned} J_3 = -\frac{15 \sin B_0'}{\sin B_0} \int_{a=0}^{y=b_0} \frac{\sin (B_0 - ky)}{(d + y)} \Bigg[\Bigg\{ \frac{(a_0 - a)}{r_6} \sin kr_6 \\ + \frac{(a_0 + a)}{r_7} \sin kr_7 - \frac{2a_0}{r_8} \cos G \sin kr_8 \Bigg\} \Bigg] \\ + j \Bigg\{ \frac{(a_0 - a)}{r_6} \cos kr_6 + \frac{(a_0 + a)}{r_7} \cos kr_7 \\ - \frac{2a_0}{r_8} \cos G \cos kr_8 \Bigg\} \Bigg] dy \end{aligned} \tag{171}$$

where,

$$\begin{aligned} r_6 &= \sqrt{(a_0 - a)^2 + (d + y)^2} \\ r_7 &= \sqrt{(a_0 + a)^2 + (d + y)^2} \\ r_8 &= \sqrt{a_0^2 + (d + y)^2}. \end{aligned} \tag{172}$$

These expressions look rather formidable, but experience with them shows that an answer can be obtained in an hour or two by plotting each integrand and traversing with a planimeter. A curve showing the mutual impedance between a particular tower and a T antenna, calculated from the above relations, has already been published.[7]

Appendix II

The Vertical Radiation Characteristics as Derived from the Rigorous Field Expressions

The usual method of deriving the field distribution at a great distance from an antenna is to set up the expression for the field due to an infinitesimal element of current.

This expression is made simple by placing the point at which we are reckoning the field at a great distance from this current element. Then an integration is carried out which sums up the effects of all the current elements along the antenna.

[7] G. H. Brown and Ronold King, *loc. cit.*, Fig. 19.

The same ultimate answer may be arrived at by reversing the procedure, first summing over the antenna to determine the field at any arbitrary point and then moving the point to a great distance from the antenna. This method is included in this paper because it is believed that the procedure is new to the literature on the subject.

The first step in the procedure, that of summing over the antenna, has already been carried out, with the results set forth in Section II.

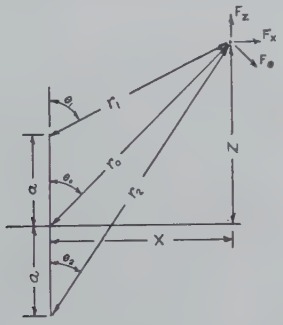

Fig. 58

To illustrate the procedure of passing to a great distance we will consider the case of the simple vertical wire antenna with no top loading, shown in Fig. 58. From (7),

$$B_\phi = j\frac{\mu I_0}{4\pi x \sin G}\left[\epsilon^{-jkr_2} + \epsilon^{-jkr_1} - 2\cos G\epsilon^{-jkr_0}\right]. \tag{173}$$

Here the magnetic flux density points into the paper when I_0 is the current flowing upward at the base of the antenna. $G = ka$. We assume r_0 so great that $\theta_2 \doteq \theta_0 \doteq \theta_1$. Then,

$$\left.\begin{aligned} r_2 &\doteq r_0 + a\cos\theta \\ r_1 &\doteq r_0 - a\cos\theta \end{aligned}\right\}. \tag{174}$$

Also,

$$\left.\begin{aligned} x/r_0 &= \sin\theta \quad \text{or} \quad \frac{1}{x} = \frac{1}{r_0\sin\theta} \\ \frac{1}{r_1} &\doteq \frac{1}{r_2} \doteq \frac{1}{r_0} \end{aligned}\right\}. \tag{175}$$

Then,

$$B_\phi = j\frac{\mu I_0}{4\pi r_0 \sin\theta \sin G}\left[\epsilon^{+jG\cos\theta} + \epsilon^{-jG\cos\theta} - 2\cos G\right]\epsilon^{-jkr_0} \tag{176}$$

or,

$$B_\phi \doteq j \frac{2 \cdot 10^{-9} I_0}{r_0 \sin G} \left[\frac{\cos (G \cos \theta) - \cos G}{\sin \theta} \right] \epsilon^{-jkr_0}. \tag{177}$$

From (5) and (6) of Section II,

$$F_z = -j \frac{30 I_0}{\sin G} \left[\frac{\epsilon^{-jkr_2}}{r_2} + \frac{\epsilon^{-jkr_1}}{r_1} - 2 \cos G \frac{\epsilon^{-jkr_0}}{r_0} \right] \tag{178}$$

and,

$$F_x = +j \frac{30 I_0}{\sin G} \left[\frac{(z-a)}{r_1} \epsilon^{-jkr_1} + \frac{(z+a)}{r_2} \epsilon^{-jkr_2} - \frac{2z}{r_0} \epsilon^{-jkr_0} \cos G \right] \tag{179}$$

Let us project these components on a line perpendicular to r_0 to form the component, F_θ.

$$F_\theta = -F_z \sin \theta + F_x \cos \theta \tag{180}$$

$$\frac{z-a}{x} \doteq \frac{z+a}{x} \doteq \frac{z}{x} = \frac{\cos \theta}{\sin \theta} \tag{181}$$

Then,

$$F_\theta = j \frac{30 I_0 \epsilon^{-jkr_0}}{r_0 \sin G} \left[\sin \theta (\epsilon^{+jG\cos\theta} + \epsilon^{-jG\cos\theta}) - 2 \cos G \sin \theta \right.$$

$$\left. + \frac{\cos^2 \theta}{\sin \theta} (\epsilon^{+jG\cos\theta} + \epsilon^{-jG\cos\theta}) - \frac{2 \cos^2 \theta \cos G}{\sin \theta} \right] \tag{182}$$

$$F_\theta = j \frac{60 I_0 \epsilon^{-jkr_0}}{r_0 \sin G} \left[\frac{\cos (G \cos \theta) - \cos G}{\sin \theta} \right]. \tag{183}$$

The projection of the components on r_0 to form F_r is

$$F_r = F_z \cos \theta + F_x \sin \theta \tag{184}$$

$$F_r = +j \frac{30 I_0 \epsilon^{-jkr_0}}{r_0 \sin G} \left[-\cos \theta (\epsilon^{+jG\cos\theta} + \epsilon^{-jG\cos\theta}) + 2 \cos G \cos \theta \right.$$

$$\left. + \cos \theta (\epsilon^{+jG\cos\theta} + \epsilon^{-jG\cos\theta}) - 2 \cos G \cos \theta \right] = 0. \tag{185}$$

We thus see that the radial field, F_r, vanishes, leaving the two mutually perpendicular vectors, B_ϕ and F_θ, which are in time phase.

Appendix III

The Derivation of the Expressions for the Electromagnetic Field in the Vicinity of a Straight Wire, End-Loaded, and of Arbitrary Length

The procedure to be carried out here is exactly the same as that of Carter in treating a similar case.[1] His wires were always integral mul-

[1] P. S. Carter, *loc. cit.*, Appendix I, pp. 1034–1037.

tiples of half waves in length so that the current at each end of the wire was always zero.

We shall consider the conductor of Fig. 59. The origin of co-ordinates is taken at the base of the antenna. The top of the wire is end-loaded so that the current is finite at the top of the wire. The current at the bottom point is finite because we are dealing with a wire of

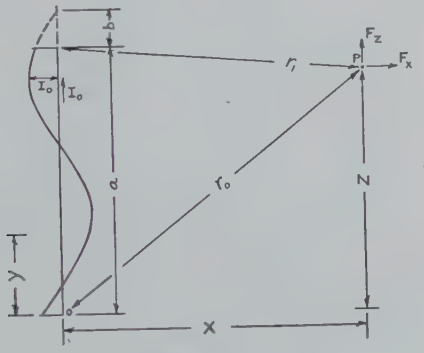

Fig. 59

arbitrary length. The length of wire which would replace the top-loading and give the same current distribution is b. Then,

$$B = \frac{2\pi b}{\lambda} \text{ radians} = \frac{360b}{\lambda} \text{ degrees}$$

$$A = \frac{2\pi a}{\lambda} \text{ radians} = \frac{360a}{\lambda} \text{ degrees}$$

where a is the length of wire. $G = A + B$.

The current distribution is

$$i_y = I_0 \sin (G - ky) \tag{186}$$

where I_0 is the current at the first loop or maximum at the top of the wire.

The vector potential at the point P due to the current on the antenna has only one component, A_z, which lies parallel to the antenna. Then,

$$A_z = \frac{\mu}{4\pi} \int_{y=0}^{y=a} i_y \frac{\epsilon^{-jkr}}{r} dy \tag{187}$$

where,

$r = \sqrt{(z-y)^2 + x^2}$

$k = 2\pi/\lambda$

μ = permeability of free space $= 4\pi \cdot 10^{-9}$.

Substituting (186) in (187),

$$A_z = \frac{\mu I_0}{4\pi} \int_{y=0}^{y=a} \sin (G - ky) \frac{\epsilon^{-jkr}}{r} dy. \tag{188}$$

This expression may be expanded to give

$$A_z = \frac{\mu I_0}{8\pi j} \left[\epsilon^{+j(G-kz)} \int_{y=0}^{y=a} \frac{\epsilon^{-jk(r+y-z)}}{r} dy \right.$$
$$\left. - \epsilon^{-j(G-kz)} \int_{y=0}^{y=a} \frac{\epsilon^{-jk(r-y+z)}}{r} dy \right]. \tag{189}$$

In the first integral, let

$$u = k(r+y-z).$$

Then,

$$du/u = dy/r.$$

The limits become

$$u_0 = k(r_0 - z) \text{ when } y = 0$$

and,

$$u_1 = k(r_1 - z) + A \text{ when } y = a$$

where,

$$r_1 = \sqrt{(z-a)^2 + x^2} \text{ and } r_0 = \sqrt{z^2 + x^2},$$

the distances shown on Fig. 59.

In the second integral, we substitute $v = k(r-y+z)$ so that $-dv/v = dy/r$.

The lower limit is $v_0 = k(r_0+z)$ while the upper limit becomes $v_1 = k(r_1+z) - A$. Thus (189) becomes

$$A_z = \frac{\mu I_0}{8\pi j} \left[\epsilon^{+j(G-kz)} \int_{u=u_0}^{u=u_1} \frac{\epsilon^{-ju}}{u} du + \epsilon^{-j(G-kz)} \int_{v=v_0}^{v=v_1} \frac{\epsilon^{-jv}}{v} dv \right]. \tag{190}$$

The magnetic flux density lies in circles about the wire. At P, the magnetic flux density points into the paper. Then

$$B_\phi = -\frac{\partial A_z}{\partial x}. \tag{191}$$

After a little manipulation, (191) becomes

$$B_\phi = -\frac{\mu I_0}{8\pi j} \left[\epsilon^{+j(G-kz)} \left\{ \frac{kx}{r_1} \frac{\epsilon^{-ju_1}}{u_1} - \frac{kx}{r_0} \frac{\epsilon^{-ju_0}}{u_0} \right\} \right.$$
$$\left. + \epsilon^{-j(G-kz)} \left\{ \frac{kx}{r_1} \frac{\epsilon^{-jv_1}}{v_1} - \frac{kx}{r_0} \frac{\epsilon^{-jv_0}}{v_0} \right\} \right]. \tag{192}$$

This folds up to give

$$B_\phi = +j\frac{I_0 \cdot 10^{-9}}{x}\left[\epsilon^{-jkr_1}\cos B - \epsilon^{-jkr_0}\cos G + j\frac{(z-a)}{r_1}\epsilon^{-jkr_1}\sin B - j\frac{z}{r_0}\epsilon^{-jkr_0}\sin G\right]. \quad (193)$$

The vertical intensity, F_z is obtained from

$$j\frac{\omega}{c^2}F_z = \frac{1}{x}\frac{\partial(xB_\phi)}{\partial x} \quad (194)$$

where $c = 3\times10^{10}$ centimeters per second = velocity of propagation of light in free space, and $\omega = 2\pi f = 2\pi c/\lambda = ck$.
Then,

$$F_z = \frac{c^2}{j\omega}\frac{1}{x}\frac{\partial(xB_\phi)}{\partial x} \quad (195)$$

and,

$$F_z = 30I_0\left[-j\frac{\epsilon^{-jkr_1}}{r_1}\cos B + j\frac{\epsilon^{-jkr_0}}{r_0}\cos G + \frac{(z-a)}{r_1^2}\epsilon^{-jkr_1}\sin B - \frac{z}{r_0^2}\epsilon^{-jkr_0}\sin G - j\frac{(z-a)}{kr_1^3}\epsilon^{-jkr_1}\sin B + j\frac{z}{kr_0^3}\epsilon^{-jkr_0}\sin G\right]. \quad (196)$$

The horizontal component of electric intensity is found from

$$F_x = \frac{-c^2}{j\omega x}\frac{\partial(xB_\phi)}{\partial z} \quad (197)$$

so that,

$$F_y = +\frac{30I_0}{x}\left[+j\frac{(z-a)}{r_1}\epsilon^{-jkr_1}\cos B - j\frac{z}{r_0}\epsilon^{-jkr_0}\cos G - \frac{(z-a)^2}{r_1^2}\epsilon^{-jkr_1}\sin B + \left(\frac{z}{r_0}\right)^2\epsilon^{-jkr_0}\sin G - j\frac{x^2}{kr_1^3}\epsilon^{-jkr_1}\sin B + j\frac{x^2}{kr_0^3}\epsilon^{-jkr_0}\sin G\right]. \quad (198)$$

Then to find the total field due to a number of current elements, we use (193), (196), and (198) to compute the contribution due to each element and combine with due care to symbolism. This is the procedure that yielded the results of Section II.

Proceedings of the Institute of Radio Engineers
Volume 25, Number 1, Part 1 *January, 1937*

DISCUSSION ON "AN URBAN FIELD STRENGTH SURVEY AT THIRTY AND ONE HUNDRED MEGACYCLES"*

R. S. Holmes and A. H. Turner

C. R. Burrows:[1] From the data presented by Holmes and Turner the authors conclude that there exists an important difference between propagation on one hundred megacycles and on thirty megacycles over urban terrain. Fig. 14 indicates that the power required by one hundred megacycles is 1300 times that required by thirty megacycles at ten miles but only one hundred times at one mile to deliver one hundred microvolts to the input of a receiver. The writer believes that judgment should be reserved in regard to the existence of this higher rate of attenuation on the higher frequency for the following reasons.

The conclusion that the rate of attenuation on one hundred megacycles is larger than that on thirty megacycles is based on the fact that the slopes of the lines drawn through the averages of the experimental data plotted in Figs. 6 and 7 are 1.84 and 2.5, respectively. It appears that the data would be as well represented by lines with a slope of two (inverse square of distance). Since there is some theoretical justification for the slope of two,[2] the writer feels that more data are desirable before concluding that the rate of attenuation is actually greater on one hundred megacycles than on thirty megacycles.

The method of averaging the radius of a contour of equal signal by determining the radius of a circle of equal area does not seem desirable since owing to the great irregularity in these contours the results obtained over a wide range of distances contributes to the value to be attributed to a single intermediate distance. Moreover, the drawing of contours presents difficulties of engineering judgment which the writer prefers to avoid if possible in determining a final average.

It is interesting to note that if the "survey average curves" of Figs. 6 and 7 were drawn with a slope of two, the deviations of the actual received field strengths from the survey average, as shown in Figs. 10, 11, 12, and 13, would in each case be decreased. While the difference between the resulting curves and the original figures is small, it may be significant that in each of the four cases the received field strength is more nearly in agreement with the inverse square of distance curve than the survey averages of the paper.

R. S. Holmes and A. H. Turner:[3] There are three possible conditions that can be considered in studying the propagation of ultra-high-frequency radio waves. Two of these conditions are almost entirely theoretical, while the third is practical for broadcast service.

First, if both the transmitting and receiving antennas were in free space entirely away from any interfering objects and from the earth, field intensity would be inversely proportional to distance and independent of frequency. Second, if both antennas were over flat earth with no obstructions between, and reflection from the earth were practically perfect, field intensity would be inversely proportional to the square of the distance over the region where the

* Proc. I.R.E., vol. 24, pp. 755–770; May, (1936).
[1] Bell Telephone Laboratories, Inc., Deal, N. J.
[2] C. R. Burrows, L. E. Hunt, and A. Decino, "Ultra-short-wave propagation: mobile urban transmission characteristics," *Elec. Eng.*, vol. 54, pp. 115–124; January, (1935): *Bell Sys. Tech. Jour.*, vol. 14, pp. 253–272; April, (1935); and "Ultra-short-wave propagation over land," Proc. I.R.E., vol. 23, 1507–1535; December, (1935).
[3] Engineering Department, RCA Victor Division, RCA Manufacturing Company, Inc., Camden, New Jersey.

distance between antennas is of the order of one to ten miles as it was in this survey. In this range the rate of attenuation should be less at one hundred megacycles than at thirty, because the reflected wave produces less cancellation at the higher frequencies. The third, and the most practical, condition is where the antennas are both close to irregular earth of variable reflecting properties, and there is not a free transmission path between them. These are most nearly the conditions under which this survey was made. The transmitting antenna was comparatively low, and the receiving antenna was only a few feet from the ground. Consequently in only a few instances was there a free path between the two antennas. The signal was therefore propagated principally either through obstructions such as buildings, trees, and hills, or by various multiple paths around them. This condition does not readily lend itself to theoretical calculation, but it seems reasonable that the attenuation should be considerably greater at the higher frequency, and this was the result found in the survey.

In drawing the straight lines of Figs. 6 and 7, little weight was given the single point at less than one mile because too few data were taken this close. The greatest part of the data was taken between one and ten miles from the transmitter. The lines could possibly have been drawn with more nearly equal slopes, but the one hundred-megacycle curve appears to be better represented by the line of slope 2.5 than it would be by a line of slope 2.

In drawing the contours of field strength on the map there were sufficient points so that very little was left to judgment in determining the exact position of the contour lines.

Proceedings of the Institute of Radio Engineers
Volume 25, Number 1, Part 1 *January, 1937*

CORRESPONDENCE

Election of Institute Officers and a New York Section

May I take the opportunity, now afforded by the Board of Directors in opening the PROCEEDINGS to correspondents, to put before the membership certain questions regarding the organization of the Institute?

The first question is the proposal (which has been favorably discussed at meetings of the Board during the past year) that only one candidate need be officially nominated for the offices of president and vice president, at least—with the understanding, of course, that additional candidates can always be nominated by petition from a proper number of members. Our present constitutional requirement that at least two candidates be nominated officially has for years been an embarrassment and a wounder of feelings. Other organizations similar to our own have nearly all—or perhaps all—come to recognize that it is unwise to turn down one good man every time another is elected. A subsequent election of a defeated candidate is of course possible; but a nominating committee naturally feels reluctant to propose a name that has been disapproved by the voters, lest a second defeat should permanently alienate the good will of a man whom the committee considers deserving of honor.

If only a single candidate were to be nominated officially, the responsibility of the nominating committee would, of course, be greatly increased; and there would arise the question of the selection of the committee in a way that would preserve—or, better, would enhance—the democratic control of the Institute. This is a particularly puzzling question in view of the geographical distribution of our membership: a large proportion in the vicinity of New York and a great many more within easy traveling distance, but yet with an important membership scattered throughout this country and Canada—some affiliated with sections, some not—and with an exceptionally large proportion in other parts of the world. Perhaps it would be possible to have one or more members of the nominating committee selected by the sections and one or more by the metropolitan membership, leaving others to be selected by the Board of Directors, as at present, to represent the remainder of the membership. If this were to be done, careful consideration would have to be given to the machinery for registering the wishes of the membership. Perhaps the Sections Committee could represent the sections in some way; and perhaps the metropolitan group could express itself through an appropriate committee.

This brings me to the second question with which I have been concerned: how to secure for the membership centered in New York the advantages and privileges enjoyed by the sections in the conduct of local meetings and generally in self-expression. By our present constitution, the New York Program Committee, appointed by the President, arranges papers for the New York meetings; and the conduct of the meetings is left to the President. Might it not be practicable to give the metropolitan membership a direct voice in the matters which affect it—say by electing one or more members to the New York Program Committee and by holding a short business meeting once a year before the presentation of the paper of the evening? The Institute might profit by the discovery in this

way of unrecognized talent that it could draw on; and there might turn out to be some unappreciated desires—such as for a social gathering after a meeting—that could be gratified.

In concluding, may I call attention to the fact that the preceding suggestions are personal ones, not sponsored by the Board of Directors on which I have the honor of serving, and may I express the hope that the Editor or the Secretary will receive comments and ideas from members as to the functioning of the Institute in ways that will increase its service?

ALAN HAZELTINE

Stevens Institute of Technology,
Hoboken, New Jersey

Proceedings of the Institute of Radio Engineers
Volume 25, Number 1, Part 1 *January, 1937*

BOOK REVIEWS

Electrical Engineers' Handbook. Volume 5. Electric Communication and Electronics. Harold Pender, editor-in-chief; Knox McIlwain, associate editor-in-chief. Third edition. 1022 pages, 981 figures. John Wiley, New York City, 1936. Price $5.00.

This new complete handbook for the communication and electronics fields—a part of the Pender's Electrical Engineers' Handbook—is a most welcome volume. Being ordinary book size, even as to thickness, instead of the very thick "pocket size," the convenience of its use is much enhanced. The excellence of the list of contributors is probably chiefly responsible for its great value as a source. Of the list of more than fifty a third are associated with the Bell Laboratories, a third connected with RCA, and the other third scattered.

The volume is divided into seventeen sections ranging from seventeen to one hundred and sixty pages in length. Except for the general section on mathematical formulas and physical constants, the section entitled "Acoustics" is the only one which is not directly electrical. Many of the sections, however, are devoted to the arts which combine the electrical with other branches of physics. Among these are "Electromechanical-Acoustic Devices," "Sound-Reproduction Systems," "Facsimile Transmission and Reception," "Television," "Electronic Control and Navigation Equipment," and "Medical Applications of Electricity." With the emphasis throughout upon the communication field, the two sections last mentioned (each is quite short) seem perhaps somewhat out of place. However, with the concentration of the electronic part of the entire handbook series in the present volume, it was presumably best to place these two in the present volume and to give emphasis to "Electronics" in the title. Of course, a fair part of the entire volume involves electronics. There is a section entitled "Electron Tubes" while a second section, more than twice as long as any other, entitled "Circuit Elements," is devoted largely to vacuum tube circuits.

Among the articles of which the reviewer made particular note, in going through the volume, were (1) in the mathematical section, a decibel conversion table and one of physical constants; (2) in the section on properties of materials, an article on luminescent materials, an extensive descriptive list of solid dielectric materials and special articles on quartz and piezoelectric materials, the latter seems to be one of the few subjects not well provided with bibliographical references; (3) vacuum tube operating data, where standard makes of tubes are listed in seventeen groups according to their characteristics.

The scope of the contents of the handbook, which is surprising at first sight for an Electrical Engineers' Handbook, is such as to make it a valuable addition to the physicist's desk as well as to that of the communication engineer. Noting the presence of a section on acoustics and the absence of a similar section on optics suggests that, if a period of fourteen years elapses again between editions the fourth edition may possibly contain a special optical section. At present what material there is in this field is scattered through the articles "Phototubes," "Photoluminescence," "Television," and "Optical Recording and Reproducing."

*Karl S. Van Dyke

* Wesleyan University, Middletown, Connecticut.

The Earth's Magnetism, by S. Chapman. Published by Methuen and Company, Ltd., 36 Essex St., London, W.C.2, England. 116 pages, price 3s.6d.

A pocket-size monograph containing "a brief but fairly broad account of our present knowledge of the earth's magnetic field and its changes." Written by one of the foremost authorities, this book can be recommended as a valuable contribution to the subject.

In the first chapter "The Main Field and the Secular Variation" are discussed. Among the subjects considered are: "The Magnetic Elements," "Isomagnetic Maps," "Units and Force Values," "Absolute Magnetic Measurements and Instruments," "Magnetic Observatories, Variometers and Magnetographs," "Magnetic Surveys," etc.

"The Transient Magnetic Variations" are discussed in the second chapter. Some of the subjects discussed are: "The Sunspot Cycle; Sunspot Numbers," "Quiet and Disturbed Days; Character Figures," and "The Annual Variation of the Magnetic Elements."

"The Quiet-Day Solar Daily Magnetic Variation" is the subject of the third chapter while the fourth chapter is concerned with the Lunar Daily Magnetic Variation. In the fifth chapter, The Morphology of the Magnetic Disturbance is discussed. Under this heading are included: "Magnetic Disturbance and Storms," "The Storm-Time Variations," etc.

The subject of the last chapter (Chapter VI) is: "Solar Relations with Magnetic Disturbance."

The mathematical development is touched only briefly and no attempt is made to do more than mention the importance of radio research in the study of the earth's magnetism. The methods used in separating the various causes of observed changes in the field are well described and similar methods might be used to advantage in other types of work. The clear readable style will attract many a lay reader as well as the experienced student of this subject.

The author admits that there are many problems yet unsolved, but the reader will look forward to further enlightenment in the more extensive and detailed account of the subject which the author hopes to publish shortly in collaboration with Professor J. Bartels.

*T. R. Gilliland

* National Bureau of Standards, Washington, D. C.

CONTRIBUTORS TO THIS ISSUE

Brown, George H.: Born October 14, 1908, at North Milwaukee, Wisconsin. Received B.S. degree, University of Wisconsin, 1930; M.S. degree, 1931; Ph.D. degree, 1933. Research Fellow, electrical engineering department, University of Wisconsin, 1930–1933. Research division, RCA Victor Company, Inc., 1933 to date. Member, Sigma Xi. Associate member, Institute of Radio Engineers, 1930.

Colwell, Robert C.: Born October 14, 1884, at Fredericton, N. B., Canada. Received A.B. degree, Harvard University; M.A. degree, University of New Brunswick; Ph.D. degree, Princeton University. Professor of Physics, Geneva College, 1913–1923; assistant director of radio laboratory, West Virginia University, 1924 to date. Member, American Physical Society; Franklin Institute; American Mathematical Society. Associate member, Institute of Radio Engineers, 1921; Member, 1929.

Epstein, D. W.: Born January 11, 1908, in Russia. Received B.S. degree in engineering physics, Lehigh University, 1930; M.S. degree in electrical engineering, University of Pennsylvania, 1934. Research division, engineering department, RCA Victor Company, Inc., 1930–1935; RCA Victor Division, RCA Manufacturing Company, Inc., 1935 to date. Member, American Physical Society. Associate member, Institute of Radio Engineers, 1934.

Friend, A. W.: Born January 24, 1910, at Morgantown, West Virginia. Received B.S.E.E. degree, West Virginia University, 1932; M.S. degree in physics, 1936. Transmission and distribution engineer, Ohio Power Company, 1933–1934; instructor in physics, West Virginia University, 1934 to date. Associate member, American Institute of Electrical Engineers. Associate member, Institute of Radio Engineers, 1934.

Judson, E. B.: Born December 3, 1898, at Washington, D. C. Naval radio service, 1917–1919; United States Naval Radio Research Laboratory, 1919–1923; assistant to Dr. L. W. Austin, radio transmission research laboratory, Bureau of Standards, 1923–1932; wave phenomena group, National Bureau of Standards, 1932 to February, 1936; Bureau of Yards and Docks, Navy Department, February, 1936 to date. Associate member, Institute of Radio Engineers, 1926.

Poch, W. J.: Born July 11, 1905, at London, England. Received B.S. degree, University of Michigan, 1928; M.S. degree, University of Pennsylvania, 1933. General Electric Company, 1928–1929; RCA Manufacturing Company, Inc., 1930 to date. Associate member, Institute of Radio Engineers, 1928.

Wagener, Winfield G.: Born July 11, 1906, ar San Jose, California. Received B.S. degree, 1928; M.S. degree in electrical engineering, 1929, University of California. Antenna and vacuum tube development, Federal Telegraph Company, 1929–1933; research and development laboratory, RCA Manufacturing Company, Inc., Radiotron Division, 1933 to date. Associate member, Institute of Radio Engineers, 1929.